Reviews of Geophysics

REVIEW ARTICLE
10.1029/2018RG000636

Key Points:
- Tidal properties have changed, and continue to evolve, due to nonastronomical factors
- Attributing causation remains challenging
- Regionally coherent increases/decreases in tidal properties are likely to occur over the next centuries

Correspondence to:
I. D. Haigh,
i.d.haigh@soton.ac.uk

Citation:
Haigh, I. D., Pickering, M. D., Green, J. A. M., Arbic, B. K., Arns, A., Dangendorf, S., et al. (2019). The tides they are a-changin': A comprehensive review of past and future nonastronomical changes in tides, their driving mechanisms and future implications. *Reviews of Geophysics*, *57*, e2018RG000636. https://doi.org/10.1029/2018RG000636

Received 30 NOV 2018
Accepted 18 NOV 2019
Accepted article online 13 DEC 2019

The Tides They Are A-Changin': A Comprehensive Review of Past and Future Nonastronomical Changes in Tides, Their Driving Mechanisms, and Future Implications

Ivan D. Haigh[1], Mark D. Pickering[1], J. A. Mattias Green[2], Brian K. Arbic[3], Arne Arns[4], Sönke Dangendorf[5], David F. Hill[6], Kevin Horsburgh[7], Tom Howard[8], Déborah Idier[9], David A. Jay[10], Leon Jänicke[11], Serena B. Lee[12], Malte Müller[13], Michael Schindelegger[14], Stefan A. Talke[10,15], Sophie-Berenice Wilmes[2], and Philip L. Woodworth[7]

[1]Ocean and Earth Science, National Oceanography Centre Southampton, University of Southampton, Southampton, UK, [2]School of Ocean Sciences, Bangor University, Menai Bridge, UK, [3]Department of Earth and Environmental Sciences, University of Michigan, Ann Arbor, MI, USA, [4]Faculty of Agricultural and Environmental Sciences, University of Rostock, Rostock, Germany, [5]Center for Coastal Physical Oceanography, Department of Ocean, Earth and Atmospheric Sciences, Old Dominion University, Norfolk, VA, USA, [6]Civil and Construction Engineering, Oregon State University, Corvallis, OR, USA, [7]National Oceanography Centre, Liverpool, UK, [8]Met Office, Exeter, UK, [9]Risk and Climate Change Unit, BRGM, Orléans, France, [10]Department of Civil and Environmental Engineering, Portland State University, Portland, OR, USA, [11]Research Institute for Water and Environment, University of Siegen, Siegen, Germany, [12]Griffith Climate Change Response Program, Griffith Centre for Coastal Management, Griffith University, Southport, Queensland, Australia, [13]Research and Development Department, Norwegian Meteorological Institute, Oslo, Norway, [14]Institute of Geodesy and Geoinformation, University of Bonn, Bonn, Germany, [15]Department of Civil and Environmental Engineering, California Polytechnic State University, San Luis Obispo, CA, USA

Abstract Scientists and engineers have observed for some time that tidal amplitudes at many locations are shifting considerably due to nonastronomical factors. Here we review comprehensively these important changes in tidal properties, many of which remain poorly understood. Over long geological time scales, tectonic processes drive variations in basin size, depth, and shape and hence the resonant properties of ocean basins. On shorter geological time scales, changes in oceanic tidal properties are dominated by variations in water depth. A growing number of studies have identified widespread, sometimes regionally coherent, positive, and negative trends in tidal constituents and levels during the 19th, 20th, and early 21st centuries. Determining the causes is challenging because a tide measured at a coastal gauge integrates the effects of local, regional, and oceanic changes. Here, we highlight six main factors that can cause changes in measured tidal statistics on local scales and a further eight possible regional/global driving mechanisms. Since only a few studies have combined observations and models, or modeled at a temporal/spatial resolution capable of resolving both ultralocal and large-scale global changes, the individual contributions from local and regional mechanisms remain uncertain. Nonetheless, modeling studies project that sea level rise and climate change will continue to alter tides over the next several centuries, with regionally coherent modes of change caused by alterations to coastal morphology and ice sheet extent. Hence, a better understanding of the causes and consequences of tidal variations is needed to help assess the implications for coastal defense, risk assessment, and ecological change.

Plain Language Summary Tides are one of the most persistent and dominant forces that shape our planet. The regular and predictable daily, fortnightly, monthly, annual, interannual, and longer-term changes in tides, driven by astronomical forces, are well understood. However, scientists and engineers have observed for some time that tides at many locations are shifting considerably due to nonastronomical factors. Here, we carry out a review of these important changes in tides, many of which remain poorly understood. We highlight that over long geological time scales, changes in tides are driven by tectonic processes, which alter the size, depth, and shape of the ocean. Over shorter geological time scales, changes in tides are mainly driven by changes in water depth. In recent decades, a growing number of studies have identified widespread, and sometimes regionally coherent, changes in tides during the last 150 years. However, determining exactly what has caused these more recent changes in tides has proven difficult. We discuss the local and regional/global mechanisms that might be responsible for the observed changes.

Modeling studies predict that sea level rise and climate change will continue to alter tides over the next several centuries. Therefore, a better understanding of what is causing changes in tides is needed.

1. Introduction

Tides remain one of the most persistent and dominant forces that shape our planet. They exert a crucial physical control on the coastal zone, shelf seas, and open ocean. At the coast, tides impact the timing and magnitude of storm surges and waves (Horsburgh & Wilson, 2007; Prandle & Wolf, 1978) and therefore modulate high sea levels and strongly influence coastal flooding and erosion (Pugh & Woodworth, 2014). Navigation to and from ports is constrained by tidal stage, currents, and swell steepened by tidal currents (e.g., Akan et al., 2017), while tidal range largely determines the vertical zonation of species in coastal intertidal ecosystems (Stumpf & Haines, 1998). In estuaries, the interplay between tidal currents, tidal mixing, and river flow helps to determine the extent of salinity intrusion (Jay, 1991; Geyer & MacCready, 2014), impacts sediment transport, sets system morphology, and overall is a determining factor in the mass, momentum, and energy budgets of the river/estuary/shelf continuum (Burchard et al., 2018; Jay, 1991). In shelf seas, tidal currents control sediment transport (Simpson & Sharples, 2012) and tidal renewable energy potential (Robins et al., 2015). Vigorous tidal currents produce coherent turbulent structures and surface boils (Nimmo-Smith et al., 1999; Talke et al., 2013), leading to the small-scale mixing and energy dissipation necessary for air/water gas exchange (Talke et al., 2013; Zappa et al., 2007), which impacts the drawdown of atmospheric CO_2 (Thomas et al., 2004) and alters the oxygenation of hypoxic waters (Talke et al., 2009). Tidal currents affect the formation and evolution of river plumes (Horner-Devine et al., 2009) and help to determine the dynamics of shelf sea fronts, therefore influencing primary productivity and fisheries (Simpson & Hunter, 1974). In the open-ocean, tidal dissipation affects the large-scale circulation and vertical mixing (Green et al., 2009; Munk, 1966; Wunsch & Ferrari, 2004). Furthermore, tidal levels (relative to chart datum) provide the physical basis for many national and international boundaries and, historically at least, geodetic systems (Shalowitz, 1962, 1964). Changes to tidal levels and tidal currents, therefore, have wide-ranging and important scientific and practical implications.

Tidal levels (e.g., mean high and low water), tidal range (i.e., the vertical difference between a tidal high and the following low water), and tidal currents vary on regular daily, fortnightly, monthly, annual, interannual, and longer-term time scales, driven by astronomical variations in the orbits and relative positions of the Sun, Moon, and Earth (Pugh & Woodworth, 2014). Because planetary orbital motions are stable and predictable, the astronomical forcing of tidal motions is well characterized and tide predictions can be made far into the future (Cartwright, 1985). Due to their repeatability and importance for navigation, the study of tides is the oldest branch of physical oceanography (Cartwright, 1999). Perhaps because of the reliability of tide predictions, casual observers might assume that tidal prediction is a solved problem and that tidal constituents are stationary over time. Nonetheless, both scientists and engineers have long observed that tidal levels in many locations change considerably due to nonastronomical factors over seasonal, decadal, and secular time scales (e.g., Doodson, 1924).

Our review of scientific literature indicates that changes in tides due to nonastronomical factors have primarily been noted at local scales over the past two centuries. For example, in rivers and estuaries, it has long been known that tides are greatly influenced by seasonal changes to river flow, with tidal motion completely disappearing in fluvial reaches during flood conditions (Powell, 1884). Similarly, engineers in Germany used theory and/or physical models to determine that building a weir on the Ems Estuary would amplify tides, due to increased reflection and local resonance (Keller, 1901). Engineering changes to the River Thames similarly had a big impact on its tidal history: the tidal range at London increased from 2 m during Roman times to 7–8 m during the nineteenth and twentieth centuries (Amin, 1983; Reidy, 2008). Scientifically, studies such as Doodson (1924), Schureman (1934), and Marmer (1935) observed that tides can vary significantly, most obviously due to harbor modifications and dredging. However, detailed explanations were usually lacking. Moreover, there was an apparent historical reluctance to explore methods for analysis of nonstationary time series in order to investigate these changes further. Part of this conservatism might be assigned to the stationarity assumption inherent in the harmonic analysis methodology that originated at the end of the nineteenth century (e.g., Darwin, 1898), although later pioneering works on tides such as Cartwright (1968) did recognize nonstationary behavior related to nonastronomical forcing.

Only over the past 20 years (since the digitization, concatenation, and public dissemination of regional and global databases of tide gauge records; Woodworth et al., 2017) has it been determined that significant and widespread positive and negative trends in tidal levels (and tidal currents) are occurring at many locations around the world (e.g., Devlin et al., 2014; Feng et al., 2015; Flick et al., 2003; Jay, 2009; Müller et al., 2011; Ray, 2006; Talke et al., 2018; Talke & Jay, 2017; Woodworth, 2010). Remarkably, the rates of tidal level changes observed are of similar magnitudes to the rate of mean sea level (MSL) rise at some sites; for example, Mawdsley et al. (2015) found increases in tidal range at Astoria (USA), Wilmington (USA), Delfzijl (the Netherlands), Cuxhaven (Germany), and Calais (France) of >25 cm over the last century. Furthermore, a number of modeling studies at local (e.g., Chernetsky et al., 2010; Familkhalili & Talke, 2016; Holleman & Stacey, 2014; Lee et al., 2017; Orton et al., 2015), regional (e.g., Arns et al., 2015, 2017; Devlin et al., 2018; Greenberg et al., 2012; Idier et al., 2017; Luz Clara et al., 2015; Pickering et al., 2012; Pelling, Green, et al., 2013; Pelling, Uehara, et al., 2013; Ross et al., 2017; Ward et al., 2012), and global scales (e.g., Müller et al., 2011; Pickering, 2014; Pickering et al., 2017; Schindelegger et al., 2018; Wilmes et al., 2017) confirm that altered conditions (e.g., MSL, bathymetry, or stratification) affect tide levels and currents. Moving forward, these studies suggest that further changes to tidal levels and currents due to nonastronomical causes are possible over the 21st century and beyond.

Despite these recent advances, important gaps remain in our ability to interpret and predict past and future changes in tides over the century time scale (e.g., Müller et al., 2011), possibly because multiple processes and spatial scales are involved (e.g., Devlin et al., 2018). Over longer time scales, studies suggest that tides have also markedly changed in open-ocean and shelf sea regions over millennial (e.g., Gehrels et al., 1995; Hill et al., 2011; Hinton, 1995, 1996; Shennan et al., 2000) and longer time scales (e.g., Arbic et al., 2004, 2008; Arbic & Garrett, 2010; Egbert et al., 2004; Green, 2010; Griffiths & Peltier, 2008, 2009; Müller, 2007; Platzmann, 1978; Wilmes & Green, 2014; Green et al., 2017). These changes have been driven by large (>100 m) variations in MSL and basin geometry, which has altered water depths, frictional energy loss, and the resonant properties of specific basins. While these studies suggest important mechanisms, the trends over the past few centuries occurred with considerably smaller perturbations to water depth and other factors (Woodworth et al., 2010; Ray, 2006) and remain challenging to reproduce with large-scale numerical models (Müller et al., 2011). Instead, changes at multiple time and length scales may be occurring (e.g., Devlin et al., 2018), with effects that can accentuate or counteract each other. At small scale, tidal amplitudes and circulation have changed with harbor depths, many of which have been drastically altered by a factor of 2 to 4, to enable ever larger ships to enter ports (Chant et al., 2018; Familkhalili & Talke, 2016). Also, coastlines have been altered considerably by human development. Simultaneously, a combination of MSL rise, ongoing vertical land motion, and climate evolution has changed the water depth and possibly stratification of numerous shallow shelf seas over secular time scales, causing changes to tides (Ray, 2006). Consequently, several questions remain unanswered; for example,

1. Why are tides in some locations and regions particularly sensitive to changing boundary conditions and environmental factors, while tides at other locations have remained relatively stationary?
2. What are the mechanisms underlying these variations and how large are the respective contributions of basin geometry, water depth, ice extent, bottom roughness, and stratification?
3. Are changes being primarily driven by the effects of climate change, particularly MSL rise, and/or are they being caused by local anthropogenic factors such as channel deepening, harbor development, wetland reclamation, and any other activity that affects the small to large-scale geometry of coastal regions?

The aim of this paper is to review and synthesize nonastronomical changes in tides locally, regionally and globally in an attempt to answer these important questions. Particularly when combined with data archaeology and the recovery/analysis of historic tide data from the 19th century (Dangendorf et al., 2014; Haigh et al., 2009; Talke & Jay, 2013; Talke & Jay, 2017; Woodworth, 2006), the opportunity now exists to review our current understanding, analyze instrumental data, determine local, regional, and global footprints of change, and separate out local anthropogenic influences from larger spatial-scale processes (e.g., changes in climate) through a combination of statistical techniques and retrospective numerical modeling. Our primary goal is to better understand the spatial patterns of change that have been observed over the last two centuries and that are predicted in coming centuries, and their causes and implications. However, to put these "modern" changes into context, we also briefly consider changes on paleo–time scales.

We start in section 2 by reviewing the modeling and observational studies that have investigated past changes in tides on (1) paleo–time scales from deep time to the Year 1800 (section 2.1) and (2) for the instrumental period from 1800 to present (section 2.4). We then go on in section 3 to evaluate and discuss our current understanding of the range of different mechanisms causing changes in tides over varying time scales, first at a local (e.g., estuary) scale (section 3.1) and then regionally and globally (section 3.3). We follow this in section 4 with a review of the modeling studies that have predicted future changes in tides (section 4.1) and then discuss important implications of these potential changes (section 4.2). Finally, we end in section 5 with conclusions and highlight key knowledge gaps and future research challenges.

2. Past Changes in Tides

Studies of paleotides are generally model based (see, e.g., Arbic et al., 2004; Egbert et al., 2004; Green et al., 2017; Kagan & Sundermann, 1996; Uehara et al., 2006; Wilmes & Green, 2014, and references below) because of a lack of direct proxies for tides, and the proxies that do exist often lack spatial and/or temporal detail. Here, we give a brief overview of the methods that have been applied to infer past tidal conditions. Numerous studies have used cyclical sedimentary sequences, morphosedimentary data (e.g., coastline structure), salt marsh sedimentary deposits, and ecological indicators (e.g., species ranges across the intertidal zone) to classify paleoenvironments as microtidal, mesotidal, or macrotidal regimes (see Hinton, 1996, and references therein for a detailed overview of sedimentary records used for reconstruction of tidal environments). However, all rely on adequate preservation of the paleoenvironment, which is often hampered (Middleton, 1991). For example, using sublittoral sediment sequences Amos and Zaitlin (1985) and Amos et al. (1991) inferred that transitions in tidal regimes and tidal range changes had occurred throughout the deglaciation and Holocene in Chigneto Bay in the Bay of Fundy. Tidal laminations (rythmites), which are formed by varying amounts and types of sediment deposited on the flood and the ebb tide (e.g., Dalrymple, 1992), can be used to infer tidal components and longer-term variations but are highly localized in time and space and can give a range of potential tidal amplitudes (e.g., Tanavsuu-Milkeviciene & Plink-Bjorklund, 2009; Williams, 2000). Attempts have also been made to reconstruct tidal dynamics by linking sea bed sediment types from sediments cores to bed shear stress in order to infer tidal current strength (Ward et al., 2015) but were hampered by limitations of the sedimentary records. Studies reconstructing changes in stratification in paleo–shelf seas from plankton assemblages (e.g., Scourse et al., 2002; Woods et al., 2019) can provide an indication of the strength of tidal currents by tracking tidal mixing fronts but again only provide an indication of regional tidal conditions. In the late twentieth century, a number of studies highlighted the possibility of using tidally driven microgrowth patterns in bivalve shells to reconstruct paleo–tidal dynamics (e.g., Pannella, 1976)—this method has been used to infer Late Pleistocene tides in Osaka Bay (Japan) (Ohno, 1989; Tojo et al., 1999) but has not been widely applied since. Other approaches, again based on cyclicity in sediments, constrain global dissipation rates through the lunar effects on Milankovitch cycle (e.g., Waltham, 2015), but this can introduce large errors in the recession rate if care is not taken. For example, Zeeden et al. (2014) concluded that the globally integrated dissipation rate 11 Ma must have been either within 10% or half of the present rate (the latter is the most likely one; Green et al., 2017). To date, however, no single method has been applied over a geographically wide range and proved to be a reliable method for reconstructing paleotides.

2.1. Paleotidal Changes

Global MSL has generally been much higher than today over the past 500 Myr because of an absence of ice sheets, greenhouse climates, and younger (and hence lighter) tectonic plates (e.g., Hallam, 1984). The exception is the late Triassic (~200 Ma), when sea level was at a low-stand 50 m below present day (Haq, 2018). Over the past 2 Myr, however, MSL has fluctuated rapidly (in geological terms) by up to 130 m between glaciations and interglacial warm periods (e.g., Peltier, 2004). The present-day North Atlantic tides are large because the basin is near resonant (e.g., Arbic et al., 2004, 2008, 2009; Arbic & Garrett, 2010; Egbert et al., 2004; Green, 2010; Griffiths & Peltier, 2008, 2009; Müller, 2007; Platzman, 1978; Platzman et al., 1981)—see section 3.3 for further details. Consequently, it can be argued that on shorter geological time scales, up to 2 Myr, changes in tides were mainly due to changes in MSL and ocean stratification (Egbert et al., 2004; Schmittner et al., 2015; Müller, 2012 gives a nice description of how changes in stratification in coastal areas can change tides), because continental drift is a very slow process (the average drift speed at present is ~5–6

cm/year; e.g., Müller et al., 2008). Further back in time, however, MSL becomes a second-order effect, because large-scale tectonic changes affected basin size, and hence the resonant properties, more than a high stand in MSL did (see Green & Huber, 2013, for simulations of the sensitivity of present-day tides to large-scale changes in bathymetry and MSL). Further back in time, beyond ~250 Ma, both tectonics and changes in the Earth's rotation rate control the resonant properties of the tide and need to be explicitly accounted for in numerical model experiments (e.g., Green et al., 2019; Kagan, 1997; Webb, 1982).

2.2. Deep-Time Tides

An early attempt to simulate the tidal evolution over the past 570 Myr was done by Kagan and Sundermann (1996), but at a resolution we today know is too coarse to accurately simulate basic tidal processes (Egbert et al., 2004). Their study also excluded tidal conversion, that is, the transfer of energy from the barotropic to the baroclinic tide, which is a crucial dissipation process in the global ocean (e.g., Egbert & Ray, 2001; Green & Nycander, 2013). Due to recent advances in tectonic modeling, and hence in the accuracy and resolution of the reconstructions (e.g., Matthews et al., 2016), Green and Huber (2013) and Green et al. (2017) revisited the subject and performed the first deep-time simulations with improved accuracy. Going back to the Permian-Triassic boundary, 252 Myr BP, and then simulating a further five slices (118, 55, 25, and 2 Myr), it was shown that tides are currently very large, and for most of the past 252-Myr tidal dissipation rates have been less than half of the present rates. This makes sense dynamically: There is no reason to have large tides during a supercontinental gathering, because basins are too large to be resonant. Also, sensitivity simulations in Green et al. (2017) indicated that with higher MSL, the tides became even less energetic, something Wilmes et al. (2017) also note.

From 2 Myr onward, on the other hand, MSL changes dominate long-term changes in the tides. The continental configuration over this period is virtually the same as today, at least at the resolution used in many paleotidal simulations (typically (1/4)°–(1/8)°, plates have moved ~100 km over the past 2 Myr). The tides at 2 Myr BP were still smaller than at present, however, because MSL was some 25 m higher than today (Green et al., 2017). This is an interesting result, because we would then expect the tides in the future to be smaller than today if MSL keeps rising. It also indicates that interglacial periods over the past 2 Myr may have had reduced tides, because they are associated with high MSL.

2.3. Tides During the Last Glacial Maximum, Deglaciation, and Holocene

During the Last Glacial Maximum (26.5–19 kyr BP; henceforth LGM; Clark et al., 2009; Peltier et al., 2015) large parts of the Northern Hemisphere land masses were covered by extensive ice sheets which lowered global MSL by 120–130 m, which led to the exposure of most continental shelves. The MSL decrease and associated ocean basin shape change is thought to have shifted tidal dissipation from the shelf seas into the open ocean, thus profoundly altering the tides during this period. At the present, the largest tidal amplitudes are found in the shallow continental shelf seas, and analysis of satellite-constrained tide models has shown that out of a global total of 3.5 TW tidal energy dissipation, 1 TW (30%) of energy is lost to the internal tide in the abyssal ocean (Egbert & Ray, 2001; Munk & Wunsch, 1998; Nycander, 2005). Modeling of the global LGM tides (Arbic et al., 2004; Arbic et al., 2008; Egbert et al., 2004; Green, 2010; Griffiths & Peltier, 2008, 2009; Thomas & Sündermann, 1999; Uehara et al., 2006; Wilmes & Green, 2014) suggests that the principal semidiurnal M_2 tide was especially sensitive to the LGM bathymetry changes. In the North Atlantic, M_2 amplitudes increased by several meters and reached amplitudes of over 6 m in some areas in the Labrador Sea (see Figures 1a and 1b). Increases can also be seen for the South Atlantic, the Gulf of,Mexico and New Zealand. For K_1, the open-ocean amplitudes show little change but certain regions experience larger diurnal tides such as the margins of Antarctica, the South China Sea, and Sea of Okhotsk (Griffiths & Peltier, 2008, 2009; Wilmes & Green, 2014). These estimates are somewhat sensitive to the abyssal stratification adopted (Arbic et al., 2008; Egbert et al., 2004; Griffiths & Peltier, 2009), the sea level model used (Arbic et al., 2008) and, relating to the latter, local ice sheet extent. For example, the margins of the Antarctic Basin and in the Weddell and Ross Sea may have experienced megatides during the LGM. However, their amplitude is strongly sensitive to ice sheet extent and grounding line location (Griffiths & Peltier, 2008, 2009) with local ice extent changes showing basin-wide tide effects (Rosier et al., 2014; Wilmes & Green, 2014). Globally integrated dissipation for M_2 increased by around 1.5 TW to around 4 TW and energy losses in the abyssal ocean increased by a factor of 2–3 to 1.5–3 TW (Egbert et al., 2004; Green, 2010; Griffiths & Peltier, 2009;

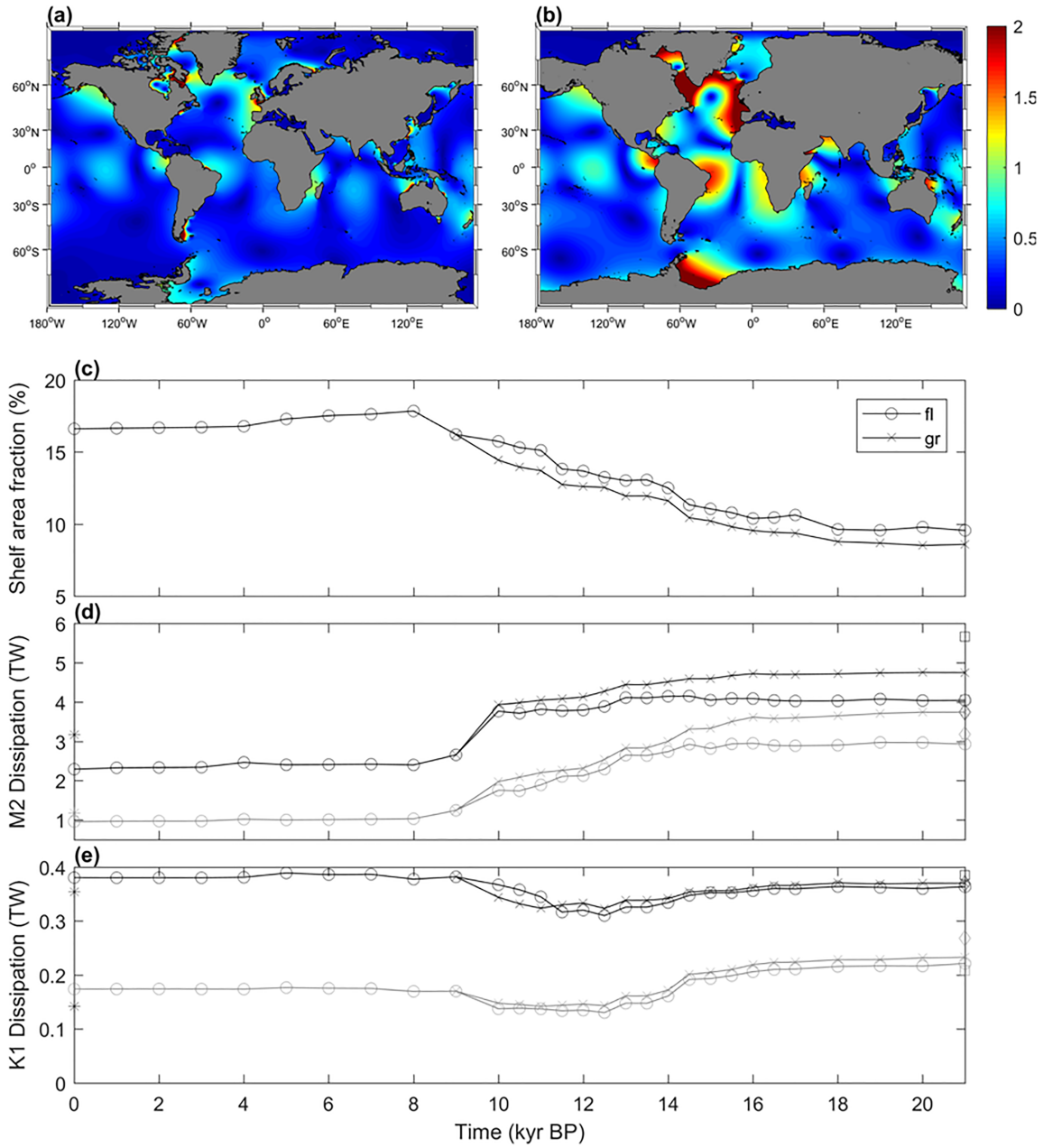

Figure 1. M_2 tidal amplitudes for (a) present-day and (b) LGM (21 kyr BP). (c) Shelf area fraction throughout the deglacial period allowing for grounded ("gr," crosses) and floating Antarctic ice shelves ("fl," circles). (d) M_2 tidal dissipation throughout the deglacial. Black lines denote total dissipation, gray lines deep (water depth >500 m) dissipation. For 21 kyr BP the squares (diamonds) denote sensitivity experiments with stronger (weaker) stratification and for 0 kyr BP the stars show the effect of a more extensive Antarctic Ice Sheet at present. Adapted from Wilmes and Green (2014, Figures 2, 4, and 7).

Wilmes & Green, 2014). The increases in amplitudes and dissipation during the LGM can be explained with the help of a damped harmonic oscillator model (Egbert et al., 2004), as discussed in section 3.3.3.

At the onset of the deglacial period (19–16 kyr BP) MSL increased by ~5 m/kyr (Peltier et al., 2015), and corresponding shelf area changes were initially small (see Figure 1c). As a consequence, amplitude changes were restricted to the edges of the European shelf, so that open-ocean dissipation remained high and close to LGM values (Figure 1d; Egbert et al., 2004; Uehara et al., 2006; Wilmes & Green, 2014). Between 16- and 8-kyr global MSL increased at rates of up to 15 m/kyr (Stanford et al., 2011), leading to the flooding of all major shelf seas. As an example, tides in the southern North Sea shifted from mesotidal to macrotidal between 8,000 and

6,000 years ago, as the land bridge to England was flooded and the system approached resonance (van der Molen & de Swart, 2001). Large tidal amplitudes can be seen on the emerging European Shelf and Patagonian Shelf, while open Atlantic Ocean amplitudes remained enhanced during the middeglaciation period. M_2 dissipation began to shift from the open ocean into the shelf seas (Egbert et al., 2004; Uehara et al., 2006; Wilmes & Green, 2014). Large drops in open-ocean amplitudes and dissipation can be seen between 10 and 8 kyr, corresponding with the retreat of the Laurentide Ice Sheet and opening of Hudson Bay and Strait (Wilmes & Green, 2014). For example, around this time regional deglacial enhancements in near-coastal tidal amplitudes can be seen across the European Shelf (Uehara et al., 2006; Ward et al., 2016), the northwest coast of the United States (Hill et al., 2011), and the western central Labrador Sea (Arbic et al., 2008).

Throughout the remainder of the Holocene (7 kyr to present) MSL adjustments were small and supraregional amplitudes and dissipation closely reflected the present-day state (Egbert et al., 2004; Hill et al., 2011; Uehara et al., 2006; Wilmes & Green, 2014). However, numerous studies have shown that local changes took place during the mid-Holocene across the European Shelf (Austin, 1991; Hinton, 1995, 1996; Shennan et al., 2000; Shennan & Horton, 2002), along the east coast of America (Hall et al., 2013; Hill et al., 2011; Leorri et al., 2011), in the Bay of Fundy (Gehrels et al., 1995; Scott & Greenberg, 1983) and in the China Sea (Uehara, 2001), but these are generally smaller than the changes experienced during the deglacial period and early Holocene.

2.4. The 19th, 20th, and Early 21st Century Changes

Changes in the tides over the last ~220 years have generally been studied using long tide gauge records. Only a small number of records are available with start dates during the first half of the nineteenth century; Brest (Pouvreau et al., 2006), Marseille (Wöppelmann et al., 2014), New York (Talke et al., 2014), and Boston (Talke et al., 2018) are notable examples from Europe and North America, respectively. Automatic tide gauges became more reliable and common during the second half of the nineteenth century (e.g., Talke & Jay, 2013), and such gauges were increasingly installed in many ports during the late nineteenth and early twentieth centuries. Many of the data collected before the advent and adoption of digital recorders in the 1970s to 1990s remain in analog format (see, e.g., Talke & Jay, 2013, 2017), and, as a consequence, one is often constrained to using information from approximately the last half-century to assess and interpret global trends (e.g., Mawdsley et al., 2015; Woodworth, 2010). Multiple projects are in progress to improve the historical data set (known as "data archaeology," see, e.g., Bradshaw et al., 2015; Haigh et al., 2009; Talke & Jay, 2017).

Two questions arise prior to the analysis of any long tidal record. The first is whether there have been any changes in the tide gauge location or changes in instrument type that could introduce discontinuities or spurious trends in tides at that location (see section 3.2.5 for a discussion). The second is whether there have been local changes to the hydrological regime, bathymetry, and related processes (e.g., sedimentation rates), in the vicinity of the tide gauge (see sections 3.2 to 3.2.4 for a detailed review of local mechanisms). This is a particular concern for gauges installed in rivers and estuaries, where many ports are located, or in coastal lagoons. These two concerns can be addressed by having information from as many stations as possible along the same coastline. Consistency of findings provides confidence that one is observing a genuine regional ocean process. Interpretation is more difficult along an irregular coastline with many rivers (e.g., NW Europe or SE Asia) and at isolated locations such as remote ocean islands.

Most tide gauge data from the nineteenth century comprise tabulations of heights and times of high and low waters, with the difference between monthly or annual Mean High Water and Mean Low Water being mean tidal range (MTR). Even after automatic tide gauges were introduced in the 1830s (Matthäus, 1972), tidal charts at many ports were simply used to note the highs and lows. The full digitization of the charts to provide time series of typically hourly heights throughout the tidal curve became routine later, alongside the increasing use of the harmonic analysis of tide gauge data (Cartwright, 1999; Talke & Jay, 2017). Consequently, the two types of data commonly employed in studies of changes in the tide are records of MTR or of harmonic constituents derived from the hourly time series. In areas of predominantly semidiurnal tides, MTR is approximately twice the amplitude of the M_2 constituent, although all other constituents also contribute to some extent (see appendices in Woodworth et al., 1991). Studies that have used MTR instead of harmonic constituents to explore changes in the tide include Flick et al. (2003) and Mawdsley et al. (2015).

2.5. Studies at Individual Stations

Both continuous tide gauge time series and short sets of measurements taken some years apart provide an opportunity to examine possible long-term tidal changes. For example, Cartwright (1971) used short sets of data collected in 1761 and 1969 from St. Helena in the South Atlantic, finding little change in the dominant semidiurnal tide but apparent changes in diurnal phase lag. Cartwright (1972a) performed a similar study of historical data from Brest, finding a significant decrease in semidiurnal amplitude of order 1% per century between 1771 and 1936 (see also Cartwright, 1972b). Pouvreau et al. (2006) updated that work, concluding that the amplitude of the semidiurnal tide had increased in recent years from its smallest values around 1960 and that the tide had been smaller than average prior to 1880, indicating some kind of cyclic variation. Wöppelmann et al. (2014) found little change in the small (decimetric) tide at Marseille since the 1840s, other than those which can be explained by instrumental effects (see section 3.2.5). In New York Harbor, measurements suggest that tide amplitudes decreased slightly from the 1840s to the early 1900s and increased thereafter by 5–10%, depending on location (Chant et al., 2018; Talke et al., 2014). In Boston, Talke et al. (2018) discussed, in the contexts of both local engineering changes and wider regional tidal changes, a large (~5.5%) decrease in MTR during the nineteenth century, after which it was relatively stable and even increased slightly after 1930 (see also Ray & Foster, 2016). The latter rate (19 mm per century) is somewhat less than half the rate of change in M_2 range (54 mm per century) reported for Boston by Ray (2009) over the period 1935–2005, suggesting other tidal changes (such as altered M_4 and M_6, as shown in Talke et al., 2018) are at work.

Other examples of studies of individual records include that of Plag (1985), who found increasing amplitudes of semidiurnal and diurnal tides at two stations in southern Norway, and Ray (2016), who found the amplitude of M_2 to have decreased significantly at Churchill, Hudson Bay since 1990. Santamaria-Aguilar et al. (2017) recently detected significant trends in the four major tidal constituents (M_2, S_2, K_1, O_1, and overtide M_4) at two Argentinian tide gauge locations, expressing themselves in tidal range decreases of about ~0.6 mm/year. Other examples at individual remote locations can be found in the quasi-global surveys of Woodworth (2010) and Müller et al. (2011). In most cases the changes in amplitudes, both positive and negative, are of order several percent per century and in most cases tend to be statistically significant.

For the reasons given above, it is hard to make firm conclusions from individual station records regarding the validity of the findings, let alone determine the reasons for them. To do better, it is necessary to take a wider perspective and test for tidal changes in denser networks.

2.6. Regional Studies

A number of regional investigations have been made over the past decade. One example concerns the Gulf of Maine for which changes in the tide have been suspected for many years (Doodson, 1924; Godin, 1995). Ray (2006) concluded that M_2 amplitudes had been increasing at stations in the Gulf of Maine for most of the twentieth century, at rates ranging from 43 mm per century (Boston) to 133 mm per century (Eastport). More recently, Ray and Talke (2019) showed that the secular change in Gulf of Maine tides does not extend into the nineteenth century. Greenberg et al. (2012) determined that trends in M_2 amplitude after 1982 at Portland, Eastport, and Saint John were essentially half of those observed previously due to an apparent regime shift, which was also reflected in changes in trend in MSL. This reduction was accompanied by a positive trend in tidal phase throughout the entire North Atlantic (Müller, 2011). In addition, Ray (2009) found S_2 amplitude to have reduced along the entire east coast of North America, and at Bermuda, over the period 1935–2005. These S_2 amplitude changes were enormous (order of 10% per century) and are considered as the largest and most coherent changes of ocean tides on supraregional scales.

The tides of the west coast of North America contain much larger diurnal components than on the east coast, so both species can contribute to significant changes in high and low water levels. Jay (2009) used 34 records with lengths more than 44 years, concluding that diurnal (K_1) and semidiurnal (M_2) amplitudes had increased by ~2% per century since the midtwentieth century. The Ray (2009) and Jay (2009) findings are important indicators that ocean tides are changing faster than expected. Confidence in this conclusion comes from the large number of stations along the tested coastlines, the regional coherence in the findings, and the fact that the tide gauge data in North America are among the best quality in the world.

Elsewhere, Hollebrandse (2005) and Jensen et al. (2003) reported for the Dutch and German coasts that the tidal range was nearly constant in the first half of the twentieth century, while a very strong (average) increase of 25 mm per decade emerged in the second half of the century. Likewise, increases in M_2 amplitude over recent decades have been documented at stations along the northern China coastline, and partly in the south (Feng et al., 2015). Shaw and Tsimplis (2010) detected no significant trends in tides at Mediterranean stations, although their records spanned only a couple of decades.

2.7. Quasi-Global Studies

Attempts to achieve a global understanding of tides have a long history, dating back to just after the invention of the recording tide gauge in the early 1830s. The first global survey was carried out by British authorities in June 1835 under the direction of William Whewell, with the cooperation of the United States and other powers, a total of nine countries (Reidy, 2008; Whewell, 1836). Up to 2 weeks of data were collected at 15-min intervals at some 700 stations, an astonishing logistical feat for the time given the many competing national interests. Determination of the basic properties of tides globally was the priority, and no consideration was given at that time to the idea that tides might change over the years. Further data archaeology of Whewell's 1835 tidal information, before the large-scale development of many harbors, might well prove valuable.

Comprehensive recent compilations of tide gauge data by the University of Hawaii Sea Level Center (https://uhslc.soest.hawaii.edu/) and the Global Extreme Sea Level Analysis project (Woodworth et al., 2017; https://www.gesla.org) have enabled quasi-global studies of changes in tides (Müller et al., 2011; Woodworth, 2010). These surveys confirmed results of Ray (2009) and Jay (2009) for North America and identified robust features of tidal evolution in other areas (Figure 2). Positive changes in M_2 amplitude were found in the eastern North Sea and Norway, while estimated trends appeared to be spatially more variable around the United Kingdom and the southern European Atlantic coastline. Increasing amplitudes for S_2, K_1, and O_1 were also found on eastern North Sea coasts, whereas both the diurnal and semidiurnal amplitudes have increased at most Australian locations and decreased at most northern Japanese stations. This is consistent with the results in Rasheed and Chua (2014). The signals at Pacific Ocean islands were more spatially variable, although stations in the Hawaiian Islands analyzed by both Woodworth (2010) and Müller et al. (2011) indicated increasing amplitudes. Mawdsley et al. (2015) made use of MTR data instead of harmonic constants, and came to similar conclusions regarding regional changes, for example, in the NE Pacific, German Bight, and Australasia.

This body of work has demonstrated that regionally coherent changes in the tide have occurred along particular coastlines. However, the tides have changed differently in different regions, thereby preventing overall conclusions on common forcing factors. Regressions of tidal estimates against the low-frequency components of MSL from sea level records suggest some degree of association between perturbations in water depth and the tide; see, for example, the analysis of UK MTR data (Woodworth et al., 1991) and more recent larger-scale studies (Devlin, Jay, Talke, et al., 2017; Devlin, Jay, Zaron, et al., 2017; Devlin et al., 2018; Schindelegger et al., 2018). Moreover, recent papers have attempted to include changes in phase as well as amplitude, to provide a more complete picture of the response of tides to potential forcing factors. On the other hand, Mawdsley et al. (2015) did not find such an association in a composite regression of MTR versus MSL trend estimates from a fully global in situ network, and areas of pronounced MSL rise did not exhibit unusually large tidal variations. Therefore, links between changes in tides and changes in MSL (which is discussed in detail in section 3.3.3) will only be partial at best.

Another question is whether the observed regional tidal changes are purely coastal ones or also occur across the shelf and in the neighboring deep ocean. An "open-ocean" island sites analysis such as that of Zaron and Jay (2014) for 30 gauges at Pacific island sites provides one way of addressing this question. They found that statistically significant increases in M_2 and K_1 amplitudes were occurring at 12 and 4 stations respectively, with decreases at only one and two stations, respectively. However, another conclusion was that instrumental improvements in tide gauge recording at most of the same sites could have contributed to an apparent increase in M_2 tidal amplitudes and were dominant for four sites. Even at remote island locations, harbor modifications have occurred and were dominant at two stations. This provides a further warning that the combination of historical and modern data can introduce biases in an analysis. In principle, long records of precise altimeter data could contribute to elucidating the spatial extent of changes in tides. However,

the existing coastal altimeter record is still short and substantial averaging at crossover locations will be required to arrive at noise levels at which tidal trends can be detected (Ray et al., 2011).

3. Potential Mechanisms Causing Changes

The synthesis above points to both local and regionally coherent changes in the tide over large portions of the world coastline. In this section we review the range of mechanisms that can cause these changes in tides, first at local scales (section 3.1) and then at regional/global scales (section 3.3), with most of the emphasis given to the instrumental period of the 19th, 20th, and early 21st centuries. Tidal variability induced by gravitational forces warrants a prior mention, as the astronomical tide-generating potential undergoes modulations on a multitude of time scales, from intra-annual, to interannual (the 4.4- and 8.8-year perigean and 18.6-year nodal cycles; Haigh et al., 2011) to the 21,000-year cycle in the longitude of solar perigee (Pugh & Woodworth, 2014). As an example, the recession of the Moon from the Earth must be explicitly accounted for in deep-time tidal simulations; Green et al. (2017) state the lunar distance at 252 Ma was 96% of the present, leading to an increase of the tide-generating potential of some 13%. However, secular rates of tidal potential coefficients in modern catalogues (e.g., Hartmann & Wenzel, 1995) are miniscule, typically 0.02% per century or less for leading semidiurnal constituents and somewhat larger (0.1% per century) for declinational tides (i.e., K_2 and Mf) that are affected by the current decrease of the Earth's obliquity (Cartwright & Tayler, 1971). Hence, on nongeological time scales and over the era of instrumental measurements, gravitational forcing is usually considered stationary.

3.1. Mechanisms Causing Changes on a Local Scale

Worldwide, the most dramatic recent changes in tidal properties have occurred in estuaries and tidal rivers (Talke & Jay, 2020; Winterwerp, 2013). For example, tidal ranges have more than doubled since the late nineteenth century in the upper reaches of the Hudson and Ems Rivers (Ralston et al., 2019; Schureman, 1934; Talke & Jay, 2013; Winterwerp, 2013) and the Cape Fear River at Wilmington (Familkhalili & Talke, 2016). Tidal ranges have similarly doubled for high flows (above 10,000 m^3/s) in the tidal river part of the Columbia River estuary (Jay et al., 2011). By contrast, a sharp reduction in tidal range in some Dutch estuaries has occurred, apparently due to changes in resonance associated with port development (Vellinga et al., 2014). Tidal trends are often larger at estuary stations (order 5–10% per century) than nearby coastal stations (Jay, 2009). Why are estuary and tidal rivers so sensitive to changing conditions? The scientific literature on tides suggests that changes in the following factors may cause changes in tides, or at least in the measured tides: (1) dissipation and turbulent mixing; (2) depth of channels and flats; (3) surface area, width, and convergence; (4) resonance and reflection; (5) river flow; and (6) changes in instrumentation.

Two additional factors, tectonic activity and changes in sea ice cover, may influence tides on small physical scales but are discussed in section 3.3, because their main effects are at larger scales. More comprehensive reviews of long-wave dynamics in estuaries and tidal rivers are given in Hoitink and Jay (2016) and Talke and Jay (2020).

3.2. Dissipation and Turbulent Mixing

Within estuaries and rivers, tides are affected to leading order by frictional damping, which tends to reduce tidal amplitudes, and bathymetric funneling, which tends to amplify tides (Friedrichs & Aubrey, 1994; Jay, 1991). Hence, any change to frictional resistance alters this balance. To understand how frictional damping can change, one needs to examine the turbulent mixing characteristics of the system, because turbulence extracts energy from the mean flow and is eventually dissipated by the action of viscosity (e.g., Tennekes & Lumley, 1990).

Turbulent mixing and dissipation in estuaries are typically produced by tidal and river flow over bottom roughness features such as dunes and ripples (McLean & Smith, 1979; Talke et al., 2013) but are inhibited or reduced by stratification, which responds to river flow variations and the spring-neap cycle (Geyer & MacCready, 2014; Kay & Jay, 2003). The large vertical density gradients found in estuaries, caused by salinity, water temperature, and/or sediment concentration, inhibit turbulent mixing and effectively decrease the drag on a tide wave (e.g., Geyer & Farmer, 1989; Giese & Jay, 1989; Jay, 1991). The first quantitative estuarine classification system described this balance of vertical mixing and stratification in terms of the

ratio, G/J, of dissipation (G) to buoyancy (J) (Ippen & Harleman, 1961). However, transverse (secondary) circulations caused by salinity gradients, topography, and other factors (e.g., Huijts et al., 2009; Lacy & Monismith, 2001) are also important. In addition, geometric features such as islands and channel bifurcation cause chaotic mixing (Zimmerman, 1986), by producing 2-D eddies with vertical vorticity that serve to distribute both scalars and momentum and (by necessity) are influenced by bottom friction. Particularly at the estuary mouth but also on intertidal flats, wave-current interactions greatly influence the bed stress (e.g., Talke & Stacey, 2003.

Changes to any of these small-scale (relative to the tidal wavelength) factors affect the G/J ratio and have the potential to alter tidal properties. In the Ems River, the formation of a 30- to 40-km-long blanket of fluid mud (de Jonge et al., 2014; Talke et al., 2009) reduced hydraulic roughness and inhibited turbulence (Winterwerp, 2013), thereby contributing to increased tidal range. Similarly, episodic sediment transport events linked to river floods in the Guadalquivir Estuary, Spain temporarily amplified the tidal range in the upper part of a tidal river; as fluid mud concentrations decreased, tides returned to normal (Losada et al., 2017; Wang et al., 2014). In California, shoaling and very high concentrations of coarse sediment caused by hydraulic mining eliminated tides in the landward part of the Sacramento River Delta in the late nineteenth century (Gilbert, 1917; Moftakhari et al., 2015), with tidal influence returning as the sediment pulse worked its way through the system. More recently, sediment supply has decreased sharply (Schoellhamer, 2011) and changes to the dune field in the ebb-tidal delta have been implicated as one of the reasons for increasing tide range in San Francisco Bay (Rodríguez-Padilla & Ortiz, 2017). Tides (and storm surge) are also affected by changes to wetland and intertidal fauna and biota, since the effective drag is increased by features such as oyster reefs and marsh plants (e.g., Orton et al., 2015). Other factors such as changes in sediment supply, dredging, and altered circulation patterns can alter dune fields and, therefore, bed roughness. Though field studies and analytical/numerical models support this inference, studies definitively linking altered roughness features to changed tidal properties have rarely been attempted, perhaps due to the logistical challenges of determining effective drag at a system scale.

3.2.1. Depth of Channels and Flats

Multiple analytical, field, and numerical studies have now established that depth changes can change estuary tides, primarily through the frictional term in the momentum balance (Chernetsky et al., 2010; DiLorenzo et al., 1993; Familkhalili & Talke, 2016). Over long time scales, channel deepening for shipping has shifted tidal processes in multiple estuaries (de Jonge et al., 2014; DiLorenzo et al., 1993; Jay et al., 2011) and is a primary factor for the long-term changes to estuary tides. Altered depths over subtidal and intertidal regions that may occur due to MSL rise may also amplify tides by reducing friction (Arns et al., 2017; Holleman & Stacey, 2014). The G/J measure mentioned above can be rephrased as U^3H^{-1}, where U is current speed and H is water depth, and a critical depth H_C separates mixing regimes (Simpson & Hunter, 1974). In systems near the critical depth, spring-neap transitions in mixing occur, affecting the spatial distribution of the S_2/M_2 amplitude ratio (Aretxabaleta et al., 2017; Kay & Jay, 2003).

3.2.2. Surface Area, Width, and Convergence

The convergence of an estuary (the rate at which cross-sectional area decreases) influences tides, with amplitudes increasing as the wave propagates into a narrower cross section. Theoretical analyses of estuarine long-wave propagation (Friedrichs & Aubrey, 1994; Godin & Gutierrez, 1986; Jay, 1991; Prandle & Rahman, 1980) suggest the depth dependence is caused by depth averaged friction, which scales inversely with depth. More detailed analysis suggests a number of nonlinear feedbacks as depth increases, including alterations in velocity, which tends to increase friction and limit the effect of convergence (which also is a function of depth). Green's law (Green, 1837) provides a simple summary of convergence effects in tidal channels. In a frictionless channel, tidal amplitudes scale as $b^{-1/2}H^{-1/4}$ (b is the channel width). For a system with a channel and flats, both the width of the channel and flat influence the tidal amplitude, such that amplitudes scale as $b^{-1/4}b_T^{-1/4}H^{-1/4}$, where b_T is the total width at mean water level. Strong convergence of width (or depth) modifies the H dependence, and frictional effects dominate if the channel is rough enough (Jay, 1991). More details are found in the review of Talke and Jay (2020).

Only a few studies have investigated the influence of changing width of channels and flats on tides from data or models. Holleman and Stacey (2014) found that allowing the tide wave to flood over current boundaries in South San Francisco Bay reduced some of the modeled amplification in the tide wave caused by MSL rise. On the other hand, Familkhalili and Talke (2016) found that an overall decrease in width contributed to

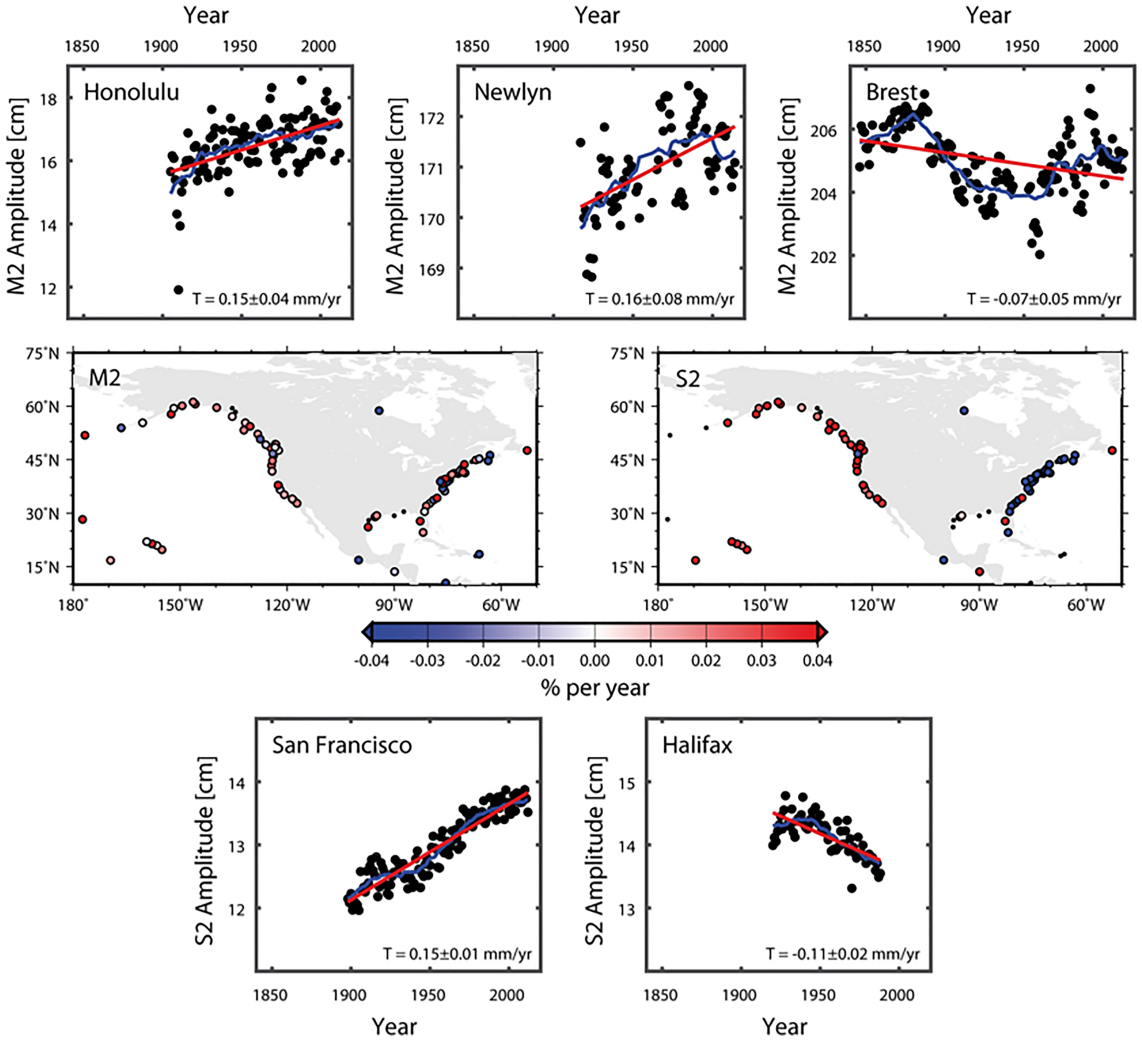

Figure 2. Maps showing percentage changes in M_2 and S_2 tidal constituent amplitudes (middle row) from tide gauge records, with M_2 amplitude time series changes shown at three sites (Honolulu, USA; Newlyn, UK; and Brest, France; upper row) and S_2 amplitude time series changes shown at two sites (San Franciosi, USA, and Halifax, Canada; lower row). Note that linear trends are shown in red and 19-year moving averages in blue.

amplified tides in the Cape Fear Estuary. Adding "retention basins" to a tide model (effectively a momentum sink) generally causes a reduction in tide amplitudes (Li et al., 2016). By contrast, an increase in tidal high water (and thus tide range) appears to have been caused by massive flooding of the Dollard subbasin in the Middle Ages, followed by a decrease when about two thirds of the Dollard was reclaimed and surface area decreased (Freund & Streif, 2000; Talke & de Swart, 2006). This suggests that the balance of channel convergence and friction can be modified by resonance and reflection, especially in short estuaries.

3.2.3. Resonance and Reflection

The reflection of a tide wave at a river boundary, and the partial reflection that occurs due to abrupt changes in width and depth, tends to cause local amplification in tides (Chernetsky et al., 2010; Jay, 1991). Estuaries that are about a quarter of a wavelength long are particularly susceptible to amplification. The usual quarter wave argument is simplistic, however, in that it neglects friction. In the absence of friction, resonance is infinitely sharp, and even a very small deviation of the actual length from the quarter wavelength criterion would essentially eliminate resonance. Thus, friction plays a dual role (Dronkers, 1964). On the one hand, some friction is needed to broaden the resonant peak (in terms of estuary length) such that resonance can actually occur. On the other, very strong friction will eliminate resonance because of the rapid damping of the tide toward the head of the estuary. In practice, strongly resonant systems almost always exhibit a convergent geometry (which increases tidal amplitude by funneling of the wave energy) and are deep enough

that tidal currents are not too strong. Two criteria are usually cited in identifying resonance: (a) an increase in tidal amplitude toward the head of an estuary and (b) a 90° phase difference between elevation and current. However, these criteria also describe the behavior of a single incident wave in a strongly and uniformly convergent channel with weak to moderate friction. Moreover, Godin (1993) showed that the actual criteria for resonance is rather more complex than the quarter wave rule, due to interaction of the tide in the estuary with the rest of the ocean. The system is not truly resonant unless there is an amphidrome within the system.

Leaving aside these dynamical complexities, changes to either length or depth of an estuary can alter tidal amplification. As discussed in Talke and Jay (2020), the largest changes occur in systems that were highly damped historically but have been significantly deepened. For example, construction of a weir in 1900 altered the length of the Ems estuary and produced an amplification in upriver tides (Chernetsky et al., 2010; Keller, 1901; Talke & Jay, 2013). Progressive deepening has further moved the system toward resonance (de Jonge et al., 2014). In the Columbia River, a bathymetric constriction caused locally amplified tides (Giese & Jay, 1989) and may contribute to the secular increase in tides at Astoria (OR). Similarly, a partial reflection was noted by Familkhalili and Talke (2016) at the end of the shipping channel in the Cape Fear estuary. Tides in the resonant Long Island Sound have amplified over secular time scales, likely due to MSL rise (Kemp et al., 2017). Tides in the Guadalquivir estuary in Spain are also affected by reflection (Dıez-Minguito et al., 2012).

3.2.4. River Flow

River flow interacts nonlinearly with tides and increases the effective frictional damping (Godin, 1986, 1991, 1999; Jay, 1991) particularly in tidal rivers, where river flow is typically strong (Hoitink & Jay, 2016). The interaction is quantitative, in the sense that it can be used to estimate river flow from tidal records (Cai et al., 2014; Moftakahri et al., 2013, 2016). Over long time scales, alteration in river flow can produce a secular trend in tides, particularly in upstream locations far from the coast. In both San Francisco Bay (Moftakahri et al., 2013; Rodríguez-Padilla & Ortiz, 2017) and the Columbia River estuary (Jay et al., 2011; Naik & Jay, 2011), long-term decreases in river inflow are a factor contributing to growth in the M_2 tide. It is important to distinguish, however, between changes in tidal amplitude related to changing river flow and changes in tidal amplitude for a given (fixed) river flow. In fact, both have occurred in the Columbia, due to an increase in hydraulic efficiency related to navigational development. The nearly linear astronomical tidal constituents are not the only components of the tide affected by river flow and changes therein. Looking landward in a river estuary, overtides typically first increase, due to frictional interactions of the main tidal constituents with each other and with river flow (e.g., Gallo & Vinzon, 2005; Godin, 1999; Guo et al., 2015; Jay & Flinchem, 1997). They then decrease, as the main tidal constituents become too small to maintain overtide generation, and frictional dissipation of the overtides increases, due to the landward increase in river flow velocity. Nonlinear fortnightly variability is typically maximal further landward in a tidal river than the overtides and may persist beyond the point where the main tidal constituents are extinguished (Buschman et al., 2009; Jay et al., 2015; Leblond, 1979), in part due to the long wavelength of this oscillation (much longer than the estuary-tidal river; Hoitink & Jay, 2016).

3.2.5. Instrumentation and Measurement Issues

The five factors considered above lead to real changes in tides at a local scale. However, water levels and tidal constituents can erroneously appear to have changed for a number of technical reasons associated with the sea level measurements (Woodworth, 2010). These include (i) an undocumented change of the tide gauge location, (ii) a change in tide gauge technology, and/or (iii) errors caused by timing problems or calibration errors. For example, recording at Liverpool on the west coast of England prior to the 1990s took place at a location 3 miles (4.83 km) south of where the current tide gauge is operated now. Although the tide is similar at the two locations, there are small differences in all tidal constituents (Lane, 2004), which could be reported as a secular change in the tide by an analyst of Liverpool data unaware of the move. A change in location can also mean that a gauge is exposed to a different wave regime, and, given that waves can bias the measurement of sea level by some types of gauge (Pugh & Woodworth, 2014), this can result in an inhomogeneous data set. Another concern is whether recording has been made by the same type of gauge (float, pressure, acoustic, and radar) as each technique has its own biases, and so a change in technology can again result in subtle changes to the data. Finally, timing errors, the symptoms of which are discussed by Zaron and Jay (2014), are often evident in sea level measurements digitized from historic tidal charts and can result in spurious changes in

calculated tidal statistics. Timing problems can be caused by clock errors or sedimentation of the stilling well (e.g., Agnew, 1986) or could occur when tidal charts were placed on the rotating drum by the operator without accurately resetting the drum offset to zero (Intergovernmental Oceanographic Commission, 1985). Before the use of digital computers for processing tide records, a tide "computer" (a person with a pencil) could only make very simple corrections for time and elevation errors in records, and reprocessing from the original paper record may allow for improvement in these corrections (e.g., Talke & Jay, 2013, 2017). The inaccurate clocks used in the first generation of "digital" gauges (those without paper records) in the 1960s to the 1980s were also subject to timing errors, which may be larger than occurred in the "marigram" period, when a paper record was used (e.g., Talke et al., 2018). The latter problem was exacerbated by the reduction in human gauge checks that accompanied the transition to digital instruments. It is therefore vital, particularly when conducting assessments of changes in tides over regional scales, that the possibility of instrument errors be considered.

3.3. Mechanisms Causing Changes on Regional/Global Scale

Spatially coherent variations observed in both tidal levels and constituents over the last century cannot be explained by the above-mentioned local mechanisms alone. Instead, at regional and global scales, the following range of possible driving mechanisms has been proposed to explain long-term secular changes in the tides (e.g., Müller, 2012; Müller et al., 2011; Woodworth, 2010): (1) tectonics and continental drift, (2) water depth, (3) shoreline position, (4) extent of (sea)ice coverage, (5) seabed roughness, (6) ocean stratification and internal tides, (7) nonlinear interactions (frictional or triad), and (8) radiational forcing.

These mechanisms are illustrated in Figure 3 and discussed below. We consider which components have contributed most to observed past changes in section 3.3.9.

3.3.1. Tectonics and Continental Drift

As discussed previously (section 2.1), it can be argued that to first order the tidal properties of a basin are set by the tectonic configuration. This is because it is the length scale of a basin, along with its depth, that determines the resonant periods, and the shape of a basin is largely set by the tectonically controlled distribution of continents and ocean. Because of the motion of the Earth's tectonic plates, it is thus expected that regions go in and out of resonance at all scales—from small inlets to ocean basins (Green et al., 2017, 2018)—depending on the tectonic configuration. Indeed, Green et al. (2018) identified a supertidal cycle that is linked to the tectonic supercontinent cycle; during a period of supercontinent aggregation, tides are very weak—close to equilibrium tides—except for isolated small inlets where local resonances can act. The reason for the overall weak tide is simply that the large horizontal scale of the ocean external to the supercontinent is out of resonance and thus not supporting a large tide. Consequently, there is no forcing in the deep ocean for large tides in local or regional basins either, although local resonances can of course still occur and lead to amplifications of up to a factor 10 (e.g., Balbus, 2014 for some theoretical considerations). As continents drift apart, basins may go in and out of resonance, thus enabling large local and regional tides. These can be generated both locally, because the basin itself is resonant (cf. the present-day Bay of Fundy), and remotely, because the regional basin is near resonant, thus allowing for a larger tidal forcing at the boundary of a region (cf. the present-day North Atlantic allowing large tides on the European shelf).

Over short time scales, earthquakes can also alter the shape and topography of coastlines, which can affect tidal dynamics, although mainly at a local scale. For example, the Christchurch earthquake in New Zealand in 2011, dramatically altered the coastline in that region (Bradley & Cubrinovski, 2011).

3.3.2. Water Depth

Changes in water depth due to geocentric (or absolute) MSL rise or geological processes such as the crust's glacial isostatic adjustment (GIA) have been explored as one of the main drivers of changes in tide at the regional/global scale (Arns et al., 2015; Flather et al., 2001; Greenberg et al., 2012; Kemp et al., 2017; Müller et al., 2011; Pickering et al., 2017; Ross et al., 2017; Schindelegger et al., 2018). Tides behave as shallow-water waves and thus are strongly affected by water depth. There are two mechanisms by which water depth changes can alter tidal dynamics.

The first mechanism is that of resonance: Large tidal amplitudes and dissipation occur when the tidal forcing frequency lies close to the natural period of an ocean basin. Therefore, increases in water depth could push an ocean basin, shelf sea, or embayment closer to resonance, increasing the tidal range, or it may be moved away from resonance, reducing the tidal range (e.g., Green, 2010; Idier et al., 2017; Kemp et al., 2017;

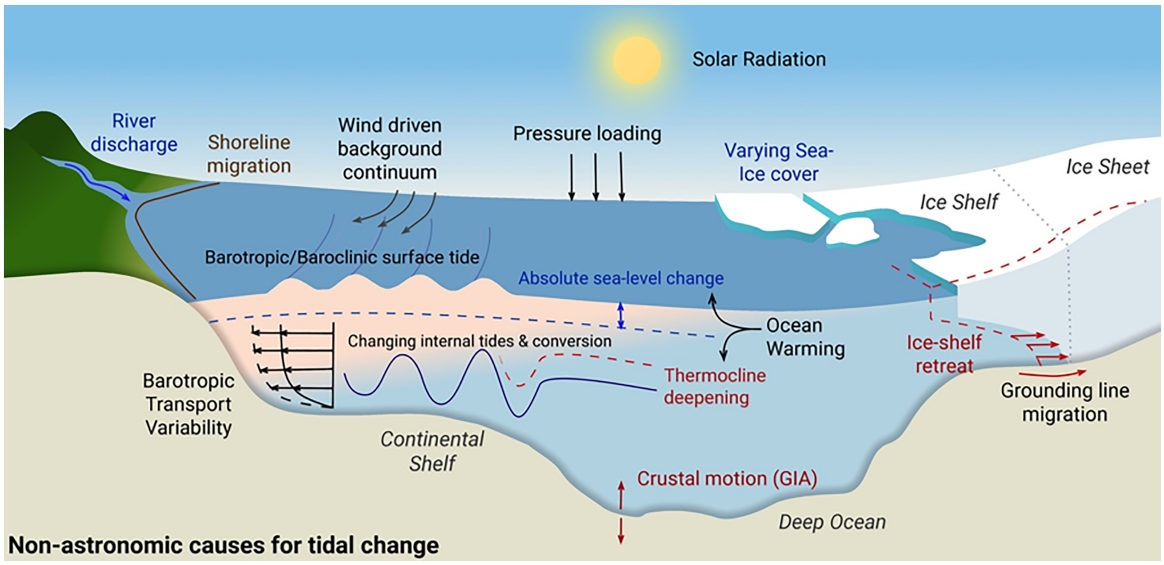

Figure 3. Illustration of the range of possible driving mechanisms have been proposed to explain long-term secular changes in the tides on regional/global scale. The image was created by Alexander Harker and Michael Schindelegger, IGG, University of Bonn.

Pickering et al., 2012). Several studies (summarized in section 2.1) have conclusively demonstrated significant deviations from present-day tides in the recent geological past, and it has been suggested that these are caused by resonance-related changes due to large relative MSL variations. For instance, Egbert et al. (2004) explained the increases in amplitudes and dissipation during the LGM with the help of a damped harmonic oscillator model. The open-ocean North Atlantic displays resonant behavior at M_2 frequency (Platzman et al., 1981; Müller, 2008); however, at present most energy dissipates in the shallow shelf seas due to bottom friction. During the LGM, most shelf seas lay dry or were occupied by ice sheets, leading to a significantly decreased damping effect. Therefore, tidal energy dissipation shifted from the shelf seas to the abyssal ocean and open-ocean amplitudes and dissipation strongly increased. The larger tides during the glacial period are thought to have increased the amount of energy available for mixing through the internal tide (Green et al., 2009; Montenegro et al., 2007; Schmittner et al., 2015; Wunsch, 2003); however, the consequences of increased tides for the LGM meridional overturning circulation (MOC) remain debated (Green et al., 2009; Montenegro et al., 2007; Schmittner et al., 2015). Furthermore, the hypothesis has been put forth that the megatides in the Labrador Sea during the last glacial period may have had decreased Laurentide Ice Sheet stability and possibly contributed to periodic ice stream instabilities (Arbic et al., 2004, 2008). Arbic et al. (2009) and Arbic and Garrett (2010) built upon the Egbert et al. (2004) damped oscillator model by constructing models of two coupled damped oscillators—one (Arbic et al., 2009) using idealized shallow-water basins and the other (Arbic & Garrett, 2010) used an even more idealized system consisting of a large mass (the open-ocean) connected via a spring to a smaller mass (the shelf). In both of these models, if the open-ocean and shelf are near resonance, the removal of the shelf yields a large increase in the amplitude of the open-ocean tide, in qualitative consistency with what is seen in numerical simulations of LGM versus present-day tides. While the damped oscillator model has been used more often to describe how tides changed in ocean basins with large MSL variations (>100 m), it has also been used to show that ~1% changes in amplitude and ~1° changes in phase can arise from ~1-m changes in sea level (Müller et al., 2011). The open-ocean/shelf coupling described above is summarized in Figure 4. This displays the coupled oscillator model of Arbic and Garrett (2010), the results of a frequency sweep of the coupled oscillator model, demonstrating that the open-ocean tide can be greatly affected if the shelf is removed, and results illustrating that blocking the Hudson Strait in a global numerical ocean tide model yields substantial changes in the open-ocean tide, in qualitative consistency with the analytical coupled oscillator model results.

The second mechanism is that a change in water depth alters the propagation speed of the tidal wave and causes a spatial reorganization amphidromes (Figure 5). In a semienclosed basin, MSL rise and thus increasing water depth causes the amphidromic point to shift toward the open boundary, leading to an increase in tidal range at the dissipative end of the basin (Taylor, 1922). The change in depth and tide range within the

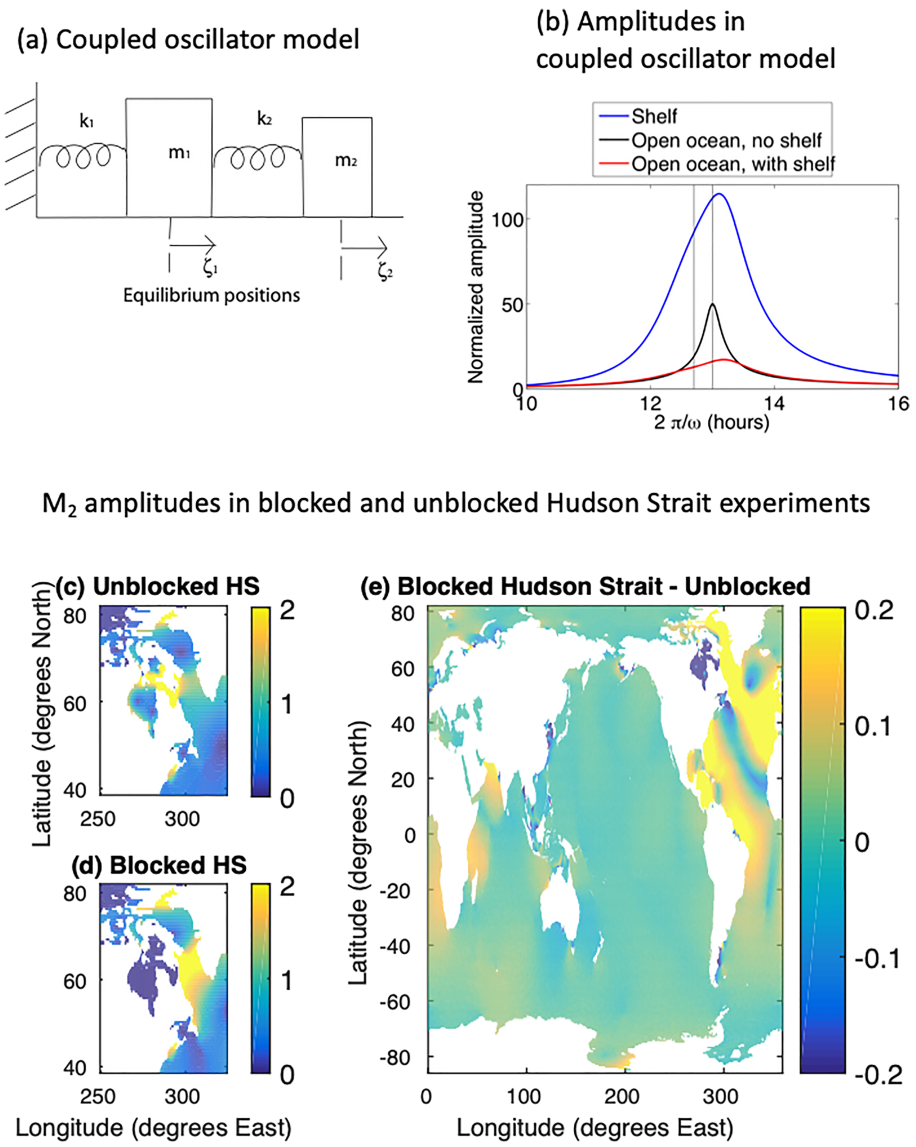

Figure 4. (a) Model of open-ocean tide (m_1) coupled to shelf tide (m_2); see Arbic and Garrett (2010) for details. (b) Normalized amplitudes in frequency sweep of the coupled oscillator model, for the open ocean without a shelf, the open ocean with a shelf included, and the shelf in the latter case. Extra vertical lines indicate the assumed resonant periods of the ocean and shelf (13 and 12.7 hr, respectively). Adapted from Figure 5 of Arbic and Garrett (2010), with a value of 0.14 for the δ_2 parameter described in that paper. (c) and (d) Amplitude (m) of M_2 elevations in simulations with unblocked and blocked Hudson Strait, respectively. (e) Difference between amplitudes in blocked and unblocked simulations. (c)–(e) are adapted from Figure 15 of Arbic et al. (2009).

amphidrome alters the spatial distribution of tidal currents and therefore the spatial pattern of energy dissipation, which is dependent on U^3/H (Garrett et al., 1978; Simpson & Hunter, 1974); where U is velocity and H is water depth. If greater tidal range at the dissipative end is associated with larger currents, the greater amount of energy lost to friction may counteract the depth effects. This in turn would shift the amphidrome to the left of the direction of propagation of the tidal wave in the Northern Hemisphere. This would increase the tidal range on one side of the basin while reducing it on the other. The increase in tidal range would also decrease the proportion of tidal energy reflected by the dissipative boundary, leading to a further displacement of the amphidrome. Taylor (1922) investigated these processes using simple analytical solutions. The shifting locations of all amphidromic points on the European Shelf with MSL rise and the associated increases or decreases in the M_2 tide are mapped in Figure 4 of Pickering et al. (2012). Idier et al. (2017) found that MSL rise leads to a small shift of the degenerate amphidromic point in the western direction (i.e., in the open-ocean direction) in the English Channel, while an overall increase of tidal range emerges in the east.

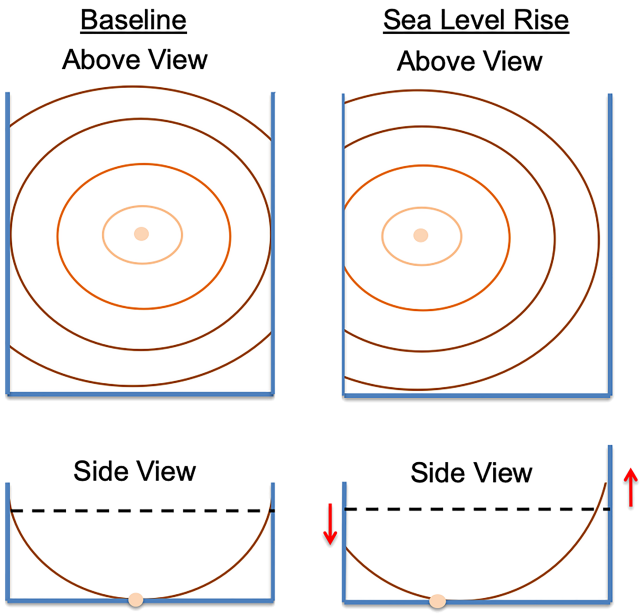

Figure 5. Illustration of how a shift in an amphidromic point induced by mean sea level rise could alter tidal range.

3.3.3. Shoreline Position

Another factor influencing tide changes is the shoreline position or the horizontal extension and surface area of the water body. Such changes imply variations in the dissipation and modifications of the natural period of oscillation of the basin. These changes can be related to water depth changes (section 3.3.2), extent of ice cover (section 3.3.4), and also shoreline dynamics (retreat, accretion) or changes in coastal defense structures. The effect of the shoreline dynamics on tide changes at a regional or global scale has not yet been investigated, except for studies of paleotides when the continents and/or ice sheets were organized differently (see section 2.1).

Coastal defense structures and flood defenses influence not only the MSL rise itself but also the landward spread of the tide and potentially the tide at the regional scale and global scale (Pelling, Green, et al., 2013; Pelling, Uehara, et al., 2013; Pelling & Green, 2014; Pickering, 2014; Pickering et al., 2017). Increasing the landward propagation of a tide wave implies an increase in the dissipation and modifications of the natural period of oscillation of the basin. For example, using a numerical experiment approach, Pelling et al. (2013) show that the tide response (to MSL rise) of the Irish Sea is controlled by the flooding of estuaries, increasing open-water tidal amplitudes through the increased dissipation in the newly flooded areas, as explained by the damped harmonic oscillator (Arbic et al., 2009). Similarly, Pelling, Green, et al. (2013), Pelling, Uehara, et al. (2013) show that the changes in the North Sea are dominated by the flooding of the Dutch coast (assuming present-day defenses are not maintained), which shifts the areas of tidal energy dissipation from the present coastline to the new flooded areas and thus moves the amphidromic points toward the coast. The same happens at the global scale (see section 4.1), where the changes in tide caused by inundation of land in tidal simulations with large-scale MSL are of the same order of magnitude as the tide changes induced by the water depth increase alone (Pickering, 2014; Pickering et al., 2017).

3.3.4. Extent of Sea Ice Cover

The interaction between sea ice and surface tidal currents can induce tidal variability, which has been, so far, mainly observed on seasonal time scales. This interactive process is described by the insulation of the ocean surface from wind forcing and the frictional effect between ocean surface currents and sea ice (Prinsenberg, 1988; St-Laurent et al., 2008). Müller et al. (2014) showed, using a coupled ocean circulation, tide, and sea ice model, and a comparison with observations, that sea ice is an important driver of seasonal variation of high-latitude tides. In the Hudson Bay and Hudson Strait, where seasonal variations in tidal amplitude can be up to 0.1 m, the amount of energy dissipated by underice friction is 21 GW, or about 10% of the bottom drag dissipation in the region.

In addition, varying sea ice cover in polar regions can drive tide changes through several of the above factors, for example, water depth (section 3.3.2) and shoreline position (section 3.3.3). Godin and Barber (1980) and Godin (1986) observed some correlation locally between tide changes and ice cover. The numerical experiment of Georgas (2011) shows that the winter ice field (and the associated friction) is an explanation for sudden tide changes in the Hudson River, both at the ice front and further afield (where reflection from the ice front may be important).

Apart from sea ice cover, ocean tide properties may also respond to variations in the geometric configuration of marine ice sheet margins, particularly the extensive ice shelves surrounding the Antarctic ice sheet. Specifically, if an ice shelf is perturbed in such a way as to alter its areal extent, thickness, and grounding line, this would affect the tide by changing local water column thickness and the position of lateral boundaries. Using a regional barotropic tide model for the Filchner-Ronne Ice Shelf and the southern Weddell Sea, Padman et al. (2018) showed that tidal currents near the Ronne ice front will decrease substantially if the ice shelf thins, with an approximate slowdown of 0.1 m/s for a hypothetical 100 m loss of vertical ice extent. In a range of sensitivity experiments, Rosier et al. (2014) modeled perturbations of tidal amplitude in an ocean domain south of 60°S for several scenarios of ice sheet evolution, including projected shifts in grounding

line up to the Year 2500 as constrained by external ice sheet models. K_1 amplitudes were found to respond to this ice shelf retreat with increases of a few decimeters in both the Ross and Weddell Seas, whereas M_2 mainly changed under the Filcher-Ronne Ice Shelf as a result of ice thickness reduction. Both Rosier et al. (2014) and Padman et al. (2018) highlight the role of tides and their variations in modulating the low-frequency dynamics of ice sheets, for example, through feedbacks on basal melt rates and ice stream velocities. However, the effect of actual (and not projected) changes of Antarctic cavity geometry on tides themselves, especially on global scales, remains unexplored.

3.3.5. Seabed Roughness

The character of the sea bed can be changed over time by many natural (e.g., including waves and tidal currents; Idier & Astruc, 2003) and human processes (e.g., trawling; Aldridge et al., 2015). Beam trawling, in particular, the process by which heavy chains and a large net attached to a beam are dragged across the sea bed, has been reported to lead to flattening of the bottom, causing a reduction in bottom friction (e.g., Schwinghamer et al., 1996). It has been suggested that changes in seabed roughness could therefore induce changes in tides. Further research in this area is therefore needed.

3.3.6. Ocean Stratification and Internal Tides

Changes in ocean stratification can have multiple effects on tidal dynamics. First, they can change the tidal conversion rate, that is, the transfer of energy from barotropic to baroclinic tides, as well as the surface expression of the internal tide. The effect on the barotropic tide through changes in the internal tide field at regional or global scales has not been well explored beyond sensitivity tests on long time scales (i.e., millennia, see Egbert et al., 2004 and Wilmes & Green, 2014). It has been shown, however, that the surface expression of internal tides can vary on seasonal time scales due to variations in the stratification and ocean currents (e.g., Müller et al., 2012). A local analysis of the tide-gauge record from Honolulu, Hawaii by Colosi and Munk (2006) attributes the recorded secular increase of the M_2 surface tide amplitude of 16.1 to 16.9 cm between 1915 and 2000 to a 28° phase change of the internal tide, induced by time-variable density stratification along the wave propagation path to the measurement site (see also Mitchum & Chiswell, 2000). Nonlinear mechanisms can also be involved. At stations around the Solomon Islands, strong connection between semidiurnal tidal anomaly trends and changes in thermocline depth, overtide generation, and the El Niño–Southern Oscillation (ENSO) have been observed. As shown by Devlin et al. (2014), this correlation could result from the changes in nonlinear triad resonance of barotropic (M_2) and internal tides (K_1 and O_1) associated with changes in stratification.

Another effect of varying stratification on tides is by means of changes in the vertical eddy viscosity profile, which is important in shallow waters. In principle, eddy viscosity can cover orders of magnitude by transitions from stable-stratified to well-mixed conditions, thereby affecting tidal current profiles. Müller et al. (2012) showed, using analytical and numerical models, that stratification changes between winter and summer can modify the tidal transport by 5% and that a deepening of the mixed-layer depth by only 10 m can induce a transport change of 1–2%, which might be relevant to understand secular trends of tides in a warming ocean. On seasonal time scales this effect has been observed in tidal current profiles (e.g., Howarth, 1998) and evoked in explanations of seasonal changes of around 6% in the M_2 surface tide in the North Sea and Yellow and East China Sea (Kang et al., 2002; Müller et al., 2014).

3.3.7. Nonlinear Interactions

Nonlinear interactions between tidal constituents and between tides and nontidal processes can lead to significant variations in tides. Regarding the former, at many locations it has been found that the 18.6-year nodal cycle variations in tidal amplitude is smaller than the 3.7% one would expect for M_2 in the tidal potential. This can be explained by the nonlinear frictional tide-tide interactions (Ku et al., 1985); for example, Ray and Foster (2016) showed that the M_2 tide in Boston (U.S. Atlantic coast) varies by 2.9% over the 18.6-year nodal cycle. Smaller variations for M_2 have also been found around the United Kingdom by Amin (1983, 1985) and Woodworth et al. (1991), around the west coast of Australia (Amin, 1993), as well as in the Bay of Fundy and Gulf of Maine (Ku et al., 1985; Müller, 2011; Ray, 2006; Ray & Talke, 2019). Feng et al. (2015) found differences from equilibrium nodal expectations for variations in both semidiurnal and diurnal tides along the coast of China. Jay et al. (2015) found that the S_2/M_2 ratio varied along an estuary-fluvial river continuum. There are two likely causes: (i) the primacy of the M_2-river flow interaction (no other constituent is as much affected by river flow as M_2) and (ii) the fact that tidal energy propagation depends on the square of tidal amplitude, while dissipation depends on its cube. A change in overtide magnitude and relative phase

can also indicate altered nonlinear interactions (e.g., Devlin et al., 2014). Thus, changes in the nonlinear tide-tide interactions at other time scales than the nodal cycle have been observed by Gräwe et al. (2014), who showed seasonal variations of the M_4/M_2 ratio in the North Sea are due to variations in the thermal structure of the water column. Given these observations, any factor that alters tide-tide interaction (such as altered bed friction) can produce a trend in one or more tidal constituents; however, extracting these (usually small) factors remains a challenging signal processing task, except when changes to nonlinear interaction are large. Moreover, closely spaced tidal constituents may respond differently to nontidal forcing.

Variations in tides caused by interactions between the tide and nontidal processes include a large spectrum of phenomena, ranging from storm events to interannual and decadal-scale variability. Examples include storm surge effects (e.g., Horsburgh & Wilson, 2007; Idier et al., 2012; Prandle & Wolf, 1978; Zhang et al., 2010), seasonal variations of mean currents and winds (e.g., Devlin, Jay, Talke, et al., 2017; Devlin et al., 2018; Müller, 2012), and climate variations such as ENSO (e.g., Devlin et al., 2014). The tide changes manifest themselves as variations in tidal constituents from year to year and can result in a long-term trend in tidal parameters if a corresponding trend exists in the nontidal forcing. Without discriminating between the sources of the sea level fluctuations, Devlin, Jay, Talke, et al. (2017), Devlin, Jay, Zaron, et al. (2017) investigated tide gauge records in the Pacific Ocean, and their results suggest that interannual tidal variability is correlated to sea level variability at most (92%) of tide gauges in the Pacific, with statistically significant rates between ±1% and ±50% of the MSL rise observed. However, the correlations of the multiple mechanisms inducing tide and sea level variability make it challenging to discern the individual causes of observed variability. For instance, Devlin et al. (2018) suggest that seasonal variability of tides in Gulf of Thailand and near Singapore could arise from monsoon-related changes in winds. Tidal current and tidal water level interact directly with wind and pressure, through the advection term in the shallow-water theory (the water depth enters in the denominator of the friction term in the shallow-water equations) and nonlinear friction term related to velocity interactions (Flather, 2001; Haigh et al., 2010a; Horsburgh & Wilson, 2007; Zhang et al., 2010). Wind-induced waves, in addition to superelevation of water, can also alter tide magnitudes during storms (e.g., Arns et al., 2017). In many cases, the dominant tide-surge interaction term comes from the friction term. Depending on the event and location, the tide-surge interaction can have a significant effect on water level at the event scale (several tens of centimeters; Idier et al., 2012). However, the long-term effect on the tidal constituents is smaller, since it would require a long-term trend in the frequency and/or magnitude of storms.

3.3.8. Radiational Forcing

The term "radiational potential" was introduced by Walter Munk to account for motions of a tidal nature, which are caused, directly or indirectly, by the Sun's radiation, instead of being of astronomical tidal origin due to the Moon or Sun (Cartwright & Tayler, 1971; Munk & Cartwright, 1966). Such radiational (or "meteorological") oscillations dominate the tides of the atmosphere, through absorption and differential heating processes, and are also important as components of the ocean tide. Relative to their astronomical counterparts, the largest radiational tides in the ocean occur due to the annual and semiannual variation in air pressure, and the ocean's subsequent response via the inverse barometer effect, and due to Sun-synchronous meteorological changes at the diurnal S_1 frequency. These meteorological forcings include diurnal variations in air pressure and also small-scale contributions from land-sea breezes (Ray & Egbert, 2004; Rosenfeld, 1988). Numerical modeling (e.g., Ray & Egbert, 2004; Schindelegger et al., 2016) shows that the radiational part of the S_1 ocean tide can have amplitudes of a few centimeters in some regions (Arabian Sea, eastern Indian Ocean, and Okhotsk Sea) and that it dominates the solar diurnal gravitational component by an approximate factor of 5 throughout the ocean. Pugh and Woodworth (2014) also point to possible spurious manifestations of S_1 in tide gauge measurements, related, for example, to the daily heating and cooling of thermally sensitive instruments.

Radiational contributions to the solar semidiurnal ocean tide S_2 are smaller than gravitational S_2 oscillations but nonetheless important. In the tropics, air pressure tends to be a maximum near 10:00 and 22:00 local time, with amplitudes that vary approximately as $125\cos^3\phi$ Pa, where ϕ is latitude (e.g., Haurwitz & Cowley, 1973). Modeling of the ocean's dynamic response to this semidiurnal pressure loading suggests that the radiational component of S_2 is about 15% of gravitational S_2 on average (Arbic, 2005). Pugh and Woodworth (2014, Section 5.5) give several determinations of this proportion at locations around the

world. The complication of S_2 having a significant radiational component, while neighboring constituents (N_2, M_2, etc.) do not, introduces difficulties in the tidal analysis using response techniques (Munk & Cartwright, 1966).

If radiational forcings vary from year to year or with a secular component, the ocean's response will change. In fact, large-scale modulations of the diurnal pressure cycle (~20 Pa) and concomitant changes in the S_1 ocean tide occur during extreme phases of ENSO (Schindelegger et al., 2017) but are restricted to time scales of less than a year. Ray (2009) summarizes reports of secular changes in the atmospheric S_2 tide, none of which points to overly large trends in available barometric records. Given the ocean's dynamic response at the S_2 frequency, secular changes seen in tide gauge data might come from pressure loading in any place, including areas of scarce meteorological observations. Hence, the relevance of radiational forcing for changes in tides remains to be confirmed by future research.

3.3.9. Attributing Past Changes

As discussed in section 2.1, on short geological time scales up to 2 Myr ago, large-scale changes in tides were mainly due to changes in water depth and to a lesser extent shoreline position and ice extent. Further back in time, however, water depth becomes a second-order effect, because large-scale tectonic changes affected basin size, and hence the resonant properties, more than water depth. Over the instrumental period of the 19th, 20th, and early 21st centuries it is much more difficult to attribute observed changes in the tide, because tide gauge measurements are affected not only by the above regional mechanisms but also by local processes (section 3.1). Overall, it has been difficult to produce unequivocal evidence of the effects of the individual local and regional mechanisms, because (i) most changes in observed tides are modestly correlated with multiple forcing factors (Devlin et al., 2014), (ii) correlation does not imply causation, and (iii) extensive modeling studies (numerical or analytical) are needed to verify any one mechanism for any location or region.

In classical tide models, effects of geocentric MSL rise and vertical land movement are explored in a comparatively simple manner through modifications of bathymetry. Müller et al. (2011) performed M_2 simulations at low ((1/2)°) and high ((1/8)°) horizontal resolution, with trend patterns from GIA models and altimetric sea levels scaled to represent water depth changes over the past 100 years. These simulations demonstrated peak sensitivities of the tide in the North Atlantic to GIA-related crustal subsidence and increases in MSL, the former accounting for 30–40% of the magnitude of measured M_2 trends on a basin-wide average. However, spatial patterns, and thus the sign of simulated M_2 changes, did not agree well with those inferred from observations. Schindelegger et al. (2018) revisited the issue with a high-resolution ((1/12)°) global tide model, in which uncertainties related to the self-attraction and loading term (the "iteration jitters" encountered by Müller et al., 2011) were greatly mitigated using an exact spectral decomposition of tidal elevations at each time step. With water depths adjusted for GIA and geocentric MSL changes, the model could reproduce the sign of the observed M_2 amplitude trends at 36 out of 45 analyzed tide gauge stations in Europe and Australia (Figure 6), and at the North Atlantic American coasts (Figure 7). Schindelegger et al. (2018) additionally reported success in capturing large fractions (order 50% or more) of the magnitude in measured M_2 changes, primarily in shallow seas dominated by frictional effects, for example, the Gulf of Mexico, the German Bight, the Northwest Australian Shelf, and the Chesapeake-Delaware Bay system; see also Ross et al. (2017) for a comparison of tide gauge data with modeling results in the latter area. Yet changes in water depth alone appear inadequate to explain some of the very large trends seen in tidal amplitude on the European Shelf (e.g., the English Channel and the Irish Sea) as well as the Gulf of Maine. In a calibration experiment, Greenberg et al. (2012) showed that an inordinate depression of ~2 m per century at the western North Atlantic shelf break would be necessary to mimic the M_2 changes observed at coastal stations in the Gulf of Maine. Hence, the twentieth century trends of the tide in that area remain a vexing signal, possibly related to a small change of the Atlantic tide at the gulf's mouth being amplified by the resonant nature of the basin (Ray, 2006).

To our knowledge, modeling studies are yet to properly address tidal impacts of past changes in ocean stratification shorter than geological time scales (i.e., several millennia). However, such efforts critically rely on quantitative knowledge of temperature and salinity, which is limited by the paucity of historical water-column measurements. For 2-D models, adjustments of buoyancy frequencies in internal tide drag parameterizations (e.g., Carless et al., 2016) can provide a rough idea of altered conversion rates and

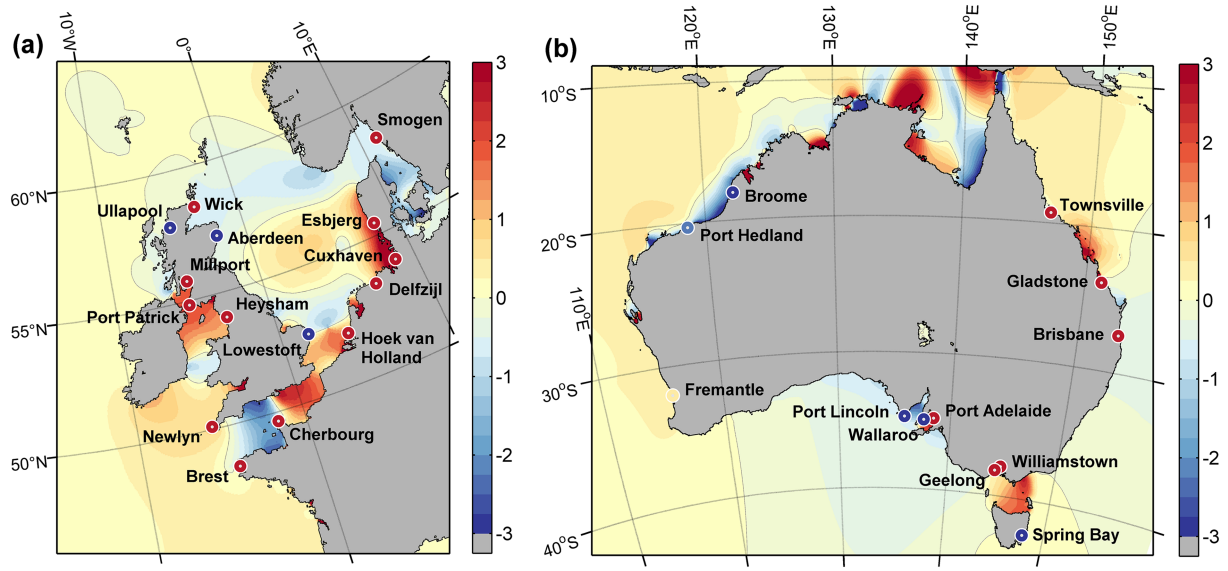

Figure 6. Modeled response of M_2 amplitudes (cm, color-filled contours) to a 0.5 m, spatially nonuniform increase in global MSL and comparisons with observations at 15 tide gauges on the European Shelf and 12 tide gauges in the coastal waters of Australia. Simulations were conducted with a quasi-global (1/20)° barotropic model and changes in water depth representing both GIA-induced crustal motion and absolute sea level trends from satellite altimetry. Colors of the tide gauge markers show measured M_2 changes in centimeters per 0.5 m of local MSL rise; see Schindelegger et al. (2018) for details.

associated modulations of the barotropic tide. Yet the wider spectrum of stratification effects on baroclinic wave propagation/generation and vertical eddy viscosity profiles must be explored in realistic 3-D simulations on both regional and global scales. Tidal changes resulting from these processes may be locally confined and patchy but of magnitudes comparable to the effects of MSL rise on tidal amplitudes (~1–2 cm per century, Colosi & Munk, 2006; Müller, 2012). Another frequently cited, although yet unproven, hypothesis is that the significant decrease of the S_2 constituent in the western North Atlantic Ocean relates to large changes in the semidiurnal atmospheric pressure tide (Ray, 2009), which might undergo modifications in a warming climate with altered stratospheric absorption characteristics (Covey et al., 2014). However, a very large (~40% per century) change in the air tide would be required to induce the observed S_2 trends, and similar amplitude decreases evidently occur in the K_2 constituent, which has only minor radiational component. Thus, as Ray (2009) suggests, attributing observed S_2 trends to atmospheric dynamics "seems premature, and may well be incorrect."

4. Future Changes in Tides and Implications

4.1. Projections of Future Changes in Tides

As Hill (2016) points out, paleo–time scales have occupied much of the attention of past modeling work on large-scale changes in tides (section 2.1), while navigational impacts over the last few centuries have been a primary focus of local modeling and data analysis (section 3.1). However, recent studies have been increasingly geared toward prediction of future changes in tides over the 21st century and beyond, motivated by concerns regarding climate change, particularly MSL rise (e.g., Holleman & Stacey, 2014) and changes in coastal flooding (see section 4.2). Climate-induced relative MSL rise will lead to increases in water depth, which will alter tidal dynamics via a range of mechanisms (section 3.3). However, studies have also assessed how tides may change in the future with large-scale land reclamation (Pelling, Green, et al., 2013) and natural and anthropogenic changes in coastal morphology (de Boer et al., 2011; Passeri et al., 2016), variations in ice sheet extent (e.g., Pickering, 2014; Rosier et al., 2014; Wilmes et al., 2017), changes in ocean warming (Carless et al., 2016), which influences tides via variations in vertical stratification (Müller, 2012) and with the introduction of tidal power stations (e.g., Ward et al., 2012).

The majority of these future tidal studies have used depth-averaged tidal models to assess changes in the main semidiurnal and/or diurnal tidal constituents and in some cases changes in tidal high and low

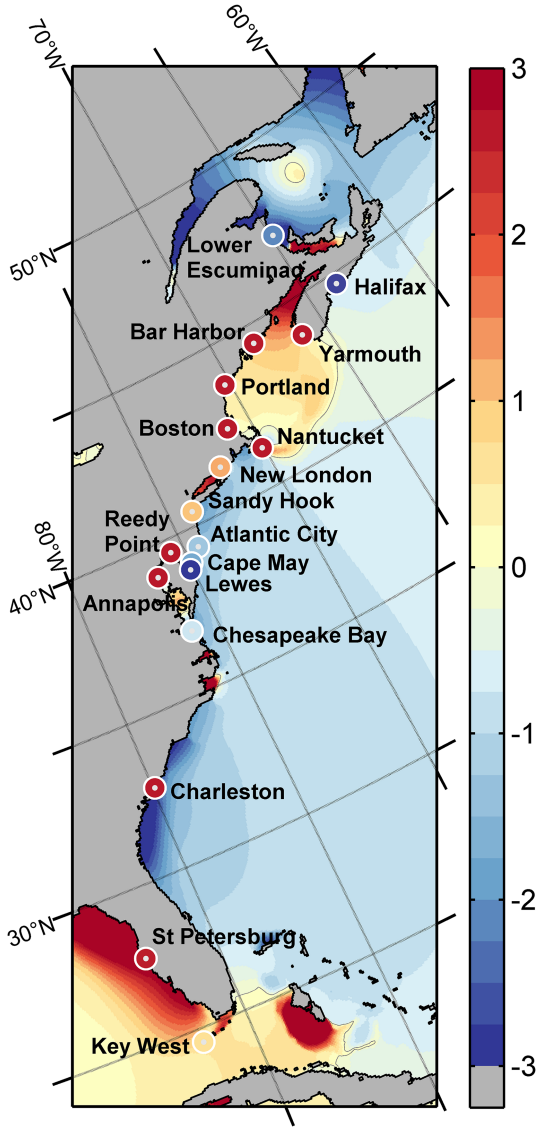

Figure 7. Modeled and observed M_2 amplitude changes (cm) as in Figure 4 but for the East Coasts of Canada and the United States, accommodating a selection of 17 tide gauges; compare Schindelegger et al. (2018).

waters, tidal range, and other parameters (e.g., tidal currents, bed shear stress, and tidal dissipation). Only in a few exceptions have baroclinic models been used (e.g., Ross et al., 2017; Valentim et al., 2013), but this has been done only on an estuary scale. The majority of modeling studies have used finite difference grids. The different studies have used a wide range of numerical software, boundary conditions, and configuration settings, with model grids of varying horizontal resolution (Hill, 2016). There has also been variability in treatment of the coastline among the investigations. Studies have considered a wide range of future projections, with MSL varying from the Intergovernmental Panel on Climate Change typical range by 2100 (i.e., up to 1 m; Church et al., 2013) to the low probability but high impact end of the scale by 2100 (~2.5 m; Lowe et al., 2009), to very high values of 10 m out to 2300 and beyond (which would require significantly ice loss from Greenland and/or Antarctic; DeConto & Pollard, 2016). Studies have also modeled future conditions in different ways, with some authors using simple spatially constant increases in water depth (equal to assumed MSL rise), while others have accounted for some assumed spatial variability in sea level change and vertical land movements (e.g., associated with GIA and other processes, such as subsidence caused by withdrawal of groundwater). These differences made it difficult to directly compare and contrast results among the analyses. Some general conclusions that can be drawn are summarized below.

We start with a review of literature that has predicted future changes in tides on the NW European Shelf, before switching to other regional and local study areas. Finally, we highlight recent papers that have predicted future changes in tides on a global scale. The different regions investigated in these studies are summarized in Figure 8.

4.1.1. Northwest European Shelf

Many studies have investigated future changes in tides on the NW European Shelf and specific areas within this domain. Results from earlier studies of the NW European Shelf tides (e.g., de Ronde, 1989; Hinton, 1996; Kauker, 1998; Flather & Williams, 2000; Flather et al., 2001; Howard et al., 2010; Kauker & Langenberg, 2000; Lowe & Gregory, 2005; Lowe et al., 2009; Plüß, 2004; Sterl et al., 2009; Vellinga et al., 2009) suggest that changes in tidal amplitudes and levels would only be a few centimeters under 0.5–2-m MSL rise. However, more dedicated explorations of future tides in this region provide evidence that changes in the M_2 amplitudes might be up to 0.1 m per meter of change in MSL. For example, Pickering et al. (2012) found significant (up to 30 cm) increases in the M_2 tidal amplitude with 2 m of MSL rise in parts of the European shelf and also areas on the shelf where the sign of the changes was reversed (up to −40 cm). Interestingly, Ward et al. (2012) obtained results with opposite signs of the amplitude changes in some regions to Pickering et al. (2012) in certain areas. Pelling, Green, et al. (2013) and Pelling and Green (2014) used numerical tidal models alongside classic tidal theory to explore why there were significant differences in the tidal changes predicted by Pickering et al. (2012) and Ward et al. (2012). They showed that the way in which MSL rise is implemented highly influences the modeled tidal response (Figure 9). When vertical walls are assumed at the present-day coastline (as in Pickering et al., 2012), predicted changes in tides due to increased water depth differ from the case where coastal areas are flooded (as Ward et al., 2012 did) and the response is largely controlled by dissipation in the newly introduced wet grid cells. Pelling and Green (2014) found that the largest changes in tides with MSL rise occurred, somewhat surprisingly, when flood defenses were accounted for (where they exist) allowing only part of the coastline (currently not protected) to flood. Idier et al. (2017) considered a greater number of tidal constituents and also nonuniform MSL rise

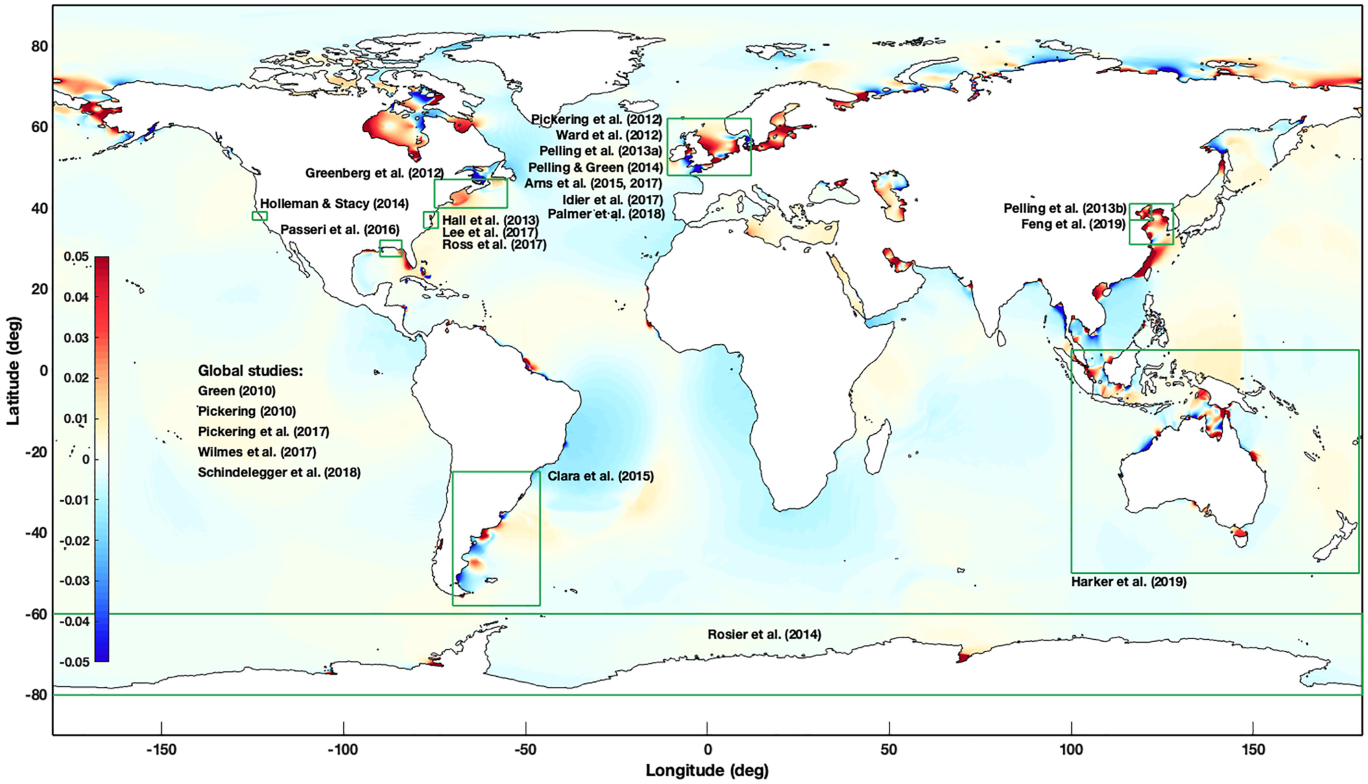

Figure 8. Approximate location of the studies that have modeled future changes in tides, overlaid on a map of changes in mean high water in meters per year from Pickering et al. (2017).

scenarios and more fully explored the physical mechanisms causing changes in tidal levels on the NW European Shelf. They found that the patterns of changes in tidal levels are spatially similar, regardless of the magnitude of MSL rise (up to 10 m), if coastal defenses are constructed along present coastlines. In this instance, the tidal changes are generally proportional to MSL change, as long as MSL rise remains smaller than 2 m. However, when flooding of dry land is allowed in the simulations the changes in tidal level are much less proportional to MSL change. Palmer et al. (2018) assess changes in tides on the NW European Shelf, with MSL rise scenarios of up to 3 m. They also found substantial changes in tidal range, and a spatially nonuniform response.

4.1.2. Other Regional and Local Analyses

Investigations of future tides have also recently been conducted in other regions, on spatial scales similar to that of the NW European Shelf. Luz Clara et al. (2015) investigated the effects of uniform 1, 2, and 10 m rises in MSL on the propagation of tides on the Patagonian Shelf. In contrast to Ward et al. (2012), Pelling, Green, et al. (2013), Pelling & Green, 2014) and Idier et al. (2017), they found that predicted changes in tidal levels were not especially sensitive to how the coastline was implemented, for the southern part of the coastline in this area. This was because the coastline south of 40°S is mostly characterized by high cliffs and due to the fact that the tide propagates northward. However, north of 40°S, where the coastline is dominated by beaches and wetlands, the response was more highly affected by added dissipation in the inundated cells. Carless et al. (2016) investigated how tides on the Patagonian Shelf might respond to various levels of nonuniform MSL change and considering different grid resolutions. They also assessed the effects of ocean warming over the area, as tides can be influenced by the strength of vertical stratification (see section 3.3.6). They predicted a decrease in tidal amplitudes along the coast as a result of a possibly more stable water column, if the surface layer heats up more than deeper waters. Rosier et al. (2014) ran hypothetical numerical simulations to assess the effect that removal or reduction in the extent and/or thickness of the Ross and Ronne-Filchner ice shelves would have on tides around Antarctica. With the removal/reduction in ice shelves changes in the M_2 amplitude of up to 50 cm in the Weddell Sea were

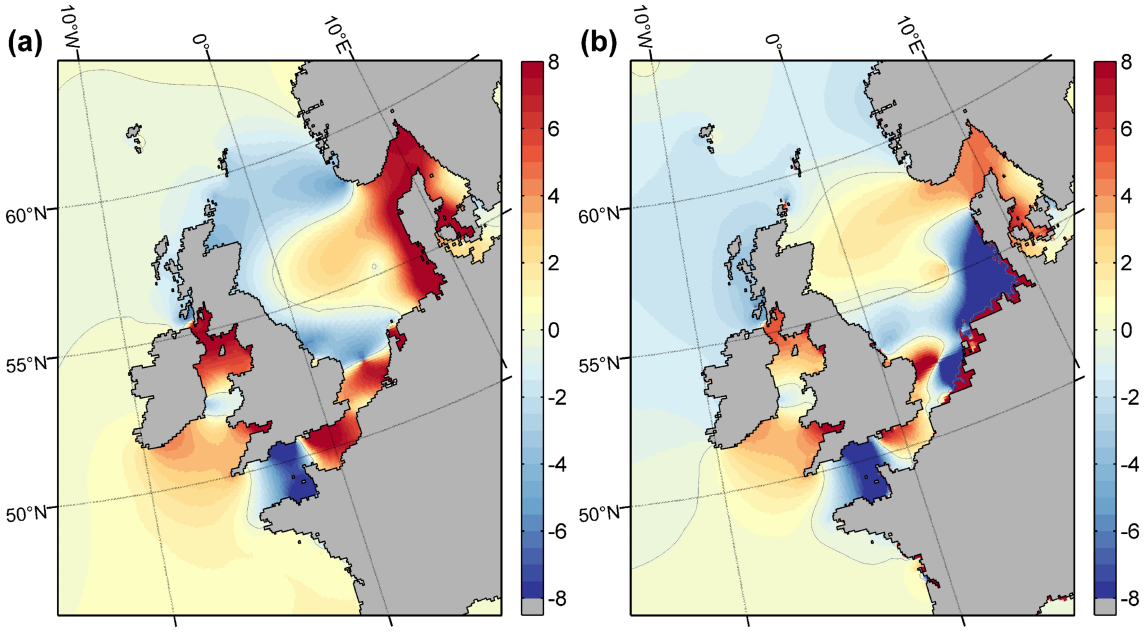

Figure 9. Modeled M_2 amplitude changes (cm) on the NW European Shelf with spatially varying water depth changes averaging 2 m, assuming: (a) invariant present-day coastlines and (b) inundation of low-lying topography. Modified from Schindelegger et al. (2018). Results were obtained from global (1/12)° tidal simulations with bathymetry adjustments constructed from altimetric sea level trends and GIA predictions.

found. These could potentially lead to tidally induced feedbacks on ice shelf/sheet dynamics which in turn would influence global MSL (as proposed in Pickering, 2014).

On the scales of large bays and estuaries, Greenberg et al. (2012) showed that the combined effects of MSL rise (partly attributed to post glacial rebound) and increasing tidal range in the Bay of Fundy could produce a significant increase in the high water levels, much greater than those seen when considering MSL rise in isolation. Pelling, Uehara, et al. (2013) investigated changes in the tidal regime in the Bohai Sea, China over the last 35 years and for the future with 1, 2, and 3 m of MSL rise. They found significant changes in the tidal regime in the Bohai Sea over the last 35 years, with M_2 amplitudes changing by up to 20 cm in some parts, due to rapid coastline changes resulting from natural developments of the Yellow River delta and large-scale anthropogenic land reclamation. In this region, their results suggested that predicted future changes in tides were sensitive to whether the coastal areas are allowed to flood, or not, in the model. They also found that changes in tidal amplitudes were not proportional to the magnitude of MSL rise. Hall et al. (2013) modeled changes in tides in the Delaware Bay (USA) for future MSL rise scenarios (~1 and 3.5 m), allowing for land inundation. They found complex spatial changes, with variations in tidal range of up to 10%. Holleman and Stacey (2014) investigated how tidal levels vary in San Francisco Bay (USA) with MSL rise of up to 1 m. They showed that tidal levels decrease in most areas, as flooding of adjacent expansive low-lying areas introduces friction. Passeri et al. (2016) assessed the integrated influence of MSL change and future morphology on tidal hydrodynamics along the northern Gulf of Mexico. Unlike previous studies, which tended to ignore changes in morphology, they updated shoreline positions and dune heights using a probabilistic model. Under the highest MSL rise scenario (2 m by 2100), tidal amplitudes within the bays along this coastline increase by up to 10 cm, because of increases in the inlet cross-sectional areas. Lee et al. (2017) and Ross et al. (2017) investigated how MSL rise and coastal change might impact tides in Chesapeake and Delaware Bays (USA). They found that when hypothetical sea walls are erected at the present coastline, tidal range increased, with greater amplification in the upper reaches of the two bays. However, when low-lying land was allowed to become inundated by MSL rise, tidal range decreased in both estuaries, similar to the global findings of Pickering et al. (2017). Harker et al. (2019) assessed how MSL rise might impact tides around the coast of Australia. They found large amplitude changes in the Arafura Sea and within embayments along Australia's northwest coast, and the generation of new amphidromic systems within the Gulf of Carpentaria and south of Papua, once water depth across the domain is increased by 3 and 7 m,

respectively. Recently, Feng et al. (2019) investigated tidal changes in the Yellow Sea. They found a notable decrease in tidal range occurs in the northern shelf, and the tide increases mainly in the southern shelf, with MSL rise.

Many other studies have predicted changes in tides with MSL change for smaller estuaries around the world (e.g., Cai et al., 2012; Valentim et al., 2013) and idealized estuaries (e.g., Du et al., 2018). The results of these are hard to generalize. Du et al. (2018) demonstrated that tidal response to MSL rise is spatially uneven and differs depending upon estuary length, bathymetry, and geometry.

4.1.3. Global-Scale Studies

Using a relatively coarse ((1/6)°) global tidal model, Green (2010) simulated changes in the M_2 and K_1 constituents with a uniform MSL rise of 5 and 60 m (akin to an almost complete melting of polar ice sheets). He found increases in tidal amplitude in many of the mixed and diurnal areas, suggesting that these areas would move closer to resonance as MSL increases. The extreme case of a 60-m MSL rise resulted in weaker global tides, as the larger shelf seas gives rise to increased tidal dampening—a result supported by sensitivity simulations of the present day tide in Green and Huber (2013). Pickering (2010) investigated uniform MSL rise scenarios of 1, 2, and 10 m with a fixed coastline and drew a similar conclusion of a sensitivity of global shelf sea tides to MSL rise, with a change in the global pattern being similar at 1- and 2-m MSL rise but differed between the 2- and 10-m scenarios.

Pickering (2014) and Pickering et al. (2017) used a fully global (1/8)° forward tidal model to assess changes in the four primary tidal constituents for MSL rise scenarios ranging from 0.5 to 10 m. With fixed coastlines, they found that tidal amplitudes responded strongly in shelf seas globally, whereas simulations with coastal recession tended to result in reductions in tidal range. Therefore, coastal management strategies could potentially influence the sign of the tidal amplitude change. With 0.5-, 1-, and 2-m MSL rise, around 10% of the 136 largest coastal cities analyzed experience changes in mean high water in excess of ±10% of the MSL change imposed (Pickering et al., 2017).

The majority of these studies have used a spatially homogeneous MSL change. When Pickering et al. (2017) introduced a spatially varying MSL change, induced by large-scale ice sheet melt of Greenland and/or West Antarctic, they found only modestly altered tidal response in low latitudes but greater differences at high latitudes. Wilmes et al. (2017) assessed how the M_2 tide responds to nonuniform sea level changes induced by complete collapses of the West Antarctic and Greenland Ice Sheets. Aside from large heterogeneous changes in tides along coastlines, these simulations point to a sensitivity of the North Atlantic tides to the West Antarctic ice sheet extent. Schindelegger et al. (2018) analyzed more modest future changes in the M_2 tidal constituent on a global scale with GIA-induced crustal motion and altimetric MSL trend patterns averaging 2 m. Again, they found that when allowing for flooding of new areas, M_2 amplitudes decreased in many basins. In contrast to Luz Clara et al. (2015) and Carless et al. (2016), their flooding run exhibited considerably larger sensitivity to water depth change than simulations with unaltered present-day coastlines for the Patagonian Shelf. This hints at feedback effects between shelf and basin tides which are difficult to account for in models configured for regional domains, in agreement with Arbic et al. (2009). These simulations indicate that changes in tidal amplitude occur particularly in shelf seas with increases of up to 15%. A key benefit of global model simulations is their inclusion of changes in coastal tides on the shelf, in deep water and the coupled interaction between the two (and a finite element approach may be the most effective way to further examine these interactions).

4.1.4. Deep-Time Future Investigations

On long time scales, MSL changes become a secondary effect in controlling future tides, as is the case for the past (see section 2.1 and Green et al., 2018). The reason MSL changes evoke large responses in today's ocean is the near-resonant state of the North Atlantic—a property largely set by tectonics. MSL changes can influence the resonant properties by drying or flooding shallow shelf seas. This effectively modulates the damping of the tidal wave, with potentially large implications for the tidal system (see Arbic & Garrett, 2010; Egbert et al., 2004; Green, 2010, for discussions). When large regions of ocean are not in a (near) resonant state, changes in MSL will have limited ability to influence the tides, and any effects are mainly local. However, the present resonant state of the North Atlantic is expected to remain for the next 25 Myr, and investigating the influence of even moderate MSL rise on tides is therefore justified.

4.2. Potential Implications of Future Changes in Tide

The influence of tides is pervasive on many aspects of human activity from commerce to coastal protection to ecosystem services. As mankind moves into an era of adaptation to our changing climate, we should consider changes to tides as another factor to plan for in our adaptation strategies. We consider implications in five main areas: (1) coastal flooding, (2) energy, (3) sediment transport, (4) tidal mixing fronts, and (5) intertidal habitats.

4.2.1. Coastal Flooding

Both trends and variations in tidal levels influence extreme sea levels and thus coastal flooding and erosion (e.g., Talke et al., 2018). Globally, up to 310 million people are at risk of coastal flooding today (Hinkel et al., 2014). Coastal flooding is already a growing threat due to MSL rise (Church et al., 2013), and changes in tidal levels will affect flood risk: Tidal range, in addition to changes in MSL (Figure 10) determines extreme sea levels so tidal range amplification will increase extreme sea levels further, exacerbating flood risk (Figure 10b), while tidal range reduction will reduce it (Figure 10c). Therefore, tidal changes must be incorporated into future flood risk assessments (i.e., tidal changes should not be treated as negligible), in areas where the changes are likely large. There are two methods of including future tidal changes into estimates of extreme sea levels. The simplest is to make a linear offset to the present-day return periods in line with the projected tidal change, in the same way as is currently done to include MSL rise itself (e.g., Haigh et al., 2010b). This method assumes the surge climatology remains unaltered by the changing tide, which is a reasonable assumption (Mawdsley & Haigh, 2016; Williams et al., 2016) but may not be correct for all coasts. The second method is to simulate the tide, surge, and MSL rise in a single model so that MSL-tide, tide-surge, and MSL-surge interactions are all included, for example, as done by Arns et al. (2015, 2017) for the German Bight. Future national flood assessments should include at least the first method, but it is only through downscaling from global tidal models, via the shelf, to estuarine models that estuarine tidal changes can be properly quantified. Tidal changes are very sensitive to coastal management practices along low-lying coasts, based on model scenarios that maintain fixed model coastlines or allow coastal recession with MSL rise (Pelling, Green, et al., 2013; Pelling, Uehara, et al., 2013; Pickering, 2014; Pickering et al., 2017). Methods to project coastline change on 100-year time scales are therefore required; studies such as Passeri et al. (2016) are making progress on this at regional scales using Bayesian Networks and decision-making trees, and others consider both geophysical and human factors influencing accommodation space with MSL rise (Schuerch et al., 2018).

4.2.2. Energy

Changes in tides will have important implications for thermal power plants and for tidal renewable energy schemes. Thermal power plants (which make up 82% of current global electricity generation) require a continuous water supply for "wet cooling" purposes. Therefore, tidal range increases could lead to the exposure of the existing intakes at low water. Further analysis of future tidal levels is required to establish how significant these range changes are in terms of maintaining a consistent supply of cooling water to power stations: in most cases increases in the maximum range are less than the MSL rise itself and extension of intake pipes into deeper water is usually straightforward.

Any economic cost benefit analysis to assess the suitability of a potential renewable tidal energy site should include possible long-term increases or decreases in the usable tidal energy. Certain locations (e.g., Bristol Channel and St. Malo in Pickering et al. (2012) under 2-m MSL rise) show substantial (−40 to −50 cm) decreases in tidal range with future MSL rise. If these future range decreases, and associated decreases in current speed, are not considered then this could lead to overestimates of the net present value of the proposed sites. A 10% reduction in tidal amplitude would cause approximately a 3% reduction in current velocity (Pickering et al., 2017). For tidal stream power, the cubic relationship between current velocity and tidal hydraulic power density (Hardisty, 2008), would lead to a 9% reduction in power generation. For tidal barrage power, owing to the quadratic relationship between tidal amplitude and hydraulic power density (MacKay, 2008), this would lead to a 19% reduction in power generation. Clearly sites with macrotidal conditions are particularly attractive for tidal barrage energy generation projects; these large amplitudes often occur where tides in estuaries are close to resonance. However, it is these resonant locations that are especially sensitive to tidal change. Tidal stream sites, on the other hand, tend to be between islands and around headlands where tides are strong but not necessarily resonant; tides in these locations may be less sensitive to nonastronomic changes. This along with the typically shorter lifespan of tidal stream sites means they may be less affected economically by tidal change than tidal barrages.

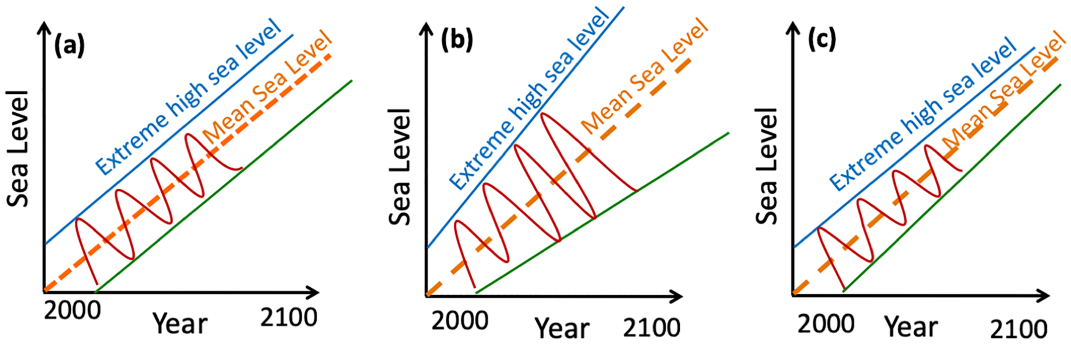

Figure 10. Diagram illustrating increases in flood risk with rises in mean sea level with: (a) no change in tidal range, (b) increases in tidal range which amplifies flood risk, and (c) decreases in tidal range which reduces the increase in flood risk relative to the other scenarios. Effects of land-level movements are in addition (e.g., coastal subsidence will increase rates of mean sea level rise) and transient weather driven components of coastal flooding such as storm surge are superimposed on these baseline changes.

4.2.3. Sediment Transport

Temporal variability of tides could lead to changes in sediment transport, with a potential to influence coastal morphology in estuaries, and therefore shipping. The magnitude of sedimentation and erosion rates is correlated to the bed shear stress and hence the square of the tidal velocity (Gerritsen & Berentsen, 1998). Consequently, even small changes in tidal range and tidal current velocities can influence coastal morphology (e.g., Chernetsky et al., 2010; Idier et al., 2017). For example, Gerritsen and Berentsen (1998) found that the MSL rise from −15 and −5 m to present day MSL reduced the erosion in the southern North Sea and increased it in the German Bight due to altered tidal dynamics. Investigations of future effects of MSL and changes in tides come to similar conclusions; see, for example, Jensen and Mudersbach (2005) and Masselink and Russell (2013). In estuaries (Bolle et al., 2010) and coastal lagoons (Araújo et al., 2008), changes to tidal asymmetry (flood-ebb dominance) could lead to associated changes in the sediment import or export. The link between increased tidal range and increased suspended sediment concentrations has been demonstrated for the Humber Estuary by Morris and Mitchell (2013). Also, depth changes in estuary may not be as large as the MSL rise itself because sediment may be imported or retained (rather than exported), depending on the local sediment supply. Failure of the sediment supply to match the rate of MSL rise would cause the estuary to "drown" (van Goor et al., 2003) as saltmarshes and spits recede or disappear as the morphology adjusts (Masselink & Russell, 2013). Furthermore, changes to the tidal range in estuaries will alter the tidal prism, that is, volume of water exchanged between the estuary and the coastal waters, with effects of the residence time for pollutants in the estuary (e.g., Dyer, 1977).

Many estuaries are critical arteries for the passage of shipping to major ports, stimulating local and national economies. Changes to tidal levels and to sedimentation have implications for both dredging operations and for navigation. For example, in Germany, navigation on the River Elbe is particularly dependent on water levels, with extended periods of low water (LW) reducing the length of the tidal cycle suitable for passage of deep draft vessels (Müller-Navarra & Bork, 2011). Plans to manage the sediment transport patterns in the Elbe could be hampered by increased tidal ranges (von Storch & Woth, 2008). Winterwerp et al. (2013) examined the tidal range evolution over the last century at five European ports with long narrow channels, where dredging and canalization has led to substantial (order of meters) increases in tidal range. These increased tidal ranges have caused problems with salt water intrusion, water quality, and increased turbidity, causing catastrophic changes in the local ecology (Winterwerp et al., 2013). A further deepening of an estuary could further exacerbate ecological problems. Many ports, such as Amsterdam in the Netherlands, are dependent on extensive lock systems as well as discharge sluices and pumping stations to create safe passage for shipping and to manage the landward water levels (Swinkels et al., 2010). Some docks have very narrow tolerances for vessel draft over the dock sills or limited clearance under bridges. Consequently, changes to tidal range, on top of a change in MSL, could change the length of the window of opportunity where safe passage could be made to the ports, as well as affecting the volume of water able to be discharged through sluices.

4.2.4. Tidal Mixing Fronts

Changes in tides could affect processes in shelf seas, which will influence primary production and fishers. Primary productivity is high in the seasonally stratified areas of shallow shelf seas due to the vertical mixing induced by (internal) tides (e.g., Sharples et al., 2007). The stratification of the water column in shelf seas plays an important role in primary productivity and hence draw down of atmospheric CO_2 through the biological carbon pump (Thomas et al., 2004). The position of tidal mixing fronts, which separate stratified and well-mixed waters, can be determined by the Simpson and Hunter criteria (1974):$c = H/U^3$. Fronts in temperate shelf seas tend to sit on contours of $c = 500$, and even small changes in tidal current amplitudes thus have the potential to alter the position of tidal mixing fronts (Carless et al., 2016; Pickering, 2014; Wilmes et al., 2017), although to some extent small increases in U may be offset by the increased water depth. In areas with high freshwater runoff, changes to tidal mixing will also influence the buoyancy-stirring competition that determines regions of freshwater influence; future stratification will depend on alterations to estuarine discharge of freshwater (due to increased precipitation) and changes to the tidal and wind mixing. Changes in stratification also directly affect primary production in coastal seas (Sharples, 2008), which may have implications for higher trophic levels such as fish and apex predators that depend on seasonal phytoplankton blooms (Embling et al., 2012; Scott et al., 2010, 2013). For example, some species of crustacean are extremely sensitive to the position of tidal mixing fronts: the Norwegian Lobster (Nephrops norvegicus) exhibits larval retention over an area of muddy substrate for settlement and during the postlarval stage for burrowing (Hill et al., 1996). Any change in the baroclinic flows that retain the larvae could have a detrimental effect on the stocks of Nephrops which have an estimated value of £10 million per year to the Irish economies (Seafish, 2007) and £84 million to the Scottish economy (Scottish Government, 2012).

Another consequence of altered tides is that changes in the tidal driven mixing, especially in the abyssal ocean, has the potential to modify the strength of the global MOC with ramifications for global climate (e.g., Green et al., 2009). However, no investigations have yet shown a link between future change in tides and changes to the MOC, but large-scale changes of paleotides have possibly influenced the MOC (e.g., Green & Huber, 2013; Munk & Bills, 2007; Schmittner et al., 2015).

4.2.5. Intertidal Habitats

Coastal habitats on rocky shores, estuaries, and saltmarshes are all strongly influenced by tidal conditions (Pugh, 1987), and changes in the MSL and MTR may therefore have implications for species that live in the intertidal zone. MSL rise will shift the intertidal zone inshore and changes in MTR will alter the spatial extent of the littoral zone, the current speeds, the bed type, the emersion/submersion curves, and the position of areas exposed during daylight. The natural response of estuaries to MSL rise is landward migration, and although coastal defenses may temporarily prevent this, the seaward edge of marshes and lower part of the intertidal zone would still erode, leading to a narrowing of the intertidal zone known as coastal squeeze (Masselink & Russell, 2013). In such cases, managed realignment of the coastal flood defenses will be required if the intertidal habitat is to be maintained (Schuerch et al., 2018). Coastal squeeze will become a particular problem along coastlines with hard engineering schemes. For example, the Dutch and German Wadden Sea is a Ramsar wetland of international importance (1987) and a UNESCO world heritage site (2009). Substantial changes to the MSL and tidal range could have large impacts on these flat intertidal habitats, which are home to over 10,000 species of flora and fauna and a haven for 10–12 million migratory birds every year. The importance of tidal range in coastal marshes for feeding of wading birds is well established (Piersma et al., 2005). Coastal squeeze and reduced tidal range could also lead to the removal of nursery habitats in high velocity environments for macrobenthic fauna such as juvenile flatfish (Rabaut et al., 2013).

Other diverse habitats, such as mangroves, saltmarshes, and corals, which are all engineered by their inhabitants (Bertness & Silliman, 2008), could be negatively impacted if MSL rise and tidal changes occurs faster than the biology can keep pace. The settling and survival of mangrove and saltmarsh seedlings depends on short, disturbance-free periods in order for roots to develop. Altered tidal dynamics could change the duration of these windows of opportunity. Seedling establishment at lower intertidal elevations is dependent on there being inundation-free periods, which would also be reduced by MSL rise and reduced tidal range (Balke et al., 2013). An additional implication of habitat loss in the coastal zone (e.g., mangroves) is the loss of their natural contribution to coastal flood defenses, and beaches where landward migration or increased erosion occurs may lead to mitigation attempts through beach nourishment programs, resulting in steeper beach slopes and loss of subtidal and intertidal habitats.

5. Conclusions and a Way Forward

This review has highlighted the considerable evidence that tidal amplitudes have changed and are continuing to change, due to nonastronomical factors. Over longer geological time scales it has been argued that variations in tides were driven by tectonic changes, which affected basin size and shape and hence the resonant properties of the basins. On shorter geological time scales, however, changes in tides were mainly due to variations in water depth, driven by large MSL fluctuations associated with glacial and interglacial cycles, and due to the extent of ice sheets. Over the 19th, 20th, and early 21st centuries, changes in tides are evident from water level records, with measured rates exceeding by far predictions related to orbital mechanics. Initially, these changes were observed at individual tide gauge sites and were thought to have arisen as a result of local natural and anthropogenic factors. However, a growing number of studies over the last decade have identified widespread, sometimes regionally coherent, positive, and negative trends in tidal constituents and levels that cannot be attributed to local mechanisms alone.

It has proved difficult to associate observed changes in tide over the instrumental period with particular forcing factors because the knowledge of past changes in tide is based on tide gauge measurements, which are affected by both local and regional mechanisms. We have highlighted six main factors that can cause changes in measured tidal statistics on local scales: (1) dissipation and turbulent mixing; (2) depth of channels and flats; (3) surface area, width, and convergence; (4) resonance and reflection; (5) river flow; and (6) changes in instrumentation. We have discussed a further eight possible regional/global driving mechanisms: (1) tectonics, (2) water depth, (3) shoreline position, (4) extent of (sea)ice coverage, (5) seabed roughness, (6) ocean stratification and internal tides, (7) nonlinear interactions (frictional or triad), and (8) radiational forcing. However, since only a few studies have combined observations and models, or modeled at a temporal/spatial resolution capable of resolving both ultralocal and large-scale global changes, the individual contributions from local and regional mechanisms remain uncertain. It is thought that changes in water depth, due to climate-related MSL rise and isostatic crustal adjustments, does contribute to the recent observed change in tides. However, any link between tidal variability and MSL is far from a one-to-one correspondence, and local factors such as navigational development are clearly dominant in many ports. One might hope that progress in understanding tidal changes at seasonal and other time scales might lead also to greater understanding of longer-term changes, but the relationship between MSL variations and tidal fluctuations is often dependent on time scale. For instance, tidal range and MSL at San Francisco both show positive, century-scale trends (not necessarily causally related), while the two are negatively correlated on seasonal scales (Devlin, Jay, Talke, et al., 2017). This example emphasizes the importance of determining whether MSL and tidal trends are causally or incidentally related. Fortunately, modeling studies are beginning to make significant progress in isolating and assessing the importance of some of the complex suite of mechanisms influencing the observed tidal signal.

Over the last decade, modeling studies have presented projections of future tidal changes over the 21st century and beyond with changes in water depth, driven by MSL rise, and other factors (e.g., ice sheet extent and, to some extent, ocean warming). This body of work demonstrates that regionally coherent increases/decreases in the tide are likely to occur, over the next centuries in response to MSL rise, changes in coastal morphology, and variations in ice sheet extents. These tidal changes will particularly affect shelf seas and coastal waters. Changes are likely to be smaller than $\pm$15% of MSL rise along most coastlines; however, at specific (often resonant) locations they can be larger.

Efforts to directly compare and contrast modeling studies on future tidal characteristics are complicated by differences in numerical software across studies, boundary conditions, configuration settings, horizontal resolutions, forcing tidal constituents, MSL rise scenarios, and analytical tidal metrics. In particular, model predictions are very sensitive to how the coastline is represented in the model set up, especially in regions with low or moderate terrestrial topographic gradients where the basins are near resonance. Decisions about boundary conditions (e.g., river flow/buoyancy input) are also likely important. More modeling studies in these areas are clearly warranted.

Accurate assessment of the spatial patterns of past changes in tides has been severely limited, in many regions, by the scarcity of long (>18 years) high-frequency tide gauge records. Hence, there is a need to continue to increase the number of sea level records available for analysis, maintain those that exist and improve their spatial distribution (e.g., in the Southern Hemisphere). Work has already begun to extend the global

tide gauge data set via a Version 3 update of the Global Extreme Sea Level Analysis database (Woodworth et al., 2017). Furthermore, we urge the community to continue to extend and improve historic data sets via data archaeology. Improved methods and expanded networks are also needed to acquire complementary information on changes in internal tides, and all the parameters likely to be associated with tidal changes on a regional/global basis.

Finally, we stress that the changes in tides predicted to occur this century and beyond are of a significant magnitude along certain stretches of coastline. Consequently, they should be accounted for in future national and international impact assessments of sea level change.

Glossary

This glossary has been adapted from Pugh and Woodworth (2014).

Amphidrome : a point in the sea where there is zero tidal amplitude due to canceling of tidal waves. Cotidal lines radiate from an amphidromic point and corange lines encircle it.

Internal tides : tidal waves which propagate at density differences within the ocean. They travel slowly compared with surface gravity waves and have wavelengths of only a few tens of kilometers, but they can have amplitudes at depth of tens of meters. Their sea surface height signals are smaller, typically of order 1–5 cm. The associated internal currents are termed baroclinic motions.

Mean sea level : the average height of the sea over longer periods of time (usually a month or year). Hence the shorter-term sea level variations (e.g., waves, tides, and storm surges) are filtered out.

Mean high water : the average of all the high water heights observed over a particular period, usually a year.

Mean low water : the average of all the low-water heights observed over a particular period, usually a year.

Mean tidal range : the difference between monthly or annual Mean High Water and Mean Low Water.

Overtides : a harmonic tidal component that has a speed that is an exact multiple of the speed of one development of the tide-producing force.

Radiational tides : tides generated by regular periodic meteorological forcing.

Resonance : The phenomenon of the large amplitudes which occur when a physical system is forced at its natural period of oscillation. Tidal resonance occurs when the natural period of an ocean or sea is close to the period of the tidal forcing.

Data Availability Statement

No data sets are analyzed directly in this paper.

Acknowledgments
We would like to thank Richard Ray and an anonymous reviewer for their insightful comments that greatly strengthened this paper. I. D. H. acknowledges funding from the Natural Environmental Research Council (Grant NE/P009069/1), which also partially supported M. D. P., and this project has received funding from the *European Research Council (ERC) under the European Union's Horizon 2020 research and innovation programme* under Grant Agreement 759677. J. A. M. G. acknowledges funding from the Natural Environmental Research Council (Grants NE/F014821/1 and NE/I030208/1). B. K. A. acknowledges support from the U.S. National Science Foundation, under CAREER Award OCE-0351837. T. H. was supported by the Met Office Hadley Centre Climate Programme funded by BEIS and Defra. M. S. thanks the Austrian Science Fund (FWF) for financial support under Grant P30097-N29. S. D. acknowledges the German Science Foundation (DFG) for financial support of the project TIDEDYN. D. I. acknowledges BRGM and the ECLISEA project which is part of ERA4CS, an ERA-NET initiated by JPI Climate with cofunding by the European Union (Grant 690462). S. A. T. was funded by the U.S. National Science Foundation, CAREER Award 1455350. S. B. W. was supported through the National Science Foundation Grant OCE-1559153. M. D. P. would like to dedicate this work to his late grandfather Peter W. Bishop.

References

Agnew, D. A. (1986). Detailed analysis of tide gauge history: A case analysis. *Marine Geodesy*, *10*(3–4), 231–255. https://doi.org/10.1080/01490418609388024

Akan, Ç., Moghimi, S., Özkan-Haller, H. T., Osborne, J., & Kurapov, A. (2017). On the dynamics of the Mouth of the Columbia River: Results from a three-dimensional fully coupled wave-current interaction model. *Journal of Geophysical Research: Oceans*, *122*, 5218–5236. https://doi.org/10.1002/2016JC012307

Aldridge, J. N., Parker, E. R., Bricheno, L. M., Green, S. L., & van der Molen, J. (2015). Assessment of the physical disturbance of the northern European Continental shelf seabed by waves and currents. *Continental Shelf Research*, *108*, 121–140. https://doi.org/10.1016/j.csr.2015.03.004

Amin, M. (1983). On perturbations of harmonic constants in the Thames Estuary. *Geophysical Journal International*, *73*(3), 587–603. https://doi.org/10.1111/j.1365-246X.1983.tb03334.x

Amin, M. (1985). Temporal variations of tides on the west coast of Great Britain. *Geophysical Journal International*, *82*(2), 279–299. https://doi.org/10.1111/j.1365-246X.1985.tb05138.x

Amin, M. (1993). Changing mean sea level and tidal constants on the west coast of Australia. *Australian Journal of Marine and Freshwater Research*, *44*(6), 911–925. https://doi.org/10.1071/MF9930911

Amos, C. L., Tee, K. T., & Zaitlin, B. A. (1991). The post-glacial evolution of Chignecto Bay, Bay of Fundy, and its modern environment of deposition. In D. G. Smith, G. E. Reinson, B. A. Zaitlin, & R. A. Rahmani (Eds.), *Clastic tidal sedimentology*, *Canadian Society of Petroleum Geologists' Memoir* (Vol. 16, pp. 59–90). Calgary: CSPG.

Amos, C. L., & Zaitlin, B. A. (1985). The effect of changes in tidal range on a sublittoral macrotidal sequence, Bay of Fundy, Canada. *Geo-Marine Letters*, *4*, 161–169.

Araújo, I. B., Dias, J. M., & Pugh, D. T. (2008). Model simulations of tidal changes in a coastal lagoon, the Ria de Aveiro (Portugal). *Continental Shelf Research*, *28*(8), 1010–1025. https://doi.org/10.1016/j.csr.2008.02.001

Arbic, B. K. (2005). Atmospheric forcing of the oceanic semidiurnal tide. *Geophysical Research Letters*, *32*, L02610. https://doi.org/10.1029/2004GL021668

Arbic, B. K., & Garrett, C. (2010). A coupled oscillator model of shelf and ocean tides. *Continental Shelf Research*, *30*(6), 564–574. https://doi.org/10.1016/j.csr.2009.07.008

Arbic, B. K., Karsten, R. H., & Garrett, C. (2009). On tidal resonance in the global ocean and the back-effect of coastal tides upon open-ocean tides. *Atmosphere-Ocean*, *47*(4), 239–266. https://doi.org/10.3137/OC311.2009

Arbic, B. K., MacAyeal, D. R., Mitrovica, J. X., & Milne, G. A. (2004). Paleoclimate: Ocean tides and Heinrich events. *Nature*, *432*(7016), 460. https://doi.org/10.1038/432460a

Arbic, B. K., MacAyeal, D. R., Mitrovica, J. X., & Milne, G. A. (2008). On the factors behind large Labrador Sea tides during the last glacial cycle and the potential implications for Heinrich events. *Paleoceanography*, *23*, PA3211. https://doi.org/10.1029/2007PA001573

Aretxabaleta, A. L., Ganju, N. K., Butman, B., & Signell, R. P. (2017). Observations and a linear model of water level in an interconnected inlet-bay system. *Journal of Geophysical Research: Oceans*, *122*, 2760–2780. https://doi.org/10.1002/2016JC012318

Arns, A., Dangendorf, S., Jensen, J., Talke, S., Bender, J., & Pattiaratchi, C. (2017). Sea-level rise induced amplification of coastal protection design heights. *Scientific Reports*, *7*, 40171. https://doi.org/10.1038/srep40171

Arns, A., Wahl, T., Dangendorf, S., & Jensen, J. (2015). The impact of sea level rise on storm surge water levels in the northern part of the German Bight. *Coastal Engineering*, *96*, 118–131. https://doi.org/10.1016/j.coastaleng.2014.12.002

Austin, R. M. (1991). Modelling Holocene tides on the NW European continental shelf. *Terra Nova*, *3*(3), 276–288. https://doi.org/10.1111/j.1365-3121.1991.tb00145.x

Balbus, S. (2014). Dynamical, biological and anthropic consequences of equal lunar and solar angular radii. *Proceedings of the Royal Society A*, *470*, 20140263. https://doi.org/10.1098/rspa.2014.0263

Balke, T., Webb, E. L., van den Elzen, E., Galli, D., Herman, P. M., & Bouma, T. J. (2013). Seedling establishment in a dynamic sedimentary environment: A conceptual framework using mangroves. *The Journal of Applied Ecology*, *50*(3), 740–747. https://doi.org/10.1111/1365-2664.12067

Bertness, M. D., & Silliman, B. R. (2008). Consumer control of salt marshes driven by human disturbance. *Conservation Biology*, *22*(3), 618–623. https://doi.org/10.1111/j.1523-1739.2008.00962.x

Bolle, A., Bing Wang, Z., Amos, C., & De Ronde, J. (2010). The influence of changes in tidal asymmetry on residual sediment transport in the Western Scheldt. *Continental Shelf Research*, *30*(8), 871–882. https://doi.org/10.1016/j.csr.2010.03.001

Bradley, B. A., & Cubrinovski, M. (2011). Near-source strong ground motions observed in the 22 February 2011 Christchurch earthquake. *Seismological Research Letters*, *82*(6), 853–865. https://doi.org/10.1785/gssrl.82.6.853

Bradshaw, E., Rickards, L., & Aarup, T. (2015). Sea level data archaeology and the Global Sea Level Observing System (GLOSS). *GeoResJ*, *6*, 9–16. https://doi.org/10.1016/j.grj.2015.02.005

Burchard, H., Schuttelaars, H. M., & Ralston, D. K. (2018). Sediment trapping in estuaries. *Annual Review of Marine Science*, *10*(1), 371–395. https://doi.org/10.1146/annurev-marine-010816-060535

Buschman, F. A., Hoitink, A. J. F., van der Vegt, M., & Hoekstra, P. (2009). Subtidal water level variation controlled by river flow and tides. *Water Resources Research*, *45*, W10420. https://doi.org/10.1029/2009WR008167

Cai, H., Savenije, H. H. G., & Toffolon, M. (2014). Linking the river to the estuary: influence of river discharge on tidal damping. *Hydrology and Earth System Sciences*, *18*(1), 287–304. https://doi.org/10.5194/hess-18-287-2014

Cai, H., Savenije, H. H. G., Yang, Q., Suying, O., & Yaping, L. (2012). Influence of river discharge and dredging on tidal wave propagation: Modaomen estuary case. *Journal of Hydraulic Engineering*, *138*(10), 885–896. https://doi.org/10.1061/(ASCE)HY.1943-7900.0000594

Carless, S. J., Green, J. A. M., Pelling, H. E., & Wilmes, S.-B. (2016). Effects of future sea-level rise on tidal processes on the Patagonian Shelf. *Journal of Marine Systems*, *163*, 113–124. https://doi.org/10.1016/j.jmarsys.2016.07.007

Cartwright, D. E. (1968). A unified analysis of tides andsurges round North and East Britain. *Philosophical Transactions of the Royal Society*, *263*, 1–55. https://doi.org/10.1098/rsta.1968.0005

Cartwright, D. E. (1971). Tides and waves in the vicinity of Saint Helena. *Philosophical Transactions of the Royal Society of London A: Mathematical, Physical and Engineering Sciences*, *270*(1210), 603–646. https://doi.org/10.1098/rsta.1971.0091

Cartwright, D. E. (1972a). Secular changes in the oceanic tides at Brest, 1711?1936. *Geophysical Journal International*, *30*(4), 433–449. https://doi.org/10.1111/j.1365-246X.1972.tb05826.x

Cartwright, D. E. (1972b). Some ocean tide measurements of the eighteenth century and their relevance today. *Proceedings of the Royal Society of Edinburgh Series B*, *72*, 331–339. https://doi.org/10.1017/S0080455X00001892

Cartwright, D. E. (1985). Tidal prediction and modern time scales. *International Hydrographic Review*, *62*, 127–138.

Cartwright, D. E. (1999). *Tides: A scientific history* (p. 292). Cambridge: Cambridge University Press.

Cartwright, D. E., & Tayler, R. J. (1971). New computations of the tide-generating potential. *Geophysical Journal of the Royal Astronomical Society*, *23*(1), 45–73. https://doi.org/10.1111/j.1365-246X.1971.tb01803.x

Chant, R. J., Sommerfeld, C. K., & Talke, S. A. (2018). Impact of channel deepening on tidal and gravitational circulation in a highly engineered estuarine basin. *Estuaries and Coasts*, *41*(6), 1587–1600. https://doi.org/10.1007/s12237-018-0379-6

Chernetsky, A. S., Schuttelaars, H. M., & Talke, S. A. (2010). The effect of tidal asymmetry and temporal settling lag on sediment trapping in tidal estuaries. *Ocean Dynamics*, *60*, 1219–1241. https://doi.org/10.1007/s10236-010-0329-8

Church, J., Clark, P., Cazenave, A., Gregory, J., Jevrejeva, S., Merrifield, M., et al. (2013). Sea Level Change, pages 1137–1216. Climate change 2013: The physical science basis. In *Contribution of Working Group I to the Fifth Assessment Report of the Intergovernmental Panel on Climate Change* (Chap. 13, pp. 1137–1216). Cambridge, UK and New York, NY, USA: Cambridge University Press.

Clark, P. U., Dyke, A. S., Shakun, J. D., Carlson, A. E., Clark, J., Wohlfarth, B., et al. (2009). The Last Glacial Maximum. *Science*, *325*(5941), 710–714. https://doi.org/10.1126/science.1172873

Colosi, J. A., & Munk, W. (2006). Tales of the venerable Honolulu tide gauge. *Journal of Physical Oceanography*, *36*(6), 967–996. https://doi.org/10.1175/JPO2876.1

Covey, C., Dai, A., Lindzen, R. S., & Marsh, D. R. (2014). Atmospheric tides in the latest generation of climate models. *Journal of the Atmospheric Sciences*, *71*(6), 1905–1913. https://doi.org/10.1175/JAS-D-13-0358.1

Dalrymple, R. W. (1992). Tidal depositional systems. In R. G. Walker & N. P. James (Eds.), *Facies models: Response to sea level change, St John's* (pp. 195–218). Geological Association of Canada: Newfoundland.

Dangendorf, S., Müller-Navarra, S., Jensen, J., Schenk, F., Wahl, T., & Weisse, R. (2014). North Sea storminess from a novel storm surge record since AD 1843. *Journal of Climate*, *27*(10), 3582–3595. https://doi.org/10.1175/JCLI-D-13-00427.1

Darwin, G. H. (1898). *The tides and kindred phenomena in the solar system: The substance of lectures delivered in 1897 at the Lowell institute, Boston, Massachusetts*. Boston: Houghton, Mifflin and company.

de Boer, W., Roos, P. C., Hulscher, S. J. M. H., & Stolk, A. (2011). Impact of mega-scale sand extraction on tidal dynamics in semi-enclosed basins: an idealized model study with application to the Southern North Sea. *Coastal Engineering*, *58*(8), 678–689. https://doi.org/10.1016/j.coastaleng.2011.03.005

de Jonge, V. N., Schuttelaars, H. M., van Beusekom, J. M. M., Talke, S. A., & de Swart, H. E. (2014). The influence of channel deepening on estuarine turbidity dynamics, as exemplified by the Ems estuary. *Estuary, Coastal and Shelf Science*, *139*, 46–59. https://doi.org/10.1016/j.ecss.2013.12.030

de Ronde, J. G. (1989). Past and Future sea level rise in the Netherlands in Workshop on Sea Level Rise and Coastal Processes, Palm Beach, Florida, 9–11 March 1988 (pp. 253–280). Washington, DC: US Department of EnergyReport DOE/NBB-0086.

DeConto, R. M., & Pollard, D. (2016). Contribution of Antarctica to past and future sea-level rise. *Nature*, *531*(7596), 591–597. https://doi.org/10.1038/nature17145

Devlin, A. T., Jay, D. A., Talke, S. A., & Zaron, E. (2014). Can tidal perturbations associated with sea level variations in the western Pacific Ocean be used to understand future effects of tidal evolution? *Ocean Dynamics*, *64*(8), 1093–1120. https://doi.org/10.1007/s10236-014-0741-6

Devlin, A. T., Jay, D. A., Talke, S. A., Zaron, E. D., Pan, J., & Lin, H. (2017). Coupling of sea level and tidal range changes, with implications for future water levels. *Scientific Reports*, *7*(1), 17021. https://doi.org/10.1038/s41598-017-17056-z

Devlin, A. T., Jay, D. A., Zaron, E. D., Talke, S. A., Pan, J., & Lin, H. (2017). Tidal variability related to sea level variability in the Pacific Ocean. *Journal of Geophysical Research: Oceans*, *122*, 8445–8463. https://doi.org/10.1002/2017JC013165

Devlin, A. T., Zaron, E. D., Jay, D. A., Talke, S. A., & Pan, J. (2018). Seasonality of tides in Southeast Asian Waters. *Journal of Physical Oceanography*, *48*, 1169–1190. https://doi.org/10.1175/JPO-D-17-0119.1

Dıez-Minguito, M., Baquerizo, A., Ortega-Sanchez, M., Navarro, G., & Losada, M. (2012). Tide transformation in the Guadalquivir estuary (SW Spain) and process-based zonation. *Journal of Geophysical Research*, *117*, C03019. https://doi.org/10.1029/2011JC007344

DiLorenzo, J. L., Huang, P., Thatcher, M. L., & Najarian, T. O. (1993). Dredging impacts on Delaware Estuary tides. Presented at Proceedings of the 3rd International Conference on Estuarine and Coastal Modeling III.

Doodson, A. T. (1924). Perturbations of harmonic tidal constants. *Proceedings of the Royal Society*, *106*(739), 513–526. https://doi.org/10.1098/rspa.1924.0085

Dronkers, J. J. (1964). *Tidal computations in rivers and coastal waters*. New York: North-Holland, Amsterdam; Interscience (Wiley).

Du, J., Shen, J., Zhang, Y. J., Ye, F., Liu, Z., Wang, Z., et al. (2018). Tidal response to sea-level rise in different types of estuaries: The Importance of Length, Bathymetry, and Geometry. *Geophysical Research Letters*, *45*, 227–235. https://doi.org/10.1002/2017GL075963

Dyer, K. R. (1977). *Estuaries: A physical introduction* (Vol. xv, p. 140). London: Wiley.

Egbert, G. D., & Ray, R. D. (2001). Estimates of M2 tidal energy dissipation from TOPEX/Poseidon altimeter data. *Journal of Geophysical Research*, *106*(C10), 22,475–22,502. https://doi.org/10.1029/2000JC000699

Egbert, G. D., Ray, R. D., & Bills, B. G. (2004). Numerical modeling of the global semidiurnal tide in the present day and in the last glacial maximum. *Journal of Geophysical Research*, *109*, C03003. https://doi.org/10.0129/2003JC001973

Embling, C. B., Illian, J., Armstrong, E., van der Kooij, J., Sharples, J., Camphuysen, K. C. J., & Scott, B. E. (2012). Investigating fine-scale spatio-temporal predator-prey patterns in dynamic marine ecosystems: A functional data analysis approach. *Journal of Applied Ecology*, *49*, 481–492. https://doi.org/10.1111/j.1365-2664.2012.02114.x

Familkhalili, R., & Talke, S. A. (2016). The effect of channel deepening on storm surge: A case study of Wilmington, NC. *Geophysical Research Letters*, *43*, 9138–9147. https://doi.org/10.1002/2016GL069494

Feng, X., Feng, H., Li, H., Zhang, F., Feng, W., Zhang, W., & Yuan, J. (2019). Tidal responses to future sea level trends on the Yellow Sea shelf. *Journal of Geophysical Research: Oceans*, *124*, 2019JC015150. https://doi.org/10.1029/2019JC015150

Feng, X., Tsimplis, M. N., & Woodworth, P. L. (2015). Nodal variations and long-term changes in the main tides on the coasts of China. *Journal of Geophysical Research: Oceans*, *120*, 1215–1232. https://doi.org/10.1002/2014JC010312

Flather, R. A. (2001). Storm surges. In J. H. Steele, S. A. Thorpe, & K. K. Turekian (Eds.), *Encyclopedia of ocean sciences* (pp. 2882–2892). San Diego, CA: Academic Press.

Flather, R. A., Baker, T. F., Woodworth, P. L., Vassie, L. M., & Blackman, D. L. (2001). Integrated effects of climate change on coastal extreme sea levels. Proudman Oceanographic Laboratory Internal Document No.140. 20pp. Retrieved from http://www.pol.ac.uk/ntslf/reports.html

Flather, R. A., & Williams, J. A. (2000). Climate change effects on storm surges: methodologies and results. In J. Beersma, M. Agnew, D. Viner, & M. Hulme (Eds.), *Climate scenarios for water-related and coastal impact*, *ECLAT-2 Workshop Report* (Vol. 3, pp. 66–78). The Netherlands: KNMI.

Flick, R. E., Murray, J. F., & Ewing, L. C. (2003). Trends in United States tidal datum statistics and tide range. *Journal of Waterway, Port, Coastal, and Ocean Engineering*, *129*(4), 155–164. https://doi.org/10.1061/(ASCE)0733-950X(2003)129:4(155)

Freund, H., & Streif, H. (2000). Natural sea level indicators recording the fluctuations of the mean high tide level in the Southern North Sea. Wadden Sea Newsletter 2000. Retrieved from https://uol.de/fileadmin/user_upload/icbm/ag/meeresstation/download/Freund_Waddensea_newsletter.pdf

Friedrichs, C. T., & Aubrey, D. G. (1994). Tidal propagation in strongly convergent channels. *Journal of Geophysical Research*, *99*(C2), 3321–3336. https://doi.org/10.1029/93JC03219

Gallo, M. N., & Vinzon, S. B. (2005). Generation of overtides and compound tides in Amazon estuary. *Ocean Dynamics*, *55*(5-6), 441–448. https://doi.org/10.1007/s10236-005-0003-8

Garrett, C. J. R., Keeley, J. R., & Greenberg, D. A. (1978). Tidal mixing versus thermal stratification in the Bay of Fundy and Gulf of Maine. *Atmosphere-Ocean*, *16*(4), 403–423. https://doi.org/10.1080/07055900.1978.9649046

Gehrels, W. R., Belknap, D. F., Pearce, B. R., & Gong, B. (1995). Modeling the contribution of M2 tidal amplification to the Holocene rise of mean high water in the Gulf of Maine and the Bay of Fundy. *Marine Geology*, *124*(1-4), 71–85. https://doi.org/10.1016/0025-3227(95)00033-U

Georgas, N. (2011). Large seasonal modulation of tides due to ice cover friction in a midlatitude estuary. *Journal of Physical Oceanography*, *42*, 352–369. https://doi.org/10.1175/JPO-D-11-063.s1

Gerritsen, H., & Berentsen, C. W. J. (1998). A modelling study of tidally induced equilibrium sand balances in the North Sea during the Holocene. *Continental Shelf Research*, *18*(2-4), 151–200. https://doi.org/10.1016/S0278-4343(97)00065-4

Geyer, W. R., & Farmer, D. M. (1989). Tide-induced variation of the dynamics of a salt wedge estuary. *Journal of Physical Oceanography*, *19*(8), 1060–1072.
Geyer, W. R., & MacCready, P. (2014). The estuarine circulation. *Annual Review of Fluid Mechanics*, *46*, 175–197. https://doi.org/10.1146/annurev-fluid-010313-141302
Giese, B. S., & Jay, D. A. (1989). Modelling tidal energetics of the Columbia River Estuary. *Estuarine, Coastal and Shelf Science*, *29*(6), 549–571. https://doi.org/10.1016/0272-7714(89)90010-3
Gilbert, G. K. (1917). *Hydraulic-mining debris in the Sierra Nevada*, *Professional Paper* (Vol. 105, p. 148). Colorado: U.S. Geological Survey.
Godin, G. (1986). Modification by an ice cover of the tide in James Bay and Hudson Bay. *Arctic*, *39*(1), 65–67.
Godin, G. (1991). Compact approximations to the bottom friction term, for the study of tides propagating in channels. *Continental Shelf Research*, *11*(7), 579–589. https://doi.org/10.1016/0278-4343(91)90013-V
Godin, G. (1993). On tidal resonance. *Continental Shelf Research*, *13*(1), 89–107. https://doi.org/10.1016/0278-4343(93)90037-X
Godin, G. (1995). Rapid evolution of the tide in the Bay of Fundy. *Continental Shelf Research*, *15*(2-3), 369–372. https://doi.org/10.1016/0278-4343(93)E0005-S
Godin, G. (1999). The propagation of tides up rivers with special considerations on the Upper Saint Lawrence River, Estuarine. *Coastal and Shelf Science*, *48*(3), 307–324. https://doi.org/10.1006/ecss.1998.0422
Godin, G., & Barber, F. G. (1980). Variability of the tide at some sites in the Canadian Arctic. *Arctic*, *33*(1), 30–37. https://doi.org/10.14430/arctic2545
Godin, G., & Gutierrez, G. (1986). Non-linear effects in the tide of the Bay of Fundy. *Continental Shelf Research*, *5*(3), 379–402. https://doi.org/10.1016/0278-4343(86)90004-X
Gräwe, U., Burchard, H., Müller, M., & Schuttelaars, H. M. (2014). Seasonal variability in M2 and M4 tidal constituents and its implications for the coastal residual sediment transport. *Geophysical Research Letters*, *41*, 5563–5570. https://doi.org/10.1002/2014GL060517
Green, G. (1837). On the motion of waves in a variable canal of small depth and width. *Transactions of the Cambridge Philosophical Society*, *6*, 457–462.
Green, J. A. M. (2010). Ocean tides and resonance. *Ocean Dynamics*, *60*(5), 1243–1253. https://doi.org/10.1007/s10236-010-0331-1
Green, J. A. M., Green, C. L., Bigg, G. R., Rippeth, T. P., Scourse, J. D., & Uehara, K. (2009). Tidal mixing and the meridional overturning circulation from the Last Glacial Maximum. *Geophysical Research Letters*, *36*, L15603. https://doi.org/10.1029/2009GL039309
Green, J. A. M., & Huber, M. (2013). Tidal dissipation in the early Eocene and implications for ocean mixing. *Geophysical Research Letters*, *40*, 2707–2713. https://doi.org/10.1002/grl.50510
Green, J. A. M., Huber, M., Waltham, D., Buzan, J., & Wells, M. (2017). Explicitly modelled deep-time tidal dissipation and its implication for Lunar history. *Earth and Planetary Science Letters*, *461*, 46–53. https://doi.org/10.1016/j.epsl.2016.12.038
Green, J. A. M., Molloy, J. L., Davies, H. S., & Duarte, J. C. (2018). Is there a tectonically driven supertidal cycle? *Geophysical Research Letters*, *45*, 3568–3576. https://doi.org/10.1002/2017GL076695
Green, J. A. M., & Nycander, J. (2013). A comparison of tidal conversion parameterizations for tidal models. *Journal of Physical Oceanography*, *43*, 104–119. https://doi.org/10.1175/JPO-D-12-023.1
Green, J. A. M., Way, M. J., & Barnes, R. (2019). Consequences of tidal dissipation in a putative Venusian ocean. *The Astrophysical Journal Letters*, *876*(2), L22. https://doi.org/10.3847/2041-8213/ab133b
Greenberg, D. A., Blanchard, W., Smith, B., & Barrow, E. (2012). Climate change, mean sea level and high tides in the Bay of Fundy. *Atmosphere-Ocean*, *50*(3), 261–276. https://doi.org/10.1080/07055900.2012.668670
Griffiths, S. D., & Peltier, W. R. (2008). Megatides in the Arctic Ocean under glacial conditions. *Geophysical Research Letters*, *35*, L08605. https://doi.org/10.1029/2008GL033263
Griffiths, S. D., & Peltier, W. R. (2009). Modelling of polar ocean tides at the Last Glacial Maximum: Amplification, sensitivity and climatological implications. *Journal of Climate*, *22*, 2905–2924. https://doi.org/10.1175/2008JCLI2540.1
Guo, L., van der Wegen, M., Jay, D. A., Matte, P., Wang, Z. B., Roelvink, D., & He, Q. (2015). River-tide dynamics: Exploration of nonstationary and nonlinear tidal behavior in the Yangtze River estuary. *Journal of Geophysical Research: Oceans*, *120*, 3499–3521. https://doi.org/10.1002/2014JC010491
Haigh, I. D., Eliot, M., & Pattiaratchi, C. (2011). Global influences of the 18.61 year nodal cycle and 8.85 year cycle of lunar perigee on high tidal levels. *Journal of Geophysical Research*, *116*, C06025. https://doi.org/10.1029/2010JC006645
Haigh, I. D., Nicholls, R. J., & Wells, N. C. (2009). Mean sea level trends around the English Channel over the 20th century and their wider context. *Continental Shelf Research*, *29*(17), 2083–2098. https://doi.org/10.1016/j.csr.2009.07.013
Haigh, I. D., Nicholls, R. J., & Wells, N. C. (2010a). Assessing changes in extreme sea levels: Application to the English Channel, 1900–2006. *Continental Shelf Research*, *30*(9), 1042–1055. https://doi.org/10.1016/j.csr.2010.02.002
Haigh, I. D., Nicholls, R. J., & Wells, N. C. (2010b). A comparison of the main methods for estimating probabilities of extreme still water levels. *Coastal Engineering*, *57*(9), 838–849. https://doi.org/10.1016/j.coastaleng.2010.04.002
Hall, G. F., Hill, D. F., Horton, B. P., Engelhart, S. E., & Peltier, W. R. (2013). A high-resolution study of tides in the Delaware Bay: Past conditions and future scenarios. *Geophysical Research Letters*, *40*, 338–342. https://doi.org/10.1029/2012GL054675
Hallam, A. (1984). Pre-Quaternary sea-level changes. *Annual Review of Earth and Planetary Sciences*, *12*(1), 205–243. https://doi.org/10.1146/annurev.ea.12.050184.001225
Haq, B. U. (2018). Triassic eustatic variations reexamined. *GSA Today*, *28*(12), 4–9. https://doi.org/10.1130/GSATG381A.1
Hardisty, J. (2008). Power intermittency, redundancy and tidal phasing around the United Kingdom. *Geographical Journal*, *174*(1), 76–84. https://doi.org/10.1111/j.1475-4959.2007.00263.x
Harker, A., Green, J. A. M., Schindelegger, M., & Wilmes, S.-B. (2019). The impact of sea-level rise on tidal characteristics around Australia. *Ocean Science*, *15*(1), 147–159. https://doi.org/10.5194/os-15-147-2019
Hartmann, T., & Wenzel, H.-G. (1995). The HW95 tidal potential catalogue. *Geophysical Research Letters*, *22*, 3553–3556. https://doi.org/10.1029/95GL03324
Haurwitz, B., & Cowley, A. D. (1973). The diurnal and semidiurnal barometric oscillations, global distribution and annual variation. *Pure and Applied Geophysics*, *102*, 193–222. https://doi.org/10.1007/BF00876607
Hill, A., Brown, J., & Fernand, L. (1996). The western Irish Sea gyre: A retention system for Norway lobster (Nephrops norvegicus)? *Oceanologica Acta*, *19*, 357–368.
Hill, D. F. (2016). Spatial and temporal variability in tidal range: Evidence, causes, and effects. *Current Climate Change Reports*, *2*(4), 232–241. https://doi.org/10.1007/s40641-016-0044-8

Hill, D. F., Griffiths, S. D., Peltier, W. R., Horton, B. P., & Törnqvist, T. E. (2011). High-resolution numerical modeling of tides in the western Atlantic, Gulf of Mexico, and Caribbean Sea during the Holocene. *Journal of Geophysical Research*, *116*, C10014. https://doi.org/10.1029/2010JC006896

Hinkel, J., Lincke, D., Vafeidis, A. T., Perrette, M., Nicholls, R. J., Tol, R. S. J., et al. (2014). Future coastal flood damage and adaptation costs. *Proceedings of the National Academy of Sciences*, *111*(9), 3292–3297. https://doi.org/10.1073/pnas.1222469111

Hinton, A. C. (1995). Holocene tides of The Wash, U.K.: The influence of water-depth and coastline-shape changes on the record of sea-level change. *Marine Geology*, *124*(1-4), 87–111. https://doi.org/10.1016/0025-3227(95)00034-V

Hinton, A. C. (1996). Tides in the northeast Atlantic: Considerations for modelling water depth changes. *Quaternary Science Reviews*, *15*(8-9), 873–894. https://doi.org/10.1016/S0277-3791(96)00061-3

Hoitink, A. J. F., & Jay, D. A. (2016). Tidal river dynamics: Implications for deltas. *Reviews of Geophysics*, *54*, 240–272. https://doi.org/10.1002/2015RG000507

Hollebrandse, F.A.P. (2005). Temporal development of the tidal range in the southern North Sea. Master's thesis, Faculty of Civil Engineering and Geosciences, Delft University of Technology.

Holleman, R. C., & Stacey, M. T. (2014). Coupling of sea level rise, tidal amplification, and inundation. *Journal of Physical Oceanography*, *44*(5), 1439–1455. https://doi.org/10.1175/JPO-D-13-0214.1

Horner-Devine, A. R., Jay, D. A., Orton, P. M., & Spahn, E. Y. (2009). A conceptual model of the strongly tidal Columbia River plume. *Journal of Marine Systems*, *78*, 460–475. https://doi.org/10.1016/j.jmarsys.2008.11.025

Horsburgh, K. J., & Wilson, C. (2007). Tide-surge interaction and its role in the distribution of surge residuals in the North Sea. *Journal of Geophysical Research*, *112*, C10009. https://doi.org/10.1029/2006JC004033

Howard, T., Lowe, J., & Horsburgh, K. (2010). Interpreting century-scale changes in southern North Sea storm surge climate derived from coupled model simulations. *Journal of Climate*, *23*, 6234–6247. https://doi.org/10.1175/2010JCLI3520.1

Howarth, M. J. (1998). The effect of stratification on tidal current profiles. *Continental Shelf Research*, *18*(11), 1235–1254. https://doi.org/10.1016/S0278-4343(98)00042-9

Huijts, K. M. H., Schuttelaars, H. M., de Swart, H. E., & Friedrichs, C. T. (2009). Analytical study of the transverse distribution of along-channel and transverse residual flows in tidal estuaries. *Continental Shelf Research*, *29*, 89–100. https://doi.org/10.1016/j.csr.2007.09.007

Idier, D., & Astruc, D. (2003). Analytical and numerical modeling of sandbanks dynamics. *Journal of Geophysical Research*, *108*(C3), 3060. https://doi.org/10.1029/2001JC001205

Idier, D., Dumas, F., & Muller, H. (2012). Tide-surge interaction in the English Channel. *Natural Hazards and Earth System Sciences*, *12*(12), 3709–3718. https://doi.org/10.5194/nhess-12-3709-2012

Idier, D., Paris, F., Cozannet, G. L., Boulahya, F., & Dumas, F. (2017). Sea-level rise impacts on the tides of the European Shelf. *Continental Shelf Research*, *137*, 56–71. https://doi.org/10.1016/j.csr.2017.01.007

Intergovernmental Oceanographic Commission (1985). Manual on sea level measurement and interpretation Volume I—Basic procedures. Report of the Intergovernmental Oceanographic Commission. https://www.psmsl.org/train_and_info/training/manuals/ioc_14i.pdf

Ippen, A. T. and D.R.F. Harleman (1961). One-ldimensional analysis of salinity intrusion in estuaries. Technical Bulletin no. 5, Committee on Tidal Hydraulics Waterways Experiment Station, Vicksburg, Mississippi. Officer, C. B. 1976

Jay, D. A. (1991). Green's law revisited: Tidal long wave propagation in channels with strong topography. *Journal of Geophysical Research*, *96*, 20,585–20,598. https://doi.org/10.1029/91JC01633

Jay, D. A. (2009). Evolution of tidal amplitudes in the eastern Pacific Ocean. *Geophysical Research Letters*, *36*, L04603. https://doi.org/10.1029/2008GL036185

Jay, D. A., & Flinchem, E. P. (1997). Interaction of fluctuating river flow with a barotropic tide: A demonstration of wavelet tidal analysis methods. *Journal of Geophysical Research*, *102*(C3), 5705–5720. https://doi.org/10.1029/96JC00496

Jay, D. A., Leffler, K., & Degens, S. (2011). Long-term evolution of Columbia River tides. *Journal of Waterway, Port, Coastal, and Ocean Engineering*, *137*(4), 182–191. https://doi.org/10.1061/(ASCE)WW.1943-5460.0000082

Jay, D. A., Leffler, K., Diefenderfer, H. L., & Borde, A. B. (2015). Tidal-fluvial and estuarine processes in the Lower Columbia River: I. Along-Channel Water Level Variations, Pacific Ocean to Bonneville Dam. *Estuaries and Coasts*, *38*(2), 415–433. https://doi.org/10.1007/s12237-014-9819-0

Jensen, J., Mudersbach, C., & Blasi, C. (2003). Hydrological changes in tidal estuaries due to natural and anthropogenic effects. 6th International MEDCOAST2003 Conference, Ravenna, Italy.

Jensen, J., & Mudersbach, C. H. (2005). Recent sea level variations at the North Sea and Baltic Sea coastlines. Book of Abstracts ICEST 2005, New Orleans, USA.

Kagan, B. A. (1997). Earth-Moon tidal evolution: Model results and observational evidence. *Progress in Oceanography*, *40*(1-4), 109–124. https://doi.org/10.1016/S0079-6611(97)00027-X

Kagan, B. A., & Sündermann, J. (1996). Dissipation of tidal energy, paleotides, and evolution of the Earth-Moon system. *Advances in Geophysics*, *38*, 179–266. https://doi.org/10.1016/S0065-2687(08)60021-7

Kang, S. K., Foreman, M. G. G., Lie, H. J., Lee, J. H., Cherniawsky, J., & Yum, K. D. (2002). Two-layer modeling of the Yellow and East China Seas with application to seasonal variability of the M2 tide. *Journal of Geophysical Research*, *107*(C3), 3020. https://doi.org/10.1029/2001JC000838

Kauker, F. (1998). Regionalisation of climate model results for the North Sea. PhD Thesis, University of Hamburg.

Kauker, F., & Langenberg, H. (2000). Two models for the climate change related development of sea levels in the North Sea. A comparison. *Climate Research*, *15*, 61–67. https://doi.org/10.3354/cr015061

Kay, D. J., & Jay, D. A. (2003). Interfacial mixing in a highly stratified estuary 1. Characteristics of mixing. *Journal of Geophysical Research*, *108*(C3), 3072. https://doi.org/10.1029/2000JC000252

Keller, H. (1901). *Weser and Ems, ihre Stromgebiete und ihre wichtigsten Nebenfluesse: Eine hydrographische, wasserwirtschaftlichte und wasserrechtliche Darstellung* (Vol. IV, p. 575). Berlin: Dietrich Reimer.

Kemp, A. C., Hill, T. D., Vane, C. H., Cahill, N., Orton, P. M., Talke, S. A., et al. (2017). Relative sea-level trends in New York City during the past 1500 years. *The Holocene*, *27*(8), 1169–1186. https://doi.org/10.1177/0959683616683263

Ku, L.-F., Greenberg, D. A., Garrett, C. J. R., & Dobson, F. W. (1985). Nodal modulations of the lunar semidiurnal tide in the Bay of Fundy and the Gulf of Maine. *Science*, *230*(4721), 69–71. https://doi.org/10.1126/science.230.4721.69

Lacy, J. R., & Monismith, S. G. (2001). Secondary currents in a curved stratified, estuarine, channel. *Journal of Geophysical Research*, *106*(C12), 31,283–31,302. https://doi.org/10.1029/2000JC000606

Lane, A. (2004). Bathymetric evolution of the Mersey Estuary, UK, 1906–1997: causes and effects. *Estuarine, Coastal and Shelf Science*, *59*(2), 249–263. https://doi.org/10.1016/j.ecss.2003.09.003

Leblond, P. H. (1979). Forced fortnightly tides in shallow rivers. *Atmosphere-Ocean*, *17*(3), 253–264. https://doi.org/10.1080/07055900.1979.9649064

Lee, S. B., Li, M., & Zhang, F. (2017). Impact of sea level rise on tidal range in Chesapeake and Delaware Bays. *Journal of Geophysical Research: Oceans*, *122*, 3917–3938. https://doi.org/10.1002/2016JC012597

Leorri, E., Mulligan, R., Mallinson, D., & Cearretta, A. (2011). Sea-level rise and local tidal range changes in coastal embayments: An added complexity in developing reliable sea-level index points. *Journal of Integrated Coastal Zone Management*, *11*(3), 307–314.

Li, C., Schuttelaars, H. M., Roos, P. C., Damveld, J. H., Gong, W., & Hulscher, S. J. M. H. (2016). Influence of retention basins on tidal dynamics in estuaries: Application to the Ems estuary. *Ocean and Coastal Management*, *134*, 216–225. https://doi.org/10.1016/j.ocecoaman.2016.10.010

Losada, M. A., Díez-Minguito, M., & Reyes-Merlo, M. (2017). Tidal-fluvial interaction in the Guadalquivir River Estuary: Spatial and frequency-dependent response of currents and water levels. *Journal of Geophysical Research: Oceans*, *122*, 847–865. https://doi.org/10.1002/2016JC011984

Lowe, J. A., & Gregory, J. M. (2005). The effects of climate change on storm surges around the United Kingdom. *Philosophical Transactions of the Royal Society A*, *363*, 1313–1328. https://doi.org/10.1098/rsta.2005.1570

Lowe, J. A., Howard, T, A. Pardaens, Tinker, J., Holt, J., Wakelin, S., et al. (2009). *UK Climate Projections science report: Marine and coastal projections*. UK Climate Projections. Exeter: Met Office Hadley Centre.

Luz Clara, M., Simionato, C. G., D'Onofrio, E., & Moreira, D. (2015). Future sea level rise and changes on tides in the Patagonian Continental Shelf. *Journal of Coastal Research*, *31*(3), 519–535. https://doi.org/10.2112/JCOASTRES-D-13-00127.1

MacKay, D. J. C. (2008). *Sustainable energy—Without the hot air* (Vol. 2008). Cambridge, UK: UIT Cambridge. ISBN: 978-0-9544529-3-3.

Marmer, H. A. (1935). *Tides and currents in New York Harbor*, *U. S. C.and G. S. Special Publication*(Vol. 111, revised edn., 198 pp.). Washington, DC: US Coast and Geodetic Survey.

Masselink, G., & Russell, P. (2013). Impacts of climate change on coastal erosion. *MCCIP Science Review*, *2013*, 71–86. https://doi.org/10.14465/2013.arc09.071-086

Matthäus, W. (1972). On the history of recording tide gauges. *Proceedings Royal Society Edinburgh, Section B*, *73*(3), 25–34.

Matthews, K. J., Maloney, K. T., Zahirovic, S., Williams, S. E., Seton, M., & Müller, R. D. (2016). Global plate boundary evolution and kinematics since the late Paleozoic. *Global and Planetary Change*, *146*, 226–250. https://doi.org/10.1016/j.gloplacha.2016.10.002

Mawdsley, R., & Haigh, I. D. (2016). Spatial and temporal variability and long-term trends in skew surges globally. *Frontiers in Marine Science*, *3*, 29.

Mawdsley, R. J., Haigh, I. D., & Wells, N. C. (2015). Global secular changes in different tidal high water, low water and range levels. *Earth's Future*, *3*(2), 66–81. https://doi.org/10.1002/2014EF000282

McLean, S. R., & Smith, J. D. (1979). Turbulence measurements in the boundary layer over a sand wave field. *Journal of Geophysical Research*, *84*(C12), 7791–7808. https://doi.org/10.1029/JC084iC12p07791

Middleton, G. V. (1991). A short historical review of clastic tidal sedimentology. In D. G. Smith, G. E. Reinson, B. A. Zaitlin, & R. A. Rahmani (Eds.), *Clastic tidal sedimentology*, *Canadian Society of Petroleum Geologists' Memoir* (Vol. 16, pp. ix–xv). Calgary: CSPG.

Mitchum, G. T., & Chiswell, S. M. (2000). Coherence of internal tide modulations along the Hawaiian Ridge. *Journal of Geophysical Research*, *105*(C12), 28,653–28,661. https://doi.org/10.1029/2000JC900140

Moftakahri, H. R., Jay, D. A., Talke, S. A., Kulkulka, T., & Bromirski, P. D. (2013). A novel approach to flow estimation in tidal rivers. *Water Resources Research*, *49*, 1–16. https://doi.org/10.1002/wrcr.20363

Moftakhari, H. R., Jay, D. A., & Talke, S. A. (2016). Estimating river discharge using multiple-tide gages distributed along a channel. *Journal of Geophysical Research: Oceans*, *121*, 2078–2097. https://doi.org/10.1002/2015JC010983

Moftakhari, H. R., Jay, D. A., Talke, S. A., & Schoellhamer, D. H. (2015). Estimation of historic flows and sediment loads to San Francisco Bay, 1849–2011. *Journal of Hydrology*, *529*, 1247–1261. https://doi.org/10.1016/j.jhydrol.2015.08.043

Montenegro, A., Eby, M., Weaver, A. J., & Jayne, S. R. (2007). Response of a climate model to tidal mixing parameterization under present day and Last Glacial Maximum conditions. *Ocean Modelling*, *19*(3–4), 125–137. https://doi.org/10.1016/j.ocemod.2007.06.009

Morris, R. K. A., & Mitchell, S. B. (2013). Has loss of accommodation space in the Humber Estuary led to elevated suspended sediment concentrations? *Journal of Frontiers in Construction Engineering*, *2*, 1–9.

Müller, M. (2007). The free oscillations of the world ocean in the period range 8 to 165 hours including the full loading effect. *Geophysical Research Letters*, *34*, L05606. https://doi.org/10.1029/2006GL028870

Müller, M. (2008). Synthesis of forced oscillations, Part I: Tidal dynamics and the influence of the loading and self-attraction effect. *Ocean Modelling*, *20*(3), 207–222. https://doi.org/10.1016/j.ocemod.2007.09.001

Müller, M. (2011). Rapid change in semi-diurnal tides in the North Atlantic since 1980. *Geophysical Research Letters*, *38*, L11602. https://doi.org/10.1029/2011GL047312

Müller, M. (2012). The influence of changing stratification conditions on barotropic tidal transport and its implications for seasonal and secular changes of tides. *Continental Shelf Research*, *47*, 107–118. https://doi.org/10.1016/j.csr.2012.07.003

Müller, M., Arbic, B. K., & Mitrovica, J. X. (2011). Secular trends in ocean tides: Observations and model results. *Journal of Geophysical Research*, *116*, C05013. https://doi.org/10.1029/2010JC006387

Müller, M., Cherniawsky, J., Foreman, M., & von Storch, J.-S. (2012). Global map of M2 internal tide and its seasonal variability from high resolution ocean circulation and tide modelling. *Geophysical Research Letters*, *39*, L19607. https://doi.org/10.1029/2012GL053320

Müller, M., Cherniawsky, J., Foreman, M., & von Storch, J.-S. (2014). Seasonal variation of the M2 tide. *Ocean Dynamics*, *64*(2), 159–177. https://doi.org/10.1007/s10236-013-0679-0

Müller-Navarra, S., & Bork, I. (2011). Development of an operational Elbe tidal estuary model. *Coastal Engineering Proceedings*, *1*, 48. https://doi.org/10.9753/icce.v32.management.48

Munk, W. (1966). Abyssal recipes. *Deep Sea Research and Oceanographic Abstracts*, *13*(4), 707–730. https://doi.org/10.1016/0011-7471(66)90602-4

Munk, W., & Bills, B. (2007). Tides and the climate: Some speculations. *Journal of Physical Oceanography*, *37*, 135–147. https://doi.org/10.1175/JPO3002.1

Munk, W., & Cartwright, D. E. (1966). Tidal spectroscopy and prediction. *Philosophical Transactions of the Royal Society*, *259*, 533–581. https://doi.org/10.1098/rsta.1966.0024

Munk, W., & Wunsch, C. (1998). Abyssal recipes II: Energetics of tidal and wind mixing. *Deep Sea Research Part I: Oceanographic Research Papers*, *45*, 1977–2010. https://doi.org/10.1016/S0967-0637(98)00070-3

Naik, P. K., & Jay, D. A. (2011). Distinguishing human and climate influences on the Columbia River: Changes in mean flow and sediment transport. *Journal of Hydrology*, *404*(3-4), 259–277. https://doi.org/10.1016/j.jhydrol.2011.04.035

Nimmo-Smith, W. A. M., Thorpe, S. A., & Graham, A. (1999). Surface effects of bottom-generated turbulence in a shallow tidal sea. *Nature*, *400*(6741), 251–254. https://doi.org/10.1038/22295

Nycander, J. (2005). Generation of internal waves in the deep ocean by tides. *Journal of Geophysical Research*, *110*, C10028. https://doi.org/10.1029/2004JC002487

Ohno, T. (1989). Palaeotidal characteristics determined by micro-growth patterns in bivalves. *Palaeontology*, *32*, 237–263.

Orton, P. M., Talke, S. A., Jay, D. A., Yin, L., Blumberg, A. F., Georgas, N., et al. (2015). Channel shallowing as mitigation of coastal flooding. *Journal of Marine Science and Engineering*, *3*(3), 654–673. https://doi.org/10.3390/jmse3030654

Padman, L., Siegfried, M. R., & Fricker, H. A. (2018). Ocean tide influences on the Antarctic and Greenland ice sheets. *Reviews of Geophysics*, *56*, 142–184. https://doi.org/10.1002/2016RG000546

Palmer, M., Howard, T., Tinker, J., Lowe. J., Bricheno, L., Calvert, D., et al.. (2018). UKCP18 Marine Report. Retrieved from https://www.metoffice.gov.uk/pub/data/weather/uk/ukcp18/science-reports/UKCP18-Marine-report.pdf

Pannella, G. (1976). Tidal growth patterns in recent and fossil mollusc bivalve shells: A tool for the reconstruction of paleotides. *The Science of Nature*, *63*, 539–543.

Passeri, D. L., Hagen, S. C., Plant, N. G., Bilskie, M. V., Medeiros, S. C., & Alizad, K. (2016). Tidal hydrodynamics under future sea level rise and coastal morphology in the Northern Gulf of Mexico. *Earth's Future*, *4*, 159176. https://doi.org/10.1002/2015EF000332

Pelling, H. E., & Green, J. A. M. (2014). Impact of flood defences and sea-level rise on the European Shelf tidal regime. *Continental Shelf Research*, *85*, 96–105. https://doi.org/10.1016/j.csr.2014.04.011

Pelling, H. E., Green, J. A. M., & Ward, S. L. (2013). Modelling tides and sea-level rise: To flood or not to flood. *Ocean Modelling*, *63*, 21–29. https://doi.org/10.1016/j.ocemod.2012.12.004

Pelling, H. E., Uehara, K., & Green, J. A. M. (2013). The impact of rapid coastline changes and sea level rise on the tides in the Bohai Sea, China. *Journal of Geophysical Research: Oceans*, *118*, 3462–3472. https://doi.org/10.1002/jgrc.20258

Peltier, W. R. (2004). Global glacial isostasy and the surface of the ice-age earth: The ICE-5G (VM2) model and GRACE. *Annual Reviews of Earth and Planetary Science*, *32*(1), 111–149. https://doi.org/10.1146/annurev.earth.32.082503.144359

Peltier, W. R., Argus, D. F., & Drummond, R. (2015). Space geodesy constrains ice age terminal deglaciation: The global ICE-6G_C (VM5a) model. *Journal of Geophysical Research: Solid Earth*, *120*, 450–487. https://doi.org/10.1002/2014JB011176

Pickering, M. D. (2010). Development and validation of a new barotropic tidal model in order to investigate the effect of future sea-level rise on the global tides. Masters Thesis, School of Ocean and Earth Science, p. 34. University of Southampton, Southampton.

Pickering, M. D. (2014). The impact of future sea-level rise on the tides. PhD Thesis, University of Southampton, Ocean and Earth Science, 347pp.

Pickering, M. D., Horsburgh, K. J., Blundell, J. R., Hirschi, J. J.-M., Nicholls, R. J., Verlaan, M., & Wells, N. C. (2017). The impact of future sea-level rise on the global tides. *Continental Shelf Research*, *142*, 50–68. https://doi.org/10.1016/j.csr.2017.02.004

Pickering, M. D., Wells, N. C., Horsburgh, K. J., & Green, J. A. M. (2012). The impact on the European Shelf tides by future sea-level rise. *Continental Shelf Research*, *35*, 1–15. https://doi.org/10.1016/j.csr.2011.11.011

Piersma, T., Rogers, D. I., González, P. M., Zwarts, L., Niles, L. J., De Lima Serrano do Nascimento, I., et al. (2005). Fuel storage rates before northward flights in red knots worldwide: Facing the severest ecological constraint in tropical intertidal environments? In R. Greenberg & P. P. Marra (Eds.), *Birds of two worlds: ecology and evolution of migration* (pp. 262–273). Baltimore: Johns Hopkins University Press.

Plag, H.-P. (1985). Temporal variations of ocean tides. In R. Viera (Ed.), Madrid, September 23-27 1985*Proceedings of the 10th International Symposium on Earth Tides (with special sessions dedicated to ocean tides)* (pp. 595–608). Madrid: Consejo Superior de Investigaciones Cientificas.

Platzman, G. W. (1978). Normal Modes of the World Ocean. Part I. Design of a Finite-Element Barotropic Model. *Journal of Physcical Oceanography*. https://doi.org/10.1175/1520-0485(1978)008<0323:NMOTWO>2.0.CO;2

Platzman, G. W., Curtis, G. A., Hansen, K. S., & Slater, R. D. (1981). Normal modes of the world ocean, Part 2. Description of modes in the range 8 to 80 hours. *Journal of Physical Oceanography*, *11*(5), 579–603. https://doi.org/10.1175/1520-0485(1981)011<0579:NMOTWO>2.0.CO;2

Plüß, A. (2004). Das Nordseemodell der BAW zur Simulation der Tide in der Deutschen Bucht. *Die K¨ uste*, *67*, 83–127.

Pouvreau, N., Miguez, B. M., Simon, B., & Wöppelmann, G. (2006). Évolution de l'onde semi-diurne M2 de la marée à Brest de 1846 à 2005. *Comptes Rendus Geoscience*, *338*(11), 802–808. https://doi.org/10.1016/j.crte.2006.07.003

Powell, C. F. (1884). *Report of Mr. J.S. Polhemus, Assistant Engineer*, *Annual Report of the Chief of Engineers, U.S. Army, Appendix QQ- 13* (p. 2406). Washington, DC: Government Printing Office.

Prandle, D., & Rahman, M. (1980). Tidal response in estuaries. *Journal of Physical Onceaography*, *10*(10), 1552–1573. https://doi.org/10.1175/1520-0485(1980)010<1552:TRIE>2.0.CO;2

Prandle, D., & Wolf, J., (1978). The interaction of surge and tide in the North Sea and River Thames. Institute of Oceanographic Sciences.

Prinsenberg, S. (1988). Damping and phase advance of the tide in western Hudson Bay by the annual ice cover. *Journal of Physical Oceanography*, *18*(11), 1744–1751. https://doi.org/10.1175/1520-0485(1988)018<1744:DAPAOT>2.0.CO;2

Pugh, D., & Woodworth, P. (2014). *Sea-level science: Understanding tides, surges, tsunamis and mean sea-level changes* (p. 395). Cambridge: Cambridge University Press.

Pugh, D. T. (1987). *Tides, surges and mean sea-level: A handbook for engineers and scientists* (p. 472). Hoboken, NJ: John Wiley.

Rabaut, M., Audfroid Calderón, M., Van de Moortel, L., van Dalfsen, J., Vincx, M., Degraer, S., & Desroy, N. (2013). The role of structuring benthos for juvenile flatfish. *Journal of Sea Research*, *84*, 70–76. https://doi.org/10.1016/j.seares.2012.07.008

Ralston, D. K., Talke, S. A., Geyer, W. R., Al-Zubaidi, H. A. M., & Sommerfield, C. K. (2019). Bigger tides, less flooding: Effects of dredging on barotropic dynamics in a highly modified estuary. *Journal of Geophysical Research: Oceans*, *124*, 196–211. https://doi.org/10.1029/2018JC014313

Rasheed, A. S., & Chua, V. P. (2014). Secular trends in tidal parameters along the Coast of Japan. *Atmosphere-Ocean*, *52*(2), 155–168. https://doi.org/10.1080/07055900.2014.886031

Ray, R. D. (2006). Secular changes of the M_2 tide in the Gulf of Maine. *Continental Shelf Research*, *26*(3), 422–427. https://doi.org/10.1016/j.csr.2005.12.005

Ray, R. D. (2009). Secular changes in the solar semidiurnal tide of the western North Atlantic Ocean. *Geophysical Research Letters*, *36*, L02610. https://doi.org/10.1029/2009GL040217
Ray, R. D. (2016). On measurements of the tide at Churchill, Hudson Bay. *Atmosphere-Ocean*, *54*(2), 108–116. https://doi.org/10.1080/07055900.2016.1139540
Ray, R. D., & Egbert, G. (2004). The global S_1 tide. *Journal of Physical Oceanography*, *34*(8), 1922–1935. https://doi.org/10.1175/1520-0485(2004)034<1922:TGST>2.0.CO;2
Ray, R. D., Egbert, G. D., & Erofeeva, S. Y. (2011). Tide predictions in shelf and coastal waters: Status and prospects. In *Coastal altimetry* (pp. 191–216). Berlin Heidelberg, Berlin, Heidelberg: Springer.
Ray, R. D., & Foster, G. (2016). Future nuisance flooding at Boston caused by astronomical tides alone. *Earth's Future*, *4*, 578–587. https://doi.org/10.1002/2016EF000423
Ray, R. D., & Talke, S. A. (2019). Nineteenth-century tides in the Gulf of Maine and implications for secular trends. *Journal of Geophysical Research: Oceans*, *124*, 7046–7067. https://doi.org/10.1029/2019JC015277
Reidy, M. S. (2008). *Tides of history: Ocean science and her majesty's navy*. Chicago: University of Chicago Press.
Robins, P. E., Neill, S. P., Lewis, M. J., & Ward, S. L. (2015). Characterising the spatial and temporal variability of the tidal-stream energy resource over the northwest European shelf seas. *Applied Energy*, *147*, 510–522. https://doi.org/10.1016/j.apenergy.2015.03.045
Rodríguez-Padilla, I., & Ortiz, M. (2017). On the secular changes in the tidal constituents in San Francisco Bay. *Journal of Geophysical Research: Oceans*, *122*, 7395–7406. https://doi.org/10.1002/2016JC011770
Rosenfeld, L. K. (1988). Diurnal period wind stress and current fluctuations over the continental shelf off northern California. *Journal of Geophysical Research*, *93*(C3), 2257–2276. https://doi.org/10.1029/JC093iC03p02257
Rosier, S. H. R., Green, J. A. M., Scourse, J. D., & Winkelmann, R. (2014). Modeling Antarctic tides in response to ice shelf thinning and retreat. *Journal of Geophysical Research: Oceans*, *119*, 87–97. https://doi.org/10.1002/2013JC009240
Ross, A. C., Najar, R. G., Li, M., Lee, S. B., Zhang, F., & Liu, W. (2017). Fingerprints of sea level rise on changing tides in the Chesapeake and Delaware Bays. *Journal of Geophysical Research: Oceans*, *122*, 8102–8125. https://doi.org/10.1002/2017JC012887
Santamaria-Aguilar, S., Schuerch, M., Vafeidis, A. T., & Carretero, S. C. (2017). Long-term trends and variability of water levels and tides in Buenos Aires and Mar del Plata, Argentina. *Frontiers in Marine Science*, *4*, 4854. https://doi.org/10.3389/fmars.2017.00380
Schindelegger, M., Einšpigel, D., Salstein, D., & Böhm, J. (2016). The global S_1 tide in Earth's nutation. *Surveys in Geophysics*, *37*, 643–680. https://doi.org/10.1007/s10712-016-9365-3
Schindelegger, M., Green, J. A. M., Wilmes, S.-B., & Haigh, I. D. (2018). Can we model the effect of observed sea level rise on tides? *Journal of Geophysical Research: Oceans*, *123*, 4593–4609. https://doi.org/10.1029/2018JC013959
Schindelegger, M., Salstein, D., Einšpigel, D., & Mayerhofer, C. (2017). Diurnal atmosphere-ocean signals in Earth's rotation rate and a possible modulation through ENSO. *Geophysical Research Letters*, *44*, 2755–2762. https://doi.org/10.1002/2017GL072633
Schmittner, A., Green, J. A. M., & Wilmes, S.-B. (2015). Glacial ocean overturning intensified by tidal mixing in a global circulation model. *Geophysical Research Letters*, *42*, 4014–4022. https://doi.org/10.1002/2015GL063561
Schoellhamer, D. H. (2011). Sudden clearing of estuarine waters upon crossing the threshold from transport to supply regulation of sediment transport as an erodible sediment pool is depleted: San Francisco Bay, 1999. *Estuaries and Coasts*, *34*(5), 885–899. https://doi.org/10.1007/s12237-011-9382-x
Schuerch, M., Spencer, T., Temmerman, S., Kirwan, M. L., Wolff, C., Lincke, D., et al. (2018). Future response of global coastal wetlands to sea-level rise. *Nature*, *561*, 231–234. https://doi.org/10.1038/s41586-018-0476-5
Schureman, P. (1934). *Tides and currents in Hudson River*, *U.S. Coast and Geodetic Survey Special Publication* (Vol. 180). Washington, DC: United States Government Printing Office.
Schwinghamer, P., Guigné, J. Y., & Siu, W. C. (1996). Quantifying the impact of trawling on benthic habitat structure using high resolution acoustics and chaos theory. *Canadian Journal of Fisheries and Aquatic Sciences*, *53*(2), 288–296. https://doi.org/10.1139/cjfas-53-2-288
Scott, B., Sharples, J., Ross, O., Wang, J., Pierce, G., & Camphuysen, C. (2010). Sub-surface hotspots in shallow seas: Fine-scale limited locations of top predator foraging habitat indicated by tidal mixing and sub-surface chlorophyll. *Marine Ecology Progress Series*, *408*, 207–226. https://doi.org/10.3354/meps08552
Scott, B., Webb, A., Palmer, M., Embling, C., & Sharples, J. (2013). Fine scale biophysical oceanographic characteristics predict the foraging occurrence of contrasting seabird species; Gannet (Morus bassanus) and storm petrel (Hydrobates pelagicus). *Progress in Oceanography*, *117*, 118–129. https://doi.org/10.1016/j.pocean.2013.06.011
Scott, D. B., & Greenberg, D. A. (1983). Relative sea-level rise and tidal development in the Fundy tidal system. *Canadian Journal of Earth Sciences*, *20*, 1554–1564. https://doi.org/10.1139/e83-145
Scottish Government, (2012). Consultation seeking views on new controls in the Scottish creel fisheries and on increasing the minimum landing size for West of Scotland. (Web publication only).
Scourse, J. D., Austin, W. E., Long, B. T., Assinder, D. J., & Huws, D. (2002). Holocene evolution of seasonal stratification in the Celtic Sea: Refined age model, mixing depths and foraminiferal stratigraphy. *Marine Geology*, *191*(3-4), 119–145. https://doi.org/10.1016/S0025-3227(02)00528-5
Seafish (2007). Retrieved from http://www.seafish.org/media/Publications/PilotPotFishery.pdf
Shalowitz, A. L. (1962). *Shore and sea boundaries: With special reference to the interpretation and use of coast and geodetic survey data* (Vol. 1). Washington, DC: Government Printing Office.
Shalowitz, A. L. (1964). *Shore and sea boundaries: With special reference to the interpretation and use of coast and geodetic survey data* (Vol. 2). Washington, DC: Government Printing Office.
Sharples, J. (2008). Potential impacts of the spring-neap tidal cycle on shelf sea primary production. *Journal of Plankton Research*, *30*, 183–197.
Sharples, J., Tweddle, J. F., Mattias Green, J. A., Palmer, M. R., Kim, Y. N., Hickman, A. E., et al. (2007). Spring-neap modulation of internal tide mixing and vertical nitrate fluxes at a shelf edge in summer. *Limnology and Oceanography*, *52*(5), 1735–1747. https://doi.org/10.4319/lo.2007.52.5.1735
Shaw, A. G. P., & Tsimplis, M. N. (2010). The 18.6yr nodal modulation in the tides of Southern European coasts. *Continental Shelf Research*, *30*(2), 138–151. https://doi.org/10.1016/j.csr.2009.10.006
Shennan, I., & Horton, B. (2002). Holocene land-and sea-level changes in Great Britain. *Journal of Quaternary Science*, *17*, 511–526. https://doi.org/10.1002/jqs.710
Shennan, I., Lambeck, K., Flather, R., Horton, B., McArthur, J., Innes, J., et al. (2000). Modelling western North Sea palaeogeographies and tidal changes during the Holocene. *Geological Society, London, Special Publications*, *166*, 299–319. https://doi.org/10.1144/GSL.SP.2000.166.01.15

Simpson, J., & Sharples, J. (2012). *Introduction to the physical and biological oceanography of shelf seas*. Cambridge: Cambridge University Press. https://doi.org/10.1017/CBO9781139034098

Simpson, J. H., & Hunter, J. (1974). Fronts in the Irish Sea. *Nature*, *250*(5465), 404–406. https://doi.org/10.1038/250404a0

Stanford, J. D., Hemingway, R., Rohling, E. J., Challenor, P. G., Medina-Elizalde, M., & Lester, A. J. (2011). Sea-level probability for the last deglaciation: A statistical analysis of far-field records. *Global and Planetary Change*, *79*(3-4), 193–203. https://doi.org/10.1016/j.gloplacha.2010.11.002

Sterl, A., van den Brink, H., de Vries, H., Haarsma, R., & van Meijgaard, E. (2009). An ensemble study of extreme storm surge related water levels in the North Sea in a changing climate. *Ocean Science*, *5*, 369–378. https://doi.org/10.5194/os-5-369-2009

St-Laurent, P., Saucier, F. J., & Dumais, J. F. (2008). On the modification of tides in a seasonally ice-covered sea. *Journal of Geophysical Research*, *113*, C11014. https://doi.org/10.1029/2007JC004614

Stumpf, R. P., & Haines, J. W. (1998). Variations in tidal level in the Gulf of Mexico and implications for tidal wetlands. *Estuarine, Coastal and Shelf Science*, *46*(2), 165–173. https://doi.org/10.1006/ecss.1997.0276

Swinkels, C., van der Zwan, S., Bijlsma, A., & Pothof, I. (2010). Technical feasibility of energy conversion from salinity gradients along the Dutch coast; A case study at IJmuiden. In *Proceedings from the 1st IAHR European Congress*. Edinburgh, UK, 4-6 May 2010: Heriot-Watt University.

Talke, S. A., & H. E. de Swart (2006). Hydrodynamics and morphology in the Ems/Dollard estuary: Review of models, measurements, scientific literature, and the effects of changing conditions. *IMAU Report R-01-06*, 78 pp.

Talke, S. A., de Swart, H. E., & de Jonge, V. N. (2009). An idealized model and systematic process study of oxygen depletion in highly turbid estuaries. *Estuaries and Coasts*, *32*(4), 602–620. https://doi.org/10.1007/s12237-009-9171-y

Talke, S. A., Horner-Devine, A. R., Chickadel, C. C., & Jessup, A. T. (2013). Turbulent kinetic energy and coherent structures in a tidal river. *Journal of Geophysical Research: Oceans*, *118*, 6965–6981. https://doi.org/10.1002/2012JC008103

Talke, S. A., & Jay, D. A. (2013). Nineteenth century North American and Pacific tidal data: Lost or just forgotten? *Journal of Coastal Research*, *291*, 118–127. https://doi.org/10.2112/JCOASTRES-D-12-00181.1

Talke, S. A., & Jay, D. A. (2017). Archival water-level measurements: Recovering historical data to help design for the future. US Army Corps of Engineers: *Civil Works Technical Series, Report CWTS-02, ~50pp*.

Talke, S. A., & Jay, D. A. (2020). Changing tides: the role of natural and anthropogenic factors. *Annual Review of Marine Science*, *12*, 31479622. https://doi.org/10.1146/annurev-marine-010419-010727

Talke, S. A., Kemp, A., & Woodruff, J. (2018). Relative sea level, tides, and extreme water levels in Boston (MA) from 1825 to 2018. *Journal of Geophysical Research: Oceans*, *123*, 3895–3914. https://doi.org/10.1029/2017JC013645

Talke, S. A., Orton, P., & Jay, D. A. (2014). Increasing storm tides in New York Harbor, 1844-2013. *Geophysical Research Letters*, *41*, 3149–3155. https://doi.org/10.1002/2014GL059574

Talke, S. A., & Stacey, M. T. (2003). The influence of oceanic swell on flows over an estuarine intertidal mudflat in San Francisco Bay. *Estuarine, Coastal and Shelf Science*, *58*(3), 541–554. https://doi.org/10.1016/S0272-7714(03)00132-X

Tanavsuu-Milkeviciene, K., & Plink-Bjorklund, P. (2009). Recognizing tTide-dDominated Vversus Ttide-Iinfluenced Ddeltas: Middle Devonian Strata of the Baltic Basin. *Journal of Sedimentary Research*, *79*(12), 887–905. https://doi.org/10.2110/jsr.2009.096

Taylor, G. I. (1922). Tidal oscillations in gulfs and rectangular basins. *Proceedings of the London Mathematical Society*, *s2-20*(1), 148–181. https://doi.org/10.1112/plms/s2-20.1.148

Tennekes, H., & Lumley, J. L. (1990). *A First Course in Turbulence*. Cambridge, MA: MIT Press.

Thomas, H., Bozec, Y., Elkalay, K., & de Baar, H. J. W. (2004). Enhanced open ocean storage of CO_2 from shelf sea pumping. *Science*, *304*(5673), 1005–1008. https://doi.org/10.1126/science.1095491

Thomas, M., & Sündermann, J. (1999). Tides and tidal torques of the world ocean since the last glacial maximum. *Journal of Geophysical Research*, *104*(C2), 3159–3183. https://doi.org/10.1029/1998JC900097

Tojo, B., Ohno, T., & Fujiwara, T. (1999). Late Pleistocene changes of tidal amplitude and phase in Osaka Bay, Japan, reconstructed from fossil records and numerical model calculations. *Marine Geology*, *157*(3–4), 241–248. https://doi.org/10.1016/S0025-3227(98)00157-1

Uehara, K. (2001). Tidal changes in the Yellow/East China Sea caused by the rapid sea-level rise during the Holocene. *Science in China, Series B Chemistry*, *44*(Suppl 1), 126–134. https://doi.org/10.1007/BF02884818

Uehara, K., Scourse, J. D., Horsburgh, K. J., Lambeck, K., & Purcell, A. P. (2006). Tidal evolution of the northwest European shelf seas from the Last Glacial Maximum to the present. *Journal of Geophysical Research*, *111*, C09025. https://doi.org/10.1029/2006JC003531

Valentim, J. M., Vaz, L., Vaz, N., Silva, H., Duarte, B., Caçador, I., & Dias, J. M. (2013). Sea level rise impact in residual circulation in Tagus estuary and Ria de Aveiro lagoon. *Journal of Coastal Research*, *165*, 1981–1986. https://doi.org/10.2112/SI65-335.1

van der Molen, J., & de Swart, H. E. (2001). Holocene tidal conditions and tide-induced sand transport in the southern North Sea. *Journal of Geophysical Research*, *106*(C5), 9339–9362. https://doi.org/10.1029/2000JC000488

van Goor, M., Zitman, T., Wang, Z., & Stive, M. (2003). Impact of sea-level rise on the morphological equilibrium state of tidal inlets. *Marine Geology*, *202*(3-4), 211–227. https://doi.org/10.1016/S0025-3227(03)00262-7

Vellinga, N. E., Hoitink, A. J. F., van der Vegt, M., Zhang, W., & Hoekstra, P. (2014). Human impacts on tides overwhelm the effect of sea level rise on extreme water levels in the Rhine-Meuse delta. *Coastal Engineering*, *90*, 40–50.

Vellinga, P., Katsman, C. A., Sterl, A., Beersma, J. J., Church, J. A., Hazeleger, W., et al. (2009). Exploring high-end climate change scenarios for flood protection of the Netherlands. In *International Scientific Assessment carried out at request of the Delta Committee*, KNMI Scientific Report WR-2009-05 (pp. 1–144). the Netherlands: KNMI/Alterra.

von Storch, H., & Woth, K. (2008). Storm surges: Perspectives and options. *Sustainability Science*, *3*(1), 33–43. https://doi.org/10.1007/s11625-008-0044-2

Waltham, D. (2015). Milankovitch period uncertainties and their impact on cyclostratigraphy. *Journal of Sedimentary Research*, *85*(8), 990–998. https://doi.org/10.2110/jsr.2015.66

Wang, Z. B., Winterwerp, J. C., & He, Q. (2014). Interaction between suspended sediment and tidal amplification in the Guadalquivir Estuary. *Ocean Dynamics*, *64*(10), 1487–1498. https://doi.org/10.1007/s10236-014-0758-x

Ward, S. L., Green, J. A. M., & Pelling, H. E. (2012). Tides, sea-level rise and tidal power extraction on the European shelf. *Ocean Dynamics*, *62*, 1153–1167.

Ward, S. L., Neill, S. P., Scourse, J. D., Bradley, S. L., & Uehara, K. (2016). Sensitivity of palaeotidal models of the northwest European shelf seas to glacial isostatic adjustment since the Last Glacial Maximum. *Quaternary Science Reviews*, *151*, 198–211. https://doi.org/10.1016/j.quascirev.2016.08.034

Ward, S. L., Neill, S. P., Van Landeghem, K. J., & Scourse, J. D. (2015). Classifying seabed sediment type using simulated tidalinduced bed shear stress. *Marine Geology*, *367*, 94–104.

Webb, D. J. (1982). Tides and the evolution of the Earth-Moon system. *Geophysical Journal of the Royal Astronomical Society*, *70*(1), 261–271 . https://doi.org/10.1111/j.1365-246X.1982.tb06404.x

Whewell, W. (1836). Researches on the tides—Sixth series. On the results of an extensive system of tide observations made on the coasts of Europe and America in June 1835. *Philosophical Transactions of the Royal Society*, *126*, 289–341. https://doi.org/10.1098/rstl.1836.0019

Williams, G. E. (2000). Geological constraints on the Precambrian history of Earth's rotation and the Moon's orbit. *Reviews of Geophysics*, *38*(1), 37–59. https://doi.org/10.1029/1999RG900016

Williams, J., Horsburgh, K. J., Williams, J. A., & Proctor, R. N. F. (2016). Tide and skew surge independence: New insights for flood risk. *Geophysical Research Letters*, *43*, 6410–6417. https://doi.org/10.1002/2016GL069522

Wilmes, S.-B., & Green, J. A. M. (2014). The evolution of tides and tidal dissipation over the past 21,000 years. *Journal of Geophysical Research: Oceans*, *119*, 4083–4100. https://doi.org/10.1002/2013JC009605

Wilmes, S.-B., Green, J. A. M., Gomez, N., Rippeth, T. P., & Lau, H. (2017). Global tidal impacts of large-scale ice-sheet collapses. *Journal of Geophysical Research: Oceans*, *122*, 8354–8370. https://doi.org/10.1002/2017JC013109

Winterwerp, J. C., Wang, Z. B., van Braeckel, A., van Holland, G., & Kösters, F. (2013). Man-induced regimeshifts in small estuaries—II: a comparison of rivers. *Ocean Dynamics*, *63*, 1293–306.

Woods, M. A., Wilkinson, I. P., Leng, M. J., Riding, J. B., Vane, C. H., Lopes dos Santos, R. A., et al. (2019). Tracking Holocene palaeostratification and productivity changes in the Western Irish Sea: A multi-proxy record. *Palaeogeography, Palaeoclimatology, Palaeoecology*, *532*, 109231. https://doi.org/10.1016/j.palaeo.2019.06.004

Woodworth, P. (2006). The meteorological data of William Hutchinson and a Liverpool air pressure time series spanning 1768–1999. *International Journal of Climatology*, *26*(12), 1713–1726. https://doi.org/10.1002/joc.1335

Woodworth, P. L. (2010). A survey of recent changes in the main components of the ocean tide. *Continental Shelf Research*, *30*(15), 1680–1691. https://doi.org/10.1016/j.csr.2010.07.002

Woodworth, P. L., Hunter, J. R., Marcos, M., Caldwell, P., Menéndez, M., & Haigh, I. D. (2017). Towards a global higher-frequency sea level dataset. *Geoscience Data Journal*, *3*(2), 50–59. https://doi.org/10.1002/gdj3.42

Woodworth, P. L., Shaw, S. M., & Blackman, D. L. (1991). Secular trends in mean tidal range around the British Isles and along the adjacent European coastline. *Geophysical Journal International*, *104*(3), 593–609. https://doi.org/10.1111/j.1365-246X.1991.tb05704.x

Wöppelmann, G., Marcos, M., Coulomb, A., Martín Míguez, B., Bonnetain, P., Boucher, C., et al. (2014). Rescue of the historical sea level record of Marseille (France) from 1885 to 1988 and its extension back to 1849–1851. *Journal of Geodesy*, *88*(9), 869–885. https://doi.org/10.1007/s00190-014-0728-6

Wunsch, C. (2003). Determining paleoceanographic circulations, with emphasis on the Last Glacial Maximum. *Quaternary Science Reviews*, *22*(2-4), 371–385. https://doi.org/10.1016/S0277-3791(02)00177-4

Wunsch, C., & Ferrari, R. (2004). Vertical mixing, energy, and the general circulation of the oceans. *Annual Review of Fluid Mechanics*, *36*(1), 281–314. https://doi.org/10.1146/annurev.fluid.36.050802.122121

Zappa, C. J., McGillis, W. R., Raymond, P. A., Edson, J. B., Hintsa, E. J., Zemmelink, H. J., et al. (2007). Environmental turbulent mixing controls on air-water gas exchange in marine and aquatic systems. *Geophysical Research Letters*, *34*, L10601. https://doi.org/10.1029/2006GL028790

Zaron, E. D., & Jay, D. A. (2014). An analysis of secular change in tides at open-ocean sites in the Pacific. *Journal of Physical Oceanography*, *44*(7), 1704–1726. https://doi.org/10.1175/JPO-D-13-0266.1

Zeeden, C., Hilgen, F. J., Hüsing, S. K., & Lourens, L. L. (2014). The Miocene astronomical time scale 9–12 Ma: New constraints on tidal dissipation and their implications for paleoclimatic investigations. *Paleoceanography*, *29*, 296–307. https://doi.org/10.1002/2014PA002615

Zhang, W.-Z., Shi, F., Hong, H.-S., Shang, S.-P., & Kirby, J. T. (2010). Tide-surge Interaction Intensified by the Taiwan Strait. *Journal of Geophysical Research*, *115*, C06012. https://doi.org/10.1029/2009JC005762

Zimmerman, J. T. F. (1986). The tidal whirlpool: A review of horizontal dispersion by tidal and residual currents. *Netherlands Journal of Sea Research*, *20*(2-3), 133–154. https://doi.org/10.1016/0077-7579(86)90037-2